

Review of “Particle hygroscopicity and its link to chemical composition in the urban atmosphere of Beijing, China during summertime” by Wu et al. This paper presents summertime measurements of aerosol chemical composition and hygroscopicity in Beijing. The authors do a good job of presenting and discussing the data and their results should be useful in increasing our understanding of aerosol chemical composition and CCN behavior in this region. I recommend that this paper be published after the following comments are addressed.

\*\*\*\*\*

The authors greatly appreciate that the reviewer spent a lot of time to review this manuscript and provide these constructive suggestions. We modified the manuscript according to the comments point by point.

\*\*\*\*\*

General Comments:

- 1) Some more discussion of the air masses and aerosol sources impacting the sampling site during the study would be very useful. What are the major local and regional aerosol sources? Is long range transport an important contributor to aerosol concentrations during this time? If so, what source regions are air masses coming from? More meteorological information should also be added. Was this time period characterized by stagnant conditions? Were there any rain events of frontal passages? If so, did these meteorological events lead to any changes in the measured aerosol properties? All of this information would greatly improve the utility of the findings presented here.

**Response:**

In the MS, one section was added to discuss the meteorological condition during the sampling period.

**Modification in the MS:**

**2.4 Meteorological parameters**

Additionally, a weather station (Met One Instruments Inc.) provided the meteorological parameters. The wind speed, wind direction, ambient temperature, and relative humidity (RH) were detected.

Air mass backward trajectories arriving at the sampling site were calculated using the NOAA “HYSPLIT-4” (Hybrid Single-Particle Lagrangian Integrated Trajectory) model (Draxler and Hess, 1998). The 48 h trajectories terminated on a height of 200 m above the ground at 00:00, 06:00, 12:00 and 18:00 local time (UTC+08). In total, 100 air mass backward trajectories were grouped by assigning to five clusters using a k-means clustering algorithm. The number of clusters was identified according to the changes of total spatial variance (TSV) (cf. HYSPLIT4 user’s guide). Five was chosen as the final number of clusters considering optimum separation of trajectories (larger number of clusters) and simplicity of display (lower number of cluster).

**4.1 Meteorological condition during the sampling period**

Fig. 1 showed the mean air mass backward trajectories for five trajectory clusters

arriving at the sampling site from May 31 to June 24, 2014. The mean backward trajectories showed the significant differences in direction and length. The air masses from the east (45%) and the south (26%) were the dominate trajectories. The short-length air mass backward trajectories in cluster 1 and 2 indicated that air parcels moved slowly and spent much more time over the industrialized regions south and east of Beijing. As a result, the southerly and easterly air masses may be heavily polluted once they arrived at Beijing (Wehner et al., 2008). Cluster 3 spent much more time over the sea and may be associated with humid air masses. Northerly (8%) and north-westerly (10%) air masses, as represented by clusters 4–5, typically lead to the advection of dry and continental air into the Beijing area.

Fig. 2 displays the time series of wind speed, wind direction, ambient temperature, and RH during the sampling period. There was a clear diurnal cycle for all meteorological parameters. During nighttime, the wind speed was usually very low (around 1 m/s) and started to increase around noon on each day. The nighttime static wind may lead to very poor dilution with clean air and dispersion of pollutants and result in the local emissions were trapped in the urban atmosphere. The ambient temperature usually was above 30 °C during daytime and around 20 °C during nighttime. The average temperature and RH were respectively  $24\pm7$  °C and  $45\pm20\%$ . It rained several times during the measuring period, as indicated in the Fig. 2 (a). The heaviest wet deposition occurred on 17, June. The wet deposition obviously removed the atmospheric particles, as can be seen from the particle number size distribution shown in Fig. 3 (a).

In summer, the new particle formation and traffic emissions are the major sources of ultrafine particles in the atmosphere of Beijing (Wu et al., 2008; Wu et al., 2007). In addition, air masses across the industrialized regions in the south and east typically bring the high concentrations of accumulation mode particles to urban areas of Beijing (Wehner et al., 2008).



Fig.1: Mean air mass backward trajectories for five clusters arriving at the sampling site.

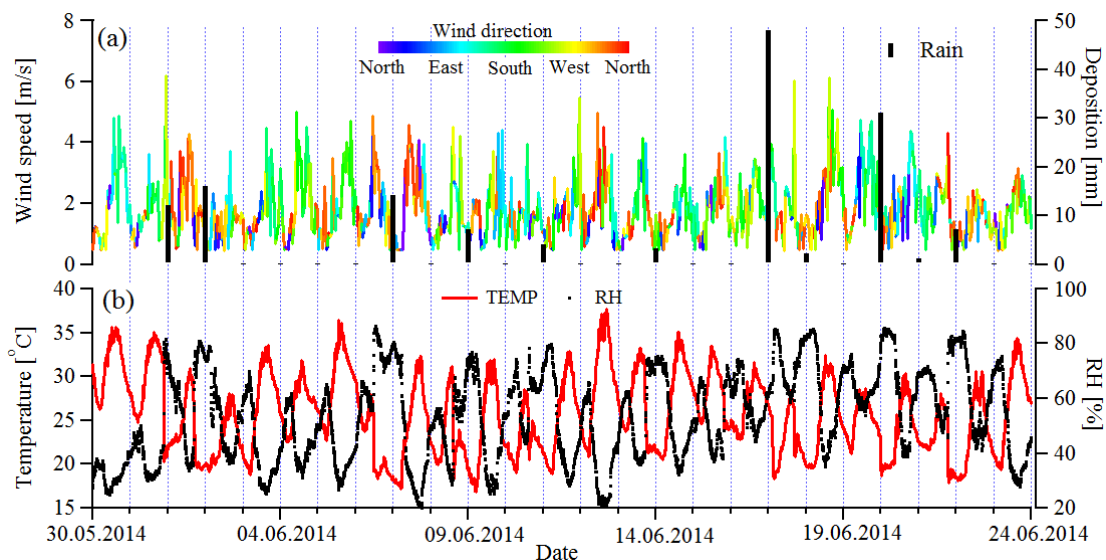


Fig.2: The time series of wind speed, wind direction, wet deposition (a) and temperature and RH (b) during the sampling period.

\*\*\*\*\*

2) *The authors include non-refractory aerosol components and black carbon in their analysis but no mention is made of other aerosol species. Please discuss the role of dust and sea salt and any potential uncertainty or bias that may be introduced by neglecting these aerosol types*

**Response:**

In this study, the particles below 350 nm in mobility diameter are concerned. The dust and sea salt exist in the coarse mode which is larger than 1 $\mu$ m. Therefore, the potential uncertainty caused by neglecting dust and sea salt are very small.

\*\*\*\*\*

3) There are a number of studies that have examined aerosol hygroscopicity and chemical composition in various environments around the world. The authors allude to a few of these in the introduction but do not discuss their findings in the context of these previous measurements or compare results. For example, Paramanov et al. (2013) present size resolved  $\kappa$  values compiled from four different studies which agree very well with those presented here, even though they were all from remote locations. The analysis performed here is also very similar to that done by Levin et al. (2012; 2014) who compared measured aerosol hygroscopicity with that calculated from aerosol composition and also measured during new particle formation events. The results presented here for the hygroscopicity of newly formed particles is actually the opposite of that found by Levin et al. (2012) who saw a decrease in  $\kappa$  for newly formed particles. This difference might indicate the different roles of organic versus inorganic condensing vapors on new particle growth in remote and urban environments. Putting the results of this paper into the context of such previous measurements would again greatly help to increase the usefulness of these findings and strengthen the paper.

**Response:**

In revised MS, we strengthened the comparisons and citation of the previous studies.

### **Modifications in the MS:**

#### ***In introduction:***

Currently, some studies had been performed to investigate the relationship between particle hygroscopicity and chemical composition based on both field measurements and laboratory experiments (Massoli et al., 2010; Wong et al., 2011; Lambe et al., 2011; Rickards et al., 2013; Moore et al., 2012; Suda et al., 2014; Paramonov et al., 2013; Levin et al., 2012). These works specially focused on parametrizing the empirical correlations between the atomic Oxygen:Carbon (O:C) ratio and organic hygroscopicity parameter  $\kappa$  derived from either hygroscopic growth factor (Wu et al., 2013; Rickards et al., 2013) or Cloud Condensation Nuclei (CCN) activity (Mei et al., 2013; Wong et al., 2011; Lambe et al., 2011; Chang et al., 2010). Typically, a linear parametrization of the correlation between  $\kappa$  and O:C was presented. Rickards et al. (2013) recently summarized the literature data and pointed out the systematic variability in parametrizations between organic  $\kappa$  and the O:C ratio determined from the different studies remains large. A recent work done by Suda et al. (2014) tested the influence of the number and location of molecular functional groups on the hygroscopicity of organic aerosols and may help us to find out the mechanisms of organics hygroscopicity from the chemistry point of view.

Over the past several decades, particle hygroscopicity measurements have been carried out world-wide, using the HTDMA technique. Atmospheric environments, in which those measurements were performed includes marine, Antarctic, boreal forest, rural, and urban areas. Swietlicki et al. (2008) and Kreidenweis and Asa-Awu (2014) compiled the existing observations on particle hygroscopic growth in the literature. Throughout these compilations, measurements of particle hygroscopicity have been rarely performed in China, which experiences frequently severe haze pollution episodes. These few particle hygroscopicity measurements using the HTDMA technique were deployed in Yangtze River Delta (Shanghai (Ye et al., 2013) and Hangzhou (Zhang et al., 2011)), Pearl River Delta (Xinken (Cheng et al., 2008) and Hong Kong (Lopez-Yglesias et al., 2014)) and North China Plain (Beijing (Massling et al., 2009; Meier et al., 2009), Yufa (Achtert et al., 2009), and Wuqing (Liu et al., 2011) ). Unfortunately, these measurements lack a linkage between particle hygroscopicity and chemical composition based on a high time resolution.

#### ***In section 4.2:***

Fig. 5 (left) shows the size-dependent particle hygroscopicity parameters and inorganic mass fraction of NR-PM<sub>1</sub> derived from averaging over the entire measuring period. The particle hygroscopicity increased with increasing particle size, displaying the same size-dependency with the mass fraction of inorganic composition in NR-PM<sub>1</sub>. This is because inorganics including ammonium sulfate and ammonium nitrate are major water-soluble chemical compounds in the atmospheric particles. Compared to inorganic components, the hygroscopicity parameter of organic aerosols were typically lower than 0.1 (Varutbangkul et al., 2006; Virkkula et al., 1999). The similar size-dependency of particle hygroscopicity was observed in various

environments. For examples, Levin et al. (2012;2014) and Paramonov et al. (2013) reported that particle hygroscopicity increased with particle size at a forested site in Colorado and a boreal environment of southern Finland at the SMEAR station, respectively. Jurányi et al (2013) observed that particle hygroscopic growth increased with increasing dry diameter in the urban areas of Paris. Swietlicki et al. (2008) compiled worldwide H-TDMA data and found that the particle hygroscopicity showed a pronounced size-dependency, with hygroscopicity increasing with particle diameter.

Over the entire study, the mean  $\kappa$ s of 50, 100, 150, 250, and 350 nm particles were  $0.16\pm 0.07$ ,  $0.19\pm 0.06$ ,  $0.22\pm 0.06$ ,  $0.26\pm 0.07$ , and  $0.28\pm 0.10$ , respectively over the entire sampling period. These values were similar to the hygroscopicity parameter  $\kappa = 0.12\text{--}0.27$  (measured at RH=90%) for 35–265 nm determined in the urban atmosphere of Paris (Jurányi et al., 2013). Yeung et al. (2014) observed that hygroscopicity  $\kappa$ s of particles with sizes of 75, 100, 150, and 200 nm were respectively 0.28, 0.29, 0.26, and 0.27 when Hong Kong experienced a continental airstream. In their study, the particle hygroscopicity showed no obvious size-dependency and was higher than our observation in Beijing. In contrast,  $\kappa$ s measured were relatively low at a forested site in Colorado ( $\kappa = 0.16\pm 0.08$  detected by CCNc), a boreal forest in Finland ( $\kappa = 0.18$  at RH=90%) (Sihto et al., 2011), and a tropical forest site in the Amazon ( $\kappa = 0.16\pm 0.06$  detected by CCNc) (Gunthe et al., 2009). At these forested locations, organic species were predominance in particles. Differently, in the atmosphere of Beijing, the inorganic fraction was relatively dominated, as shown in the Fig.3 (c).

### ***In section 4.3***

“Fig. 8 shows  $\kappa_{\text{org}}$  as a function of O:C ratio. From the degree of scatter point of view,  $\kappa_{\text{org}}$  is not correlated to the O:C ratio. Several previous studies reported the similar plots of  $\kappa_{\text{org}}$  values as a function of O:C ratios (Chang et al., 2010;Bhattu and Tripathi, 2015;Rickards et al., 2013). In order to derive an empirical relationship between  $\kappa_{\text{org}}$  and O:C ratios,  $\kappa_{\text{org}}$  values are usually binned by O:C in increments of 0.1. As displayed in Fig. 8, a linear fitting function ( $\kappa_{\text{org}}=(0.08\pm 0.02)*\text{O:C}+(0.02\pm 0.01)$ ) was obtained. Some empirical functions reported by other previous studies are also shown in Fig.8. In these previous studies (Wu et al., 2013;Jimenez et al., 2009;Rickards et al., 2013;Duplissy et al., 2011), the  $\kappa_{\text{org}}$  were derived from the measurements performed in the sub-saturation regime. In Massoli et al.’ study (2010) (not shown in the Fig. 8 due to the linear fitting based on HGF, not  $\kappa_{\text{org}}$ ), they reported a linear relationship ( $\text{HGF}_{90\%} = (0.58\pm 0.15)*\text{O:C} + (0.85 \pm 0.08)$ ) between HGF90% and O:C for the laboratory-generated SOA particles. Both results displayed in Fig. 8 and Massoli’s study showed a positive correlation between  $\kappa_{\text{org}}$  and O:C. Such positive correlation was also reported by those studies based on CCNc measurements, for examples, Chang et al. (2010) and Mei et al. (2013). We note that the slopes of the linear fitting varied with different studies, indicating there is no a simple parametrization to describe the relationship between organic hygroscopic and its oxidation state though the various atmospheric environments. Recently, Richards et al. (2013) had undertaken an extensive review of  $\kappa$  values

published in the literature and showed that  $\kappa_{\text{org}}$  vs. O:C plot has a large degree of scatter. This indicates that other factors, such as phase state (Pajunoja et al., 2015) and molecular structures (Suda et al., 2014) of organic aerosols (OA) other than oxidation state may also play a role in the determination of the OA hygroscopicity. ”

\*\*\*\*\*

4) Before publication the paper should be thoroughly proof read for English grammar and word usage.

**Response:**

We carefully read the manuscript and improve the English writing.

\*\*\*\*\*

Specific Comments:

*Page 11500, Line 8: What was the size range for the SMPS measurements?*

**Response:**

The size range is 3-800 nm.

**Modification in the MS:**

“Particle number size distributions from 3 to 800 nm were measured by TSI-SMPS (Long-DMA3081+CPC3775 and Nano-DMA3085+UCPC3776).”

\*\*\*\*\*

*Page 11501, Line 25: Was this a home built PAX instrument? Please provide more information. Page 11501, line 25: The reference here should be (Arnott et al. 1999). This is also wrong in the list of references.*

**Response:**

The PAX is not home-built one. It is product of DMT Company. The reference was corrected in the MS.

**Modification in the MS:**

“Black carbon (BC) mass concentration in  $\mu\text{g}/\text{m}^3$  is derived from Photoacoustic Extinctionmeter (PAX) measurements (DMT Company) (Arnott et al., 1999) equipped with  $\text{PM}_{10}$  cut-off inlet.”

\*\*\*\*\*

*Page 11503, line 14: Please add a figure showing the SOA and POA fractions during the study and discuss their relative importance during different time periods.*

**Response:**

In the Fig.3 (a), the organics were separated into POA and SOA fractions.

**Modification in the MS:**

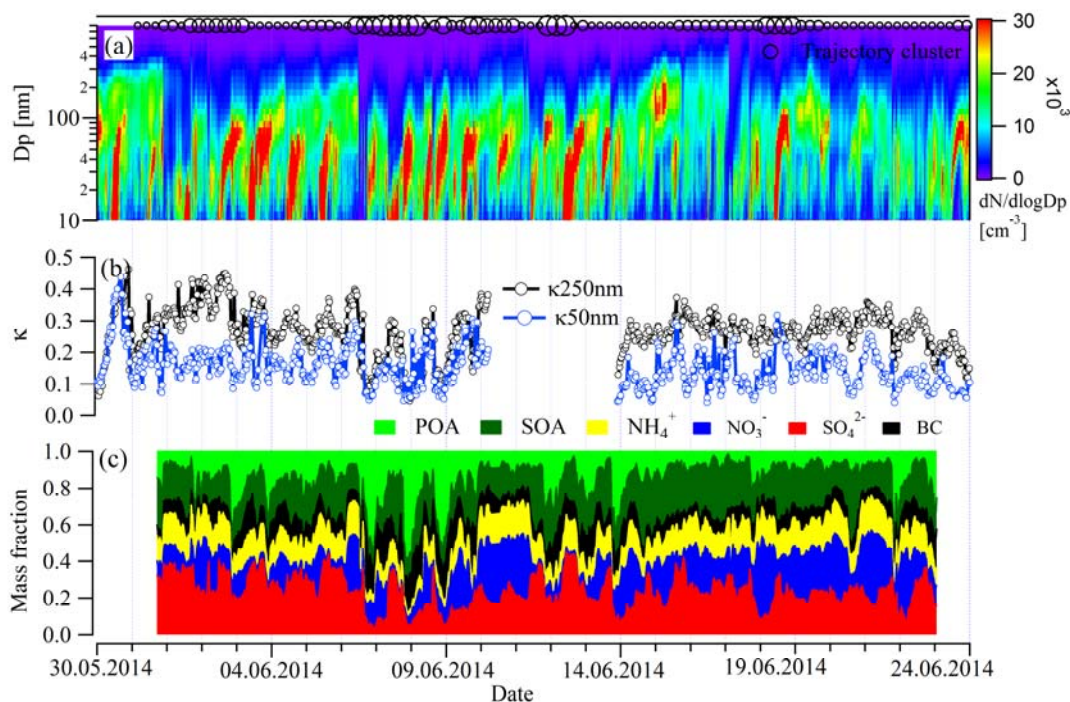


Figure 3: Time series of particle number size distribution (a), hygroscopicity parameters,  $\kappa$  (b), and chemical composition of  $PM_{10}$  (c) during the measuring period. The black circles in the upper panel indicate the trajectory clusters. The smallest circle means cluster 1, and the biggest one is cluster 5.

\*\*\*\*\*

*Page 11504, line 9: Were wind speed and direction also measured? If so, please add them to Figure 1 and discuss how they may have impacted the measured aerosol properties.*

**Response:**

Yes, the wind speed and direction were measured. A new plot was added to describe the meteorological condition.

**Modification in the MS:**

Fig.2 displays the time series of wind speed, wind direction, ambient temperature, and RH during the sampling period. There was a clear diurnal cycle for all meteorological parameters. Typically, the wind speed was very low (around 1 m/s) during the nighttime and started to increase around noon on each day. The nighttime static wind may lead to very poor dilution with clean air and dispersion of pollutants and result in the local emissions were trapped in the urban atmosphere. The ambient temperature usually is above 30 °C during daytime and around 20 °C during nighttime. The average temperature and RH was respectively  $24 \pm 7$  °C and  $45 \pm 20\%$ . It rained several times during the measuring period. The heaviest wet deposition occurred on 17, June. The wet deposition obviously removed the atmospheric particles, as can be seen from the particle number size distribution shown in Fig. 3 (a).

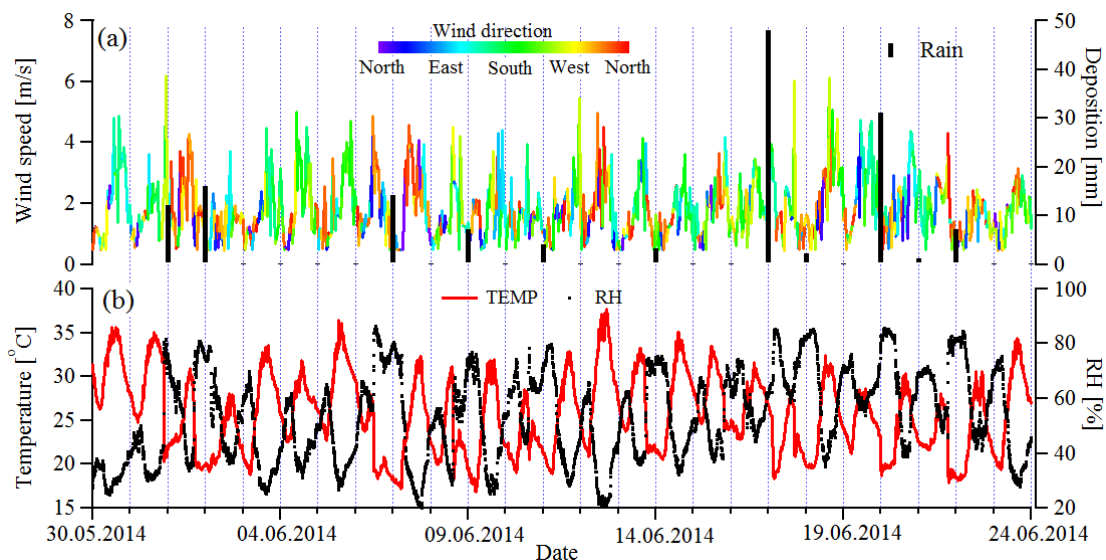


Fig.2: The time series of wind speed, wind direction, wet deposition (a) and temperature and RH (b) during the sampling period.

\*\*\*\*\*

Page 11505, Line 3: Please show the GF-PDF mentioned here.

**Response:**

One new plot was added to show the GF-PDF during the entire sampling period.

**Modification in the MS:**

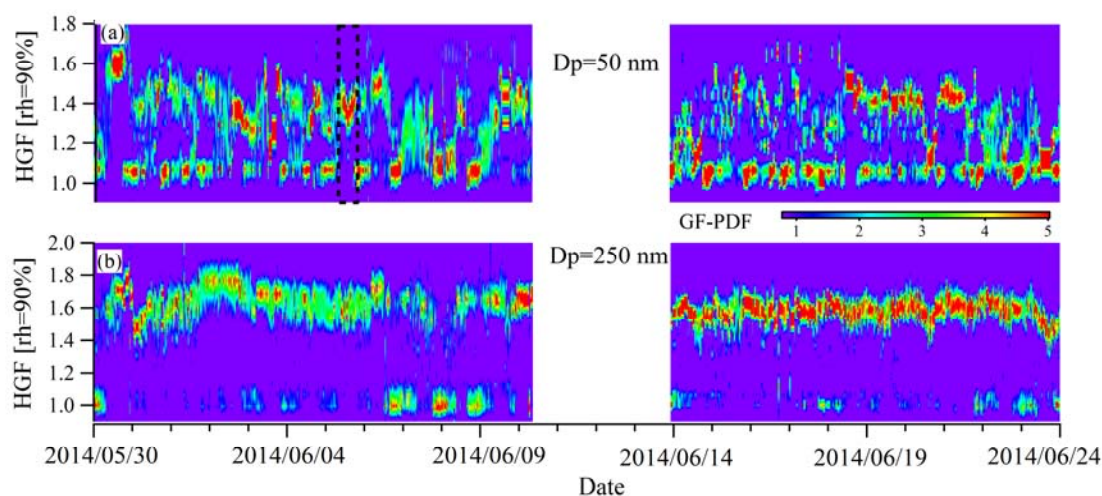


Figure 4: The time series of the GF-PDFs for 50 and 250 nm particles.

Fig. 4 gives an overview of growth factor probability density distributions (GF-PDF) for 50 and 250 nm particles during the entire field campaign. The GF-PDFs of both 50 and 250 nm showed two distinct modes, which are identified as hydrophobic mode ( $GF < 1.2$ ) and hydrophilic mode ( $GF > 1.2$ ). This implied that the particles were usually externally mixed. The hydrophilic mode of 250 nm particles is more prominent most of the time. Differently, the hydrophobic mode was dominated in 50 nm particles. As marked in the Fig. 4 (a) by the square with dashed line, the hydrophobic mode disappeared occasionally, indicating that the vast majority of particles in this size range can be fully hygroscopic. This phenomenon took place



during the NPF events. A case study of particle hygroscopic behavior during new particle formation events will be given in section 4.4.

\*\*\*\*\*

*Page 11505, Line 21: Was  $PM_{2.5}$  calculated from number size distributions or is this from a separate measurement?*

**Response:**

The  $PM_{2.5}$  mass concentration was measured by TEOM<sup>®</sup> Monitor (Series 1400ab).

**Modification in the MS:**

Here, the  $PM_{2.5}$  mass concentration which measured by TEOM<sup>®</sup> Monitor (Series 1400ab), a key factor characterizing air pollution, vs. the fraction of the hydrophilic mode is plotted (Fig. 6) to analyze the relationship between particle mixing state and air pollution.

\*\*\*\*\*

*Page 11505, Line 27: Were there other changes in aerosol characteristics (i.e. chemical composition, size distribution or  $\kappa$ ) during high PM events?*

**Response:**

The chemical composition and size distribution of particles should vary with PM concentration. In this study, the particle hygroscopicity is concerned. Other parameters will not be discussed in detail.

\*\*\*\*\*

*Page 11506, Line 16: Please show a timeline of BC concentrations. This could be added to Figure 1.*

**Response:**

The BC concentration was shown in the Fig.1 (c).

**Modification in the MS:**

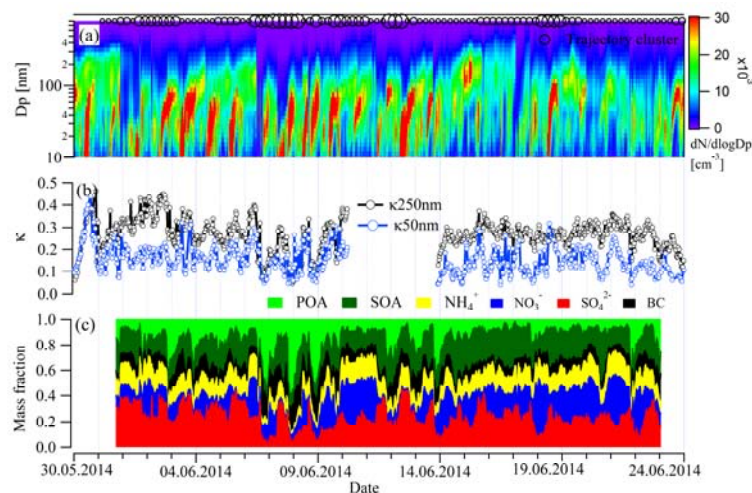


Figure 3: Time series of particle number size distribution (a), hygroscopicity parameters,  $\kappa$  (b), and chemical composition of  $PM_1$  (c) during the measuring period. The black circles in the upper panel indicate the trajectory clusters. The smallest circle means cluster 1, and the biggest one is cluster 5.

\*\*\*\*\*

*Page 11507, Line 8: While the fitted slopes are close to one, indicating no systematic*

bias, there is considerable scatter around these lines in Figure 4. This means that in specific cases  $\kappa$  may not be well predicted, as claimed here. Please mention this and discuss what might be causing the scatter.

**Response:**

The assumption of BC mass size distribution and  $\kappa_{org}$  value in the closure as well as the measurement uncertainties for both HTDMA and AMS could introduce the biases in the closure.

**Modification in the MS:**

While, one should note that the assumption of BC mass size distribution and  $\kappa_{org}$  value in the closure as well as the measurement uncertainties for both H-TDMA and AMS could introduce the biases in the closure. This may lead to a scatter of data point around the fitting line.

\*\*\*\*\*  
 Page 11508, Line 3: The slope of the  $\kappa_{org}$  vs O:C line from this work is much flatter than those of the other studies shown in Figure 5. Given the small slope and large scatter, it appears that one of the main conclusions from these measurements is that O:C is not a good predictor of  $\kappa_{org}$  for this data set (as stated in the discussion). I feel this should be stated in the abstract and conclusions instead of presenting the empirical relationship between  $\kappa_{org}$  and O:C, which is weak.

**Response:**

Yes, we agree. The abstract and conclusion were modified.

\*\*\*\*\*  
 Page 11508, Line 17: Please show, and discuss, how measured aerosol composition and  $\kappa$  changed during the NPF event.

**Response:**

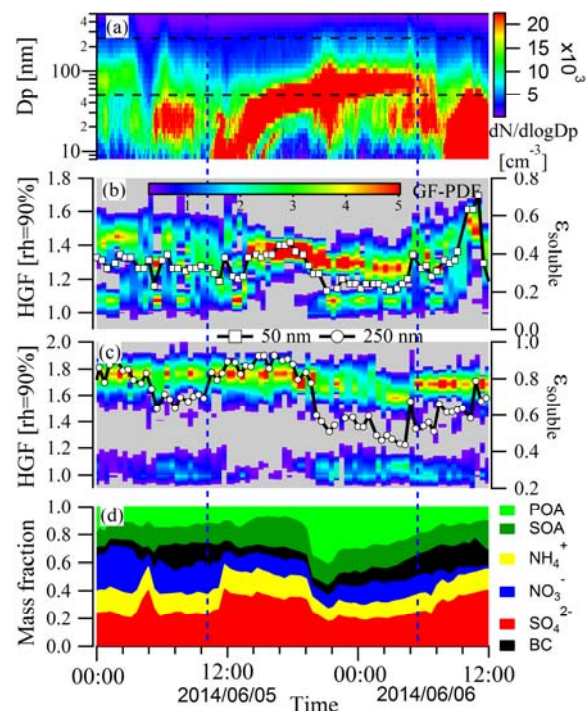
The mass fraction of PM1 during the NPF events was displayed in the Fig.9 (d). More discussions were added into the MS.

**Modification in the MS:**

The chemical composition of PM<sub>1</sub> in Fig. 9 (c) showed that the inorganic species and SOA were dominated before 8:30 p.m., while mass fraction of organic compounds, especially POA increased significantly afterwards. This variation was consistent to that in particle hygroscopicity.

Figure 9: The variation in particle hygroscopicity, water soluble volume fraction, and chemical composition during new particle formation event.

\*\*\*\*\*  
 \*\*\*\*\*



Page 11509, Line 7: It appears that there was an air mass change prior to the NPF, as indicated by the sharp decrease in aerosol concentrations. The change in 250 nm aerosol properties could just be due to this change and it may not be correct to directly compare these particles before and after the event.

**Response:**

We analyzed the local wind speed and wind direction, as shown in the Fig. 1. The wind speeds are lower than 2 m/s at the most of time. And, no significant change in wind direction was observed. This means that the decrease in aerosol concentration may not be caused by the air mass change. The possible reason may be the caused by the development of boundary layer. As a result, the pollutants were diluted by the fresh air. This analysis will be mentioned in the manuscript.

**Modification in the MS:**

“During the NPF events, the wind speeds were lower than 2 m/s, indicating a stable local meteorological condition. This means that the change in the hygroscopicity of 250 nm particle may not be caused by the air mass changes.”

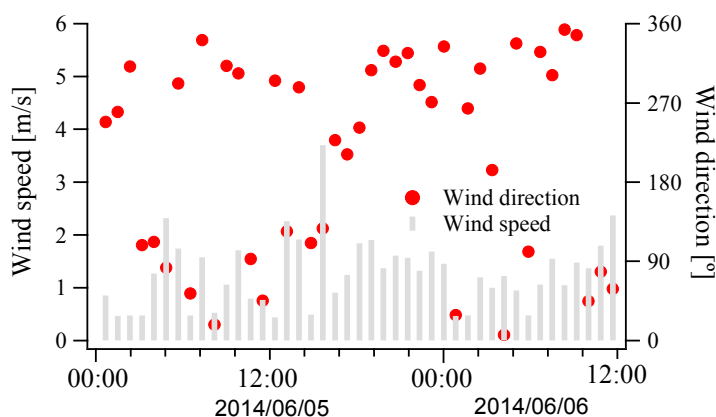


Fig 1: The wind direction and wind speed during the NPF events.

\*\*\*\*\*

Figure 2 Caption: This should say “Mass fraction of inorganics” since this is what is actually plotted.

**Response:**

Yes, it was modified in the manuscript.

\*\*\*\*\*

**References:**

Achtert, P., Birmili, W., Nowak, A., Wehner, B., Wiedensohler, A., Takegawa, N., Kondo, Y., Miyazaki, Y., Hu, M., and Zhu, T.: Hygroscopic growth of tropospheric particle number size distributions over the North China Plain, *Journal of Geophysical Research: Atmospheres*, 114, n/a-n/a, 10.1029/2008JD010921, 2009.

Arnott, P., Moosmüller, H., Fred Rogers, C., Jin, T., and Bruch, R.: Photoacoustic spectrometer for measuring light absorption by aerosol: instrument description, *Atmospheric Environment*, 33, 2845-2852, [http://dx.doi.org/10.1016/S1352-2310\(98\)00361-6](http://dx.doi.org/10.1016/S1352-2310(98)00361-6), 1999.

Bhattu, D., and Tripathi, S. N.: CCN closure study: Effects of aerosol chemical composition and mixing state, *Journal of Geophysical Research: Atmospheres*, 120, 2014JD021978,

10.1002/2014JD021978, 2015.

Chang, R. Y. W., Slowik, J. G., Shantz, N. C., Vlasenko, A., Liggio, J., Sjostedt, S. J., Leaitch, W. R., and Abbatt, J. P. D.: The hygroscopicity parameter ( $\kappa$ ) of ambient organic aerosol at a field site subject to biogenic and anthropogenic influences: relationship to degree of aerosol oxidation, *Atmos. Chem. Phys.*, 10, 5047-5064, 10.5194/acp-10-5047-2010, 2010.

Cheng, Y. F., Wiedensohler, A., Eichler, H., Heintzenberg, J., Tesche, M., Ansmann, A., Wendisch, M., Su, H., Althausen, D., Herrmann, H., Gnauk, T., Brüggemann, E., Hu, M., and Zhang, Y. H.: Relative humidity dependence of aerosol optical properties and direct radiative forcing in the surface boundary layer at Xinken in Pearl River Delta of China: An observation based numerical study, *Atmospheric Environment*, 42, 6373-6397, <http://dx.doi.org/10.1016/j.atmosenv.2008.04.009>, 2008.

Draxler, R. R., and Hess, G. D.: An overview of the HYSPLIT\_4 modelling system for trajectories dispersion and deposition, *Australian Meteorological Magazine*, 47, 295-308, 1998.

Duplissy, J., DeCarlo, P. F., Dommen, J., Alfarra, M. R., Metzger, A., Barmapadimos, I., Prevot, A. S. H., Weingartner, E., Tritscher, T., Gysel, M., Aiken, A. C., Jimenez, J. L., Canagaratna, M. R., Worsnop, D. R., Collins, D. R., Tomlinson, J., and Baltensperger, U.: Relating hygroscopicity and composition of organic aerosol particulate matter, *Atmos. Chem. Phys.*, 11, 1155-1165, 10.5194/acp-11-1155-2011, 2011.

Gunthe, S. S., King, S. M., Rose, D., Chen, Q., Roldin, P., Farmer, D. K., Jimenez, J. L., Artaxo, P., Andreae, M. O., Martin, S. T., and Pöschl, U.: Cloud condensation nuclei in pristine tropical rainforest air of Amazonia: size-resolved measurements and modeling of atmospheric aerosol composition and CCN activity, *Atmos. Chem. Phys.*, 9, 7551-7575, 10.5194/acp-9-7551-2009, 2009.

Jimenez, J. L., Canagaratna, M. R., Donahue, N. M., Prevot, A. S. H., Zhang, Q., Kroll, J. H., DeCarlo, P. F., Allan, J. D., Coe, H., Ng, N. L., Aiken, A. C., Docherty, K. S., Ulbrich, I. M., Grieshop, A. P., Robinson, A. L., Duplissy, J., Smith, J. D., Wilson, K. R., Lanz, V. A., Hueglin, C., Sun, Y. L., Tian, J., Laaksonen, A., Raatikainen, T., Rautiainen, J., Vaattovaara, P., Ehn, M., Kulmala, M., Tomlinson, J. M., Collins, D. R., Cubison, M. J., E, Dunlea, J., Huffman, J. A., Onasch, T. B., Alfarra, M. R., Williams, P. I., Bower, K., Kondo, Y., Schneider, J., Drewnick, F., Borrmann, S., Weimer, S., Demerjian, K., Salcedo, D., Cottrell, L., Griffin, R., Takami, A., Miyoshi, T., Hatakeyama, S., Shimono, A., Sun, J. Y., Zhang, Y. M., Dzepina, K., Kimmel, J. R., Sueper, D., Jayne, J. T., Herndon, S. C., Trimborn, A. M., Williams, L. R., Wood, E. C., Middlebrook, A. M., Kolb, C. E., Baltensperger, U., and Worsnop, D. R.: Evolution of organic aerosols in the atmosphere, *Science*, 326, 1525-1529, 10.1126/science.1180353, 2009.

Jurányi, Z., Tritscher, T., Gysel, M., Laborde, M., Gomes, L., Roberts, G., Baltensperger, U., and Weingartner, E.: Hygroscopic mixing state of urban aerosol derived from size-resolved cloud condensation nuclei measurements during the MEGAPOLI campaign in Paris, *Atmos. Chem. Phys.*, 13, 6431-6446, 10.5194/acp-13-6431-2013, 2013.

Kreidenweis, S. M., and Asa-Awuku, A.: 5.13 - Aerosol Hygroscopicity: Particle Water Content and Its Role in Atmospheric Processes, in: *Treatise on Geochemistry (Second Edition)*, edited by: Turekian, H. D. H. K., Elsevier, Oxford, 331-361, 2014.

Lambe, A. T., Onasch, T. B., Massoli, P., Croasdale, D. R., Wright, J. P., Ahern, A. T., Williams, L. R., Worsnop, D. R., Brune, W. H., and Davidovits, P.: Laboratory studies of the chemical composition and cloud condensation nuclei (CCN) activity of secondary organic aerosol (SOA) and oxidized primary organic aerosol (OPOA), *Atmos. Chem. Phys.*, 11, 8913-8928, 10.5194/acp-11-8913-2011, 2011.

Levin, E. J. T., Prenni, A. J., Petters, M. D., Kreidenweis, S. M., Sullivan, R. C., Atwood, S. A., Ortega,

J., DeMott, P. J., and Smith, J. N.: An annual cycle of size-resolved aerosol hygroscopicity at a forested site in Colorado, *J. Geophys. Res.*, 117, D06201, 10.1029/2011jd016854, 2012.

Levin, E. J. T., Prenni, A. J., Palm, B. B., Day, D. A., Campuzano-Jost, P., Winkler, P. M., Kreidenweis, S. M., DeMott, P. J., Jimenez, J. L., and Smith, J. N.: Size-resolved aerosol composition and its link to hygroscopicity at a forested site in Colorado, *Atmos. Chem. Phys.*, 14, 2657-2667, 10.5194/acp-14-2657-2014, 2014.

Liu, P. F., Zhao, C. S., Göbel, T., Hallbauer, E., Nowak, A., Ran, L., Xu, W. Y., Deng, Z. Z., Ma, N., Mildenerger, K., Henning, S., Stratmann, F., and Wiedensohler, A.: Hygroscopic properties of aerosol particles at high relative humidity and their diurnal variations in the North China Plain, *Atmos. Chem. Phys.*, 11, 3479-3494, 10.5194/acp-11-3479-2011, 2011.

Lopez-Yglesias, X. F., Yeung, M. C., Dey, S. E., Brechtel, F. J., and Chan, C. K.: Performance Evaluation of the Brechtel Mfg. Humidified Tandem Differential Mobility Analyzer (BMI HTDMA) for Studying Hygroscopic Properties of Aerosol Particles, *Aerosol Science and Technology*, 48, 969-980, 10.1080/02786826.2014.952366, 2014.

Massling, A., Stock, M., Wehner, B., Wu, Z. J., Hu, M., Brüggemann, E., Gnauk, T., Herrmann, H., and Wiedensohler, A.: Size segregated water uptake of the urban submicrometer aerosol in Beijing, *Atmospheric Environment*, 43, 1578-1589, <http://dx.doi.org/10.1016/j.atmosenv.2008.06.003>, 2009.

Massoli, P., Lambe, A. T., Ahern, A. T., Williams, L. R., Ehn, M., Mikkilä, J., Canagaratna, M. R., Brune, W. H., Onasch, T. B., Jayne, J. T., Petäjä, T., Kulmala, M., Laaksonen, A., Kolb, C. E., Davidovits, P., and Worsnop, D. R.: Relationship between aerosol oxidation level and hygroscopic properties of laboratory generated secondary organic aerosol (SOA) particles, *Geophysical Research Letters*, 37, n/a-n/a, 10.1029/2010GL045258, 2010.

Mei, F., Hayes, P. L., Ortega, A., Taylor, J. W., Allan, J. D., Gilman, J., Kuster, W., de Gouw, J., Jimenez, J. L., and Wang, J.: Droplet activation properties of organic aerosols observed at an urban site during CalNex-LA, *Journal of Geophysical Research: Atmospheres*, 118, 2903-2917, 10.1002/jgrd.50285, 2013.

Meier, J., Wehner, B., Massling, A., Birmili, W., Nowak, A., Gnauk, T., Brüggemann, E., Herrmann, H., Min, H., and Wiedensohler, A.: Hygroscopic growth of urban aerosol particles in Beijing (China) during wintertime: a comparison of three experimental methods, *Atmos. Chem. Phys.*, 9, 6865-6880, 10.5194/acp-9-6865-2009, 2009.

Moore, R. H., Raatikainen, T., Langridge, J. M., Bahreini, R., Brock, C. A., Holloway, J. S., Lack, D. A., Middlebrook, A. M., Perring, A. E., Schwarz, J. P., Spackman, J. R., and Nenes, A.: CCN Spectra, Hygroscopicity, and Droplet Activation Kinetics of Secondary Organic Aerosol Resulting from the 2010 Deepwater Horizon Oil Spill, *Environmental Science & Technology*, 46, 3093-3100, 10.1021/es203362w, 2012.

Pajunoja, A., Lambe, A. T., Hakala, J., Rastak, N., Cummings, M. J., Brogan, J. F., Hao, L., Paramonov, M., Hong, J., Prisle, N. L., Malila, J., Romakkaniemi, S., Lehtinen, K. E. J., Laaksonen, A., Kulmala, M., Massoli, P., Onasch, T. B., Donahue, N. M., Riipinen, I., Davidovits, P., Worsnop, D. R., Petäjä, T., and Virtanen, A.: Adsorptive uptake of water by semisolid secondary organic aerosols, *Geophysical Research Letters*, 42, 3063-3068, 10.1002/2015GL063142, 2015.

Paramonov, M., Aalto, P. P., Asmi, A., Prisle, N., Kerminen, V. M., Kulmala, M., and Petäjä, T.: The analysis of size-segregated cloud condensation nuclei counter (CCNC) data and its implications for cloud droplet activation, *Atmos. Chem. Phys.*, 13, 10285-10301, 10.5194/acp-13-10285-2013, 2013.

Rickards, A. M. J., Miles, R. E. H., Davies, J. F., Marshall, F. H., and Reid, J. P.: Measurements of the

Sensitivity of Aerosol Hygroscopicity and the  $\kappa$  Parameter to the O/C Ratio, *The Journal of Physical Chemistry A*, 117, 14120-14131, 10.1021/jp407991n, 2013.

Sihto, S. L., Mikkilä, J., Vanhanen, J., Ehn, M., Liao, L., Lehtipalo, K., Aalto, P. P., Duplissy, J., Petäjä, T., Kerminen, V. M., Boy, M., and Kulmala, M.: Seasonal variation of CCN concentrations and aerosol activation properties in boreal forest, *Atmos. Chem. Phys.*, 11, 13269-13285, 10.5194/acp-11-13269-2011, 2011.

Suda, S. R., Petters, M. D., Yeh, G. K., Strollo, C., Matsunaga, A., Faulhaber, A., Ziemann, P. J., Prenni, A. J., Carrico, C. M., Sullivan, R. C., and Kreidenweis, S. M.: Influence of Functional Groups on Organic Aerosol Cloud Condensation Nucleus Activity, *Environmental Science & Technology*, 48, 10182-10190, 10.1021/es502147y, 2014.

Swietlicki, E., Hansson, H. C., HäMeri, K., Svenningsson, B., Massling, A., McFiggans, G., McMurry, P. H., PetÄJÄ, T., Tunved, P., Gysel, M., Topping, D., Weingartner, E., Baltensperger, U., Rissler, J., Wiedensohler, A., and Kulmala, M.: Hygroscopic properties of submicrometer atmospheric aerosol particles measured with H-TDMA instruments in various environments—a review, *Tellus B*, 60, 432-469, 10.1111/j.1600-0889.2008.00350.x, 2008.

Varutbangkul, V., Brechtel, F. J., Bahreini, R., Ng, N. L., Keywood, M. D., Kroll, J. H., Flagan, R. C., Seinfeld, J. H., Lee, A., and Goldstein, A. H.: Hygroscopicity of secondary organic aerosols formed by oxidation of cycloalkenes, monoterpenes, sesquiterpenes, and related compounds, *Atmos. Chem. Phys.*, 6, 2367-2388, 10.5194/acp-6-2367-2006, 2006.

Virkkula, A., Van Dingenen, R., Raes, F., and Hjorth, J.: Hygroscopic properties of aerosol formed by oxidation of limonene,  $\alpha$ -pinene, and  $\beta$ -pinene, *J. Geophys. Res.*, 104, 3569-3579, 10.1029/1998jd100017, 1999.

Wehner, B., Birmili, W., Ditas, F., Wu, Z., Hu, M., Liu, X., Mao, J., Sugimoto, N., and Wiedensohler, A.: Relationships between submicrometer particulate air pollution and air mass history in Beijing, China, 2004–2006, *Atmos. Chem. Phys.*, 8, 6155-6168, 10.5194/acp-8-6155-2008, 2008.

Wong, J. P. S., Lee, A. K. Y., Slowik, J. G., Cziezo, D. J., Leaitch, W. R., Macdonald, A., and Abbatt, J. P. D.: Oxidation of ambient biogenic secondary organic aerosol by hydroxyl radicals: Effects on cloud condensation nuclei activity, *Geophysical Research Letters*, 38, n/a-n/a, 10.1029/2011GL049351, 2011.

Wu, Z., Hu, M., Liu, S., Wehner, B., Bauer, S., Maßling, A., Wiedensohler, A., Petäjä, T., Dal Maso, M., and Kulmala, M.: New particle formation in Beijing, China: Statistical analysis of a 1-year data set, *Journal of Geophysical Research: Atmospheres*, 112, n/a-n/a, 10.1029/2006JD007406, 2007.

Wu, Z., Hu, M., Lin, P., Liu, S., Wehner, B., and Wiedensohler, A.: Particle number size distribution in the urban atmosphere of Beijing, China, *Atmospheric Environment*, 42, 7967-7980, <http://dx.doi.org/10.1016/j.atmosenv.2008.06.022>, 2008.

Wu, Z. J., Poulain, L., Henning, S., Dieckmann, K., Birmili, W., Merkel, M., van Pinxteren, D., Spindler, G., Mueller, K., Stratmann, F., Herrmann, H., and Wiedensohler, A.: Relating particle hygroscopicity and CCN activity to chemical composition during the HCCT-2010 field campaign, *Atmospheric Chemistry and Physics*, 13, 7983-7996, 10.5194/acp-13-7983-2013, 2013.

Ye, X., Tang, C., Yin, Z., Chen, J., Ma, Z., Kong, L., Yang, X., Gao, W., and Geng, F.: Hygroscopic growth of urban aerosol particles during the 2009 Mirage-Shanghai Campaign, *Atmospheric Environment*, 64, 263-269, <http://dx.doi.org/10.1016/j.atmosenv.2012.09.064>, 2013.

Yeung, M. C., Lee, B. P., Li, Y. J., and Chan, C. K.: Simultaneous HTDMA and HR-ToF-AMS measurements at the HKUST Supersite in Hong Kong in 2011, *Journal of Geophysical Research: Atmospheres*, 119, 9864-9883, 10.1002/2013JD021146, 2014.

Zhang, J., Wang, L., Chen, J., Feng, S., Shen, J., and Jiao, L.: Hygroscopicity of ambient submicron particles in urban Hangzhou, China, *Front. Environ. Sci. Eng. China*, 5, 342-347, 10.1007/s11783-011-0358-7, 2011.

## General comments

This manuscript describes aerosol hygroscopicity determined under subsaturated conditions in Beijing, China during June 2014. The hygroscopicity parameter ( $\kappa$ ) is calculated from measurements throughout the study and a closure analysis, using the size-resolved chemical composition measured by an aerosol mass spectrometer, is presented. Overall, this study presents consistent results with previous work with careful attention to analysis. However, there is little effort in demonstrating the additional knowledge gained from this study. This is not the first HTDMA study in Beijing, but there is no comparison to previous campaigns or to other studies in urban environments (e.g. Meier et al. (2009), Juranyi et al. (2012) and Yeung et al. (2014)).

I recommend that the manuscript be accepted on the condition that a more in depth comparison with other studies is included and that the specific comments listed below are addressed. This manuscript also needs careful proofreading for grammar mistakes before it should be accepted for publication.

\*\*\*\*\*

The authors greatly thank to the referee to spend lots of time to read the manuscript and provide great comments. We realized that there is a lack of comparisons with previous studies on particle hygroscopicity in various atmospheric environments. In the revised MS, this point was strengthened.

\*\*\*\*\*

## Specific comments

Page 11501, line 14

*Why did you estimate a particle density of 1500 kg/m<sup>3</sup>? An average, or time-varying, particle density could be easily calculated using the chemical composition measured by the AMS in conjunction with the BC mass measured by the PAX.*

\*\*\*\*\*

### **Response:**

According to the particle mass concentration=volume concentration \* particle density, the particle density is estimated by comparing the AMS-measured mass concentration and BC and the particle volume concentration derived from the particle number size distribution. On average, the particle density of 1.5 kg/m<sup>3</sup> produced the best fitting between AMS-measured mass concentration and BC and the particle volume concentration. This will be clarified in the MS.

### **Modification in the MS:**

“Here, the particle density is estimated by dividing the AMS-measured PM1 and black carbon mass concentrations by the SMPS-derived particle volume concentration.”

\*\*\*\*\*

Page 11501, line 23

*Reference to the work of Lanz et al. (2007) would be appropriate.*

### **Response:**

It was modified in the MS.

HOA and COA were both anthropogenic primary organic aerosol (POA) components (Lanz et al., 2007).



\*\*\*\*\*

Page 11503, line 17

Justification should be provided for why 0.1 was chosen for SOA. Kammermann et al. (2010) determined to be > 0:2 for aged organics from HTDMA measurements at Jungfraujoch, whereas Wex et al. (2009) determined of laboratory generated SOA to be < 0:1 and Yeung et al. (2014) found urban org to be up to 0.29.

**Response:**

$\kappa_{SOA}=0.1$  was adopted from Gysel et al. (2007). By taking  $\kappa_{SOA}=0.1$ , the best fit between  $\kappa_{HTDMA}$  and  $\kappa_{chem}$  was obtained in this study. Kammermann et al., (2010) reported the mean hygroscopicity of the Aitken and accumulation mode aerosol at the free tropospheric site Jungfraujoch is  $\kappa=0.24$ , not the kappa value of organic compounds. In their study,  $\kappa_{SOA}=0.1$  was also cited from Gysel et al.’s study. Yeung et al. (2014) showed that “over 90% of measured data and predictions based on Extended Aerosol Inorganics Model with a constant GF of the organic fraction ( $GF_{org}$ ) of 1.18 are within 10% closure”.  $GF_{org}=1.18$  corresponds to  $\kappa_{SOA}\approx 0.1$ . In Yeung’s study,  $GF_{org}$  ranged from 1 to 1.5 ( $\kappa_{org}$  up to 0.29) was obtained from the best fit  $GF_{org}$  values from  $GF^*$  based on the HTDMA measurements and the predicted  $GF_{inorg}$  based on the HR-ToF-AMS composition. This method may result in the  $GF_{org}$  values include all uncertainty in the closure between particle hygroscopicity and chemical composition. The SOA hygroscopicity varies with its oxidation state (Jimenez et al., 2009). The usage of a constant value in closure study may introduce uncertainty. More discussion will be given in the MS.

**Modification in the MS:**

“thereby more hygroscopic and has a  $\kappa_{SOA}$  of 0.1, which was calculated from the hygroscopic growth factor of organics at 90% RH as given in Gysel et al. (2007) using Eq. (4) in section 3.1. By taking  $\kappa_{SOA}=0.1$ , the best fit between  $\kappa_{HTDMA}$  and  $\kappa_{chem}$  was obtained in this study. One should note that kappa of SOA may varied with its oxidation state (Jimenez et al., 2009). The usage of a constant kappa value may introduce uncertainty in the closure of particle hygroscopicity and chemical composition.”

\*\*\*\*\*

Page 11503, line 18

There is no equation 4 in the cited paper. Please update the reference.

**Response:**

The equation [4] is not cited from the reference and is from the section 3.1 in the manuscript.

**Modification in the MS:**

“thereby more hygroscopic and has a  $\kappa_{SOA}$  of 0.1, which was calculated from the hygroscopic growth factor of organics at 90% RH as given in Gysel et al. (2007) using Eq. (4) in section 3.1.”

\*\*\*\*\*

Page 11503, line 25 and Table 1

What are the references for the shown in Table 1? According to Petters and Kreidenweis (2007),  $\kappa$  for ammonium sulphate is 0.53. Was the for ammonium

*bisulphate measured by the authors?*

**Response:**

The values listed in the Table 1 are adopted from Gysel et al. (2007). In their study, the particle hygroscopic growths of different chemical species were given. According to:

$$\kappa_{HTDMA} = (HGF^3 - 1) \left( \frac{\exp\left(\frac{A}{D_{Pdry} \cdot HGF}\right)}{RH} - 1 \right)$$

The HGFs were converted into the kappa values. It will be clarified in the MS.

**Modification in the MS:**

“The  $\kappa_{HTDMA}$  values for the individual compounds listed in the Table 2 were calculated from the hygroscopic growth factor at 90% RH as given in Gysel et al. (2007) using equation [4] in the section 3.1.”

\*\*\*\*\*

*Page 11504, line 15*

*The hygroscopic growth factor was measured, from which the hygroscopicity parameter was determined. The statement should be revised to reflect this.*

**Response:**

The sentence was rearranged.

**Modification in the MS:**

“The hygroscopic growth factors of 50, 100, 150, 250, and 350 nm particles were measured at RH=90%. Hygroscopicity parameters ( $\kappa$ ) were calculated using equation [4] in section 3.1.”

\*\*\*\*\*

*Page 11506, line 15*

*Why do you limit the size range for detectable mass to be  $\pm 5$  nm when you integrate over  $\pm 50$  nm? It seems that these should be consistent.*

**Response:**

“ $\pm 5$  nm” should be “ $\pm 50$  nm”. It was corrected in the MS.

**Modifications in the MS:**

“ $\pm 5$  nm” was changed to be “ $\pm 50$  nm”.

\*\*\*\*\*

*Page 11506, lines 22–24*

*You should include a sensitivity analysis to estimate the uncertainties associated with the assumption that BC is uniformly distributed across particle size.*

**Response:**

The following figure showed the BC mass size distribution in August in the atmosphere of Beijing measured by Sun et al. (2012a). The average mass size distribution of BC had one mode peaking at a volume-equivalent diameter of 207 nm. In this study, the closure between particle hygroscopicity with diameters of 150, 250, and 350 nm and chemical composition was performed. The size range from 150-350 nm covered the peak of BC mass size distribution. As a result, the BC mass concentration for particles in diameter of 150, 250, and 350 nm should be higher than

that estimated with the assumption of uniformly distributed BC across the whole particle size range. This will be mentioned in the MS. However, due to the lack of BC size distribution measurements in our study, a sensitivity analysis cannot be given here.

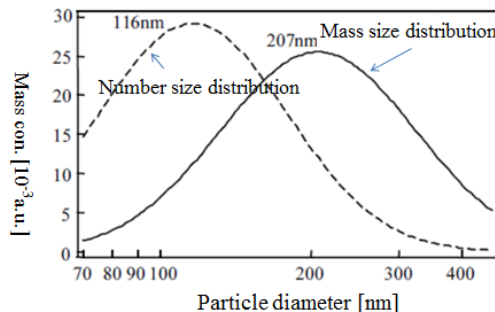


Figure: Average number size distribution and mass size distribution of BC in volume equivalent diameter (adopted from Sun et al. 2012b)

**Modifications in the MS:**

In section 4.3,

“Sun et al. (2012a) reported that the average mass size distribution of BC had one mode peaking at a volume-equivalent diameter of 207 nm in Beijing. The sizes of 150, 250, 350 nm covered the peak of BC mass size distribution. As a result, the BC mass concentration for particles in diameter of 150, 250, 350 nm should be higher than that estimated with the assumption of uniformly distributed BC across the whole particle size range.”

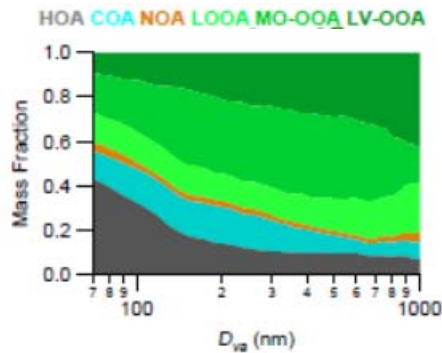
\*\*\*\*\*

Page 11507, lines 1–2

*Sun et al. (2012) have shown that this assumption is wrong since POA tends to be emitted at smaller sizes than the aerosol upon which SOA condense. Again, a sensitivity analysis could be used to estimate the uncertainties associated with this assumption if actual estimations cannot be made.*

**Response:**

Sun et al.’s (2012b) study showed a size-dependency of OA factors, as displayed in the following figure. The relative contribution of POA to OA decreased with increasing particle sizes, especially, for particles larger than 150 nm in vacuum aerodynamic diameter. In this study, the closure studies were performed for particles with mobility diameters of 150, 250, and 350 nm (larger than 200 nm in vacuum aerodynamic diameter). Using the relative contribution of POA to OA in the whole size range tends to overestimate percentage of POA for the size range focused in this study, thus, underestimate the  $\kappa$ . In our case, the POA/OA and SOA/OA are respectively 0.39 and 0.61. According to  $k_{org} = f_{POA} * k_{POA} + f_{SOA} * k_{SOA}$ , the  $\kappa_{org}$  can be calculated as 0.06 assuming  $\kappa_{SOA}=0.1$ . On the basis of Sun et al.’s study, the POA/OAs for 150, 250, and 350 nm particles are 0.30, 0.23, and 0.19, respectively. Using these ratios, the  $\kappa_{org}$ s are 0.07, 0.08, and 0.08, respectively, which are slightly higher than the one in our case. While, the differences can be ignored. These discussions will be added into the MS.



The mass fraction of OA factors as a function of size (adopted from Sun et al., 2012b).

**Modifications in the MS:**

One should note that Sun et al. (2012b) found that the contributions of POA and SOA to OA showed a size-dependency. The relative contribution of POA to OA significantly increased with decreasing particle sizes. In this study, the closure studies were performed for particles with mobility diameters of 150, 250, and 350 nm (larger than 200 nm in vacuum aerodynamic diameter). Using the relative contribution of POA to OA in PM<sub>1</sub> tends to overestimate percentage of POA for the size range focused in this study, thus underestimate the  $\kappa$ . In our case, the POA/OA and SOA/OA are respectively 0.39 and 0.61. According to equation [7], the  $\kappa_{org}$  can be calculated as 0.06 assuming  $\kappa_{SOA}=0.1$ . On the basis of Sun et al.’s study, the POA/OAs for 150, 250, and 350 nm particles are 0.30, 0.23, and 0.19, respectively. Using these ratios and equation [7], the calculated  $\kappa_{org}$ s are 0.07, 0.08, and 0.08, respectively, which are slightly higher than the one ( $\kappa_{org}=0.06$ ) in our case. This minor difference can be negligible.

\*\*\*\*\*

Page 11507, lines 15–20

*Have the authors ensured that the results are not unduly biased by restricting data to times when ammonium nitrate is below 20% and organics are greater than 50%? For example, this is likely reducing the number of night time data points included in the analysis, making the fit only representative for day time data points. A statement should be included in the text pointing this out.*

**Response:**

We made a statistics on the data points included in the analysis. The result showed that the data points for 6:00-18:00 and 18:00-6:00 (next day) are 160 and 204. The night time data points were more than daytime points. This is because that the organic mass fraction during the nighttime is higher than that during daytime. This will be mentioned in the MS.

**Modifications in the MS:**

“Restricting data to times when ammonium nitrate is below 20% and organics are greater than 50% may lead to a bias in data points between daytime and nighttime. The statistics showed that night time data points (204 data points) were more than those during daytime (160 data points). This is because that the organic mass fraction

during nighttime is higher than that during daytime. This bias could make the fit between  $\kappa_{\text{org}}$  and O:C ratio more representative for the nighttime situation than daytime.”

\*\*\*\*\*

Page 11507, lines 21–23

*Although it is mentioned later, it should be emphasized here that these studies were all performed under supersaturated conditions for CCN measurements.*

**Response:**

The studies base on the CCNc measurements were replaced by those on the basis of H-TDMA measurements.

**Modifications in the MS:**

Some empirical functions reported by other previous studies are also shown in Fig.8. In these previous studies (Wu et al., 2013;Jimenez et al., 2009;Rickards et al., 2013;Duplissy et al., 2011), the  $\kappa_{\text{org}}$  were derived from the measurements performed in the sub-saturation regime. In Massoli et al.’ study (2010) (not shown in the Fig. 8 due to the linear fitting based on HGF, not  $\kappa_{\text{org}}$ ), they reported a linear relationship ( $\text{HGF}_{90\%} = (0.58 \pm 0.15) \cdot \text{O:C} + (0.85 \pm 0.08)$ ) between  $\text{HGF}_{90\%}$  and O:C for the laboratory-generated SOA particles. Both results displayed in Fig. 8 and Massoli’s study showed a positive correlation between  $\kappa_{\text{org}}$  and O:C. Such positive correlation was also reported by those studies based on CCNc measurements, for examples, Chang et al. (2010) and Mei et al. (2013).

\*\*\*\*\*

Page 11508, lines 21–23

*“The water soluble fraction of 50 nm new particles is 42%.” Is this statement referring to the chemical composition, i.e. 42% of the particle is water soluble by mass? Or is it the number fraction of the hydrophilic mode? If the former, was this determined through Eq. 3? If the latter is this before the nucleation event? In any case, this should be clarified. These results are consistent with the findings of Shantz et al. (2012), and reference should be made to this work.*

**Response:**

The water soluble fraction is derived from:

$$\epsilon_{\text{soluble}} = \frac{\text{HGF}_{\text{measured}}^3 - 1}{\text{HGF}_{(\text{NH}_4)_2\text{SO}_4}^3 - 1}$$

It is particle volume-based method. Thus, the water soluble fraction is volume fraction, not mass or number fraction. This will be clarified in the MS.

In Shantz et al’s study (2012), they found that the 36 nm particles became increasingly CCN active within 1-4 h after the nucleation. It was hypothesized that the condensation of sulphate on these small particles enhanced their CCN activity. This article will be cited in the MS.

**Modifications in the MS:**

In section 2.2 “Then, the water-soluble volume fraction ( $\epsilon_{\text{soluble}}$ ) can be calculated by”  
In section 4.3 “Similar phenomenon was also observed by Shantz et al. (2012), which showed that the 36 nm particles became increasingly CCN active within 1-4 h after the nucleation. They hypothesized that the condensation of sulphate on these small

particles enhanced their CCN activity.”

\*\*\*\*\*

*Page 11508, line 6*

*The authors should include a discussion that compares their findings with other similar studies. This should detail the additional knowledge that their study contributes on top of the numerous other urban HTDMA studies that have previously been conducted.*

**Response:**

We cited more literature and made the comparisons with previous studies.

**Modifications in the MS:**

***In introduction:***

Currently, some studies have been performed to investigate the relationship between particle hygroscopicity and chemical composition based on both field measurements and laboratory experiments (Massoli et al., 2010;Wong et al., 2011;Lambe et al., 2011;Rickards et al., 2013;Moore et al., 2012;Suda et al., 2014;Paramonov et al., 2013;Levin et al., 2012). These works specially focused on parametrizing the empirical correlations between the atomic Oxygen:Carbon (O:C) ratio and organic hygroscopicity parameter  $\kappa$  derived from either hygroscopic growth factor (Wu et al., 2013;Rickards et al., 2013) or Cloud Condensation Nuclei (CCN) activity (Mei et al., 2013;Wong et al., 2011;Lambe et al., 2011;Chang et al., 2010). Typically, a linear parametrization of the correlation between  $\kappa$  and O:C was presented. Rickards et al. (2013) recently summarized the literature data and pointed out the systematic variability in parametrizations between organic  $\kappa$  and the O:C ratio determined from the different studies remains large. A recent work done by Suda et al. (2014) tested the influence of the number and location of molecular functional groups on the hygroscopicity of organic aerosols and may help us to find out the mechanisms of organics hygroscopicity from the chemistry point of view.

Over the past several decades, particle hygroscopicity measurements have been carried out world-wide, using the HTDMA technique. Atmospheric environments, in which those measurements were performed includes marine, Antarctic, boreal forest, rural, and urban areas. Swietlicki et al. (2008) and Kreidenweis and Asa-Awu (2014) compiled the existing observations on particle hygroscopic growth in the literature. Throughout these compilations, measurements of particle hygroscopicity have been rarely performed in China, which experiences frequently severe haze pollution episodes. These few particle hygroscopicity measurements using the HTDMA technique were deployed in Yangtze River Delta (Shanghai (Ye et al., 2013) and Hangzhou (Zhang et al., 2011)), Pearl River Delta (Xinken (Cheng et al., 2008) and Hong Kong (Lopez-Yglesias et al., 2014)) and North China Plain (Beijing (Massling et al., 2009;Meier et al., 2009), Yufa (Achtert et al., 2009), and Wuqing (Liu et al., 2011) ). Unfortunately, these measurements lack a linkage between particle hygroscopicity and chemical composition based on a high time resolution.

***In section 4.2:***

Fig. 5 (left) shows the size-dependent particle hygroscopicity parameters and

inorganic mass fraction of NR-PM<sub>1</sub> derived from averaging over the entire measuring period. The particle hygroscopicity increased with increasing particle size, displaying the same size-dependency with the mass fraction of inorganic composition in NR-PM<sub>1</sub>. This is because inorganics including ammonium sulfate and ammonium nitrate are major water-soluble chemical compounds in the atmospheric particles. Compared to inorganic components, the hygroscopicity parameter of organic aerosols were typically lower than 0.1 (Varutbangkul et al., 2006; Virkkula et al., 1999). The similar size-dependency of particle hygroscopicity was observed in various environments. For examples, Levin et al. (2012;2014) and Paramonov et al. (2013) reported that particle hygroscopicity increased with particle size at a forested site in Colorado and a boreal environment of southern Finland at the SMEAR station, respectively. Jurányi et al (2013) observed that particle hygroscopic growth increased with increasing dry diameter in the urban areas of Paris. Swietlicki et al. (2008) compiled worldwide H-TDMA data and found that the particle hgyroscopicity showed a pronounced size-dependency, with hygroscopicity increasing with particle diameter.

Over the entire study, the mean  $\kappa$ s of 50, 100, 150, 250, and 350 nm particles were  $0.16\pm 0.07$ ,  $0.19\pm 0.06$ ,  $0.22\pm 0.06$ ,  $0.26\pm 0.07$ , and  $0.28\pm 0.10$ , respectively over the entire sampling period. These values were similar to the hygroscopicity parameter  $\kappa = 0.12\text{--}0.27$  (measured at RH=90%) for 35–265 nm determined in the urban atmosphere of Paris (Jurányi et al., 2013). Yeung et al. (2014) observed that hygroscopicity  $\kappa$ s of particles with sizes of 75, 100, 150, and 200 nm were respectively 0.28, 0.29, 0.26, and 0.27 when Hong Kong experienced a continental airstream. In their study, the particle hygroscopicity showed no obvious size-dependency and was higher than our observation in Beijing. In contrast,  $\kappa$ s measured were relatively low at a forested site in Colorado ( $\kappa = 0.16\pm 0.08$  detected by CCNc), a boreal forest in Finland ( $\kappa = 0.18$  at RH=90%) (Sihto et al., 2011), and a tropical forest site in the Amazon ( $\kappa = 0.16\pm 0.06$  detected by CCNc) (Gunthe et al., 2009). At these forested locations, organic species were predominance in particles. Differently, in the atmosphere of Beijing, the inorganic fraction was relatively dominated, as shown in the Fig.3 (c).

### ***In section 4.3***

“Fig. 8 shows  $\kappa_{\text{org}}$  as a function of O:C ratio. From the degree of scatter point of view,  $\kappa_{\text{org}}$  is not correlated to the O:C ratio. Several previous studies reported the similar plots of  $\kappa_{\text{org}}$  values as a function of O:C ratios (Chang et al., 2010;Bhattu and Tripathi, 2015;Rickards et al., 2013). In order to derive an empirical relationship between  $\kappa_{\text{org}}$  and O:C ratios,  $\kappa_{\text{org}}$  values are usually binned by O:C in increments of 0.1. As displayed in Fig. 8, a linear fitting function ( $\kappa_{\text{org}}=(0.08\pm 0.02)*\text{O:C}+(0.02\pm 0.01)$ ) was obtained. Some empirical functions reported by other previous studies are also shown in Fig.8. In these previous studies (Wu et al., 2013;Jimenez et al., 2009;Rickards et al., 2013;Duplissy et al., 2011), the  $\kappa_{\text{org}}$  were derived from the measurements performed in the sub-saturation regime. In Massoli et al.’ study (2010) (not shown in the Fig. 8 due to the linear fitting based on HGF, not  $\kappa_{\text{org}}$ ), they reported a linear relationship ( $\text{HGF}_{90\%} = (0.58\pm 0.15)*\text{O:C} + (0.85$

$\pm 0.08$ )) between HGF90% and O:C for the laboratory-generated SOA particles. Both results displayed in Fig. 8 and Massoli's study showed a positive correlation between  $\kappa_{\text{org}}$  and O:C. Such positive correlation was also reported by those studies based on CCNc measurements, for examples, Chang et al. (2010) and Mei et al. (2013). We note that the slopes of the linear fitting varied with different studies, indicating there is no a simple parametrization to describe the relationship between organic hygroscopic and its oxidation state though the various atmospheric environments. Recently, Richards et al. (2013) had undertaken an extensive review of  $\kappa$  values published in the literature and showed that  $\kappa_{\text{org}}$  vs. O:C plot has a large degree of scatter. This indicates that other factors, such as phase state (Pajunoja et al., 2015) and molecular structures (Suda et al., 2014) of organic aerosols (OA) other than oxidation state may also play a role in the determination of the OA hygroscopicity. ”

\*\*\*\*\*

Page 11508, lines 26

*It is also possible that these are less hygroscopic primary aerosol that have coagulated to form larger particles.*

**Response:**

Typically, the primary particles are larger than newly formed particles. If the primary particles are pre-existing during the new particle formation events, the newly formed tiny particles will coagulate with these pre-existing particles. It is very clear that the newly formed particle continuously grew to around 50 nm before around 8:30p.m., as shown in Fig. 6. The GF-PDF shows an internal mixed state of new particles. This indicates that 50 nm particles mainly came from the new particle formation via growth, not primary particles before 8:30 p.m.. However, due to the measurements performed in urban atmosphere, the influence of primary particles cannot be excluded. Around 8:30pm, the fraction of the hydrophilic mode particles dropped to 0.6, and the hydrophobic mode appeared again. This is attributed to the intensive traffic emissions at the time of rush hour, which can clearly be seen from the particle number size distribution. More discussions will be added into the MS.

**Modifications in the MS:**

As displayed in Fig. 9 (b), the GF-PDF of 50 nm particles showed an internal mixed state, as marked by the black dashed lines. This indicates that 50 nm particles mainly came from the new particle formation via growth, not primary particles before 8:30 p.m.. Around 8:30 p.m., the fraction of the hydrophilic mode particles dropped to 0.6, and the hydrophobic mode appeared again. This is attributed to the intensive traffic emissions at the time of rush hour, which can clearly be seen from the particle number size distribution. We also note that the growth factor of hydrophilic mode particles decreased during nighttime.

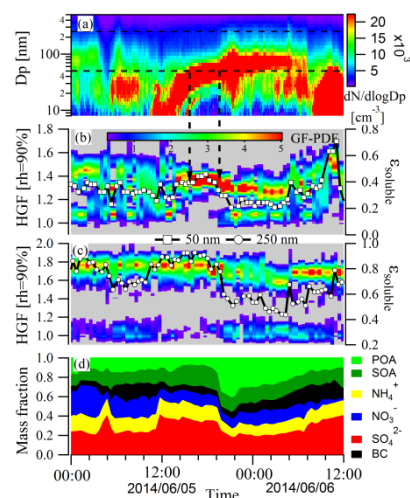


Figure 9: The variation in particle hygroscopicity, water soluble volume fraction, and



chemical composition of PM1 during the NPF event.

\*\*\*\*\*

Page 11509, lines 7–9

*This statement is confusing since 250 nm particles have a surface area that is larger than 100 nm particles but smaller than 350 nm particles. Are the authors referring to the surface area concentration?*

**Response:**

This statement is confusing and was removed from the MS.

\*\*\*\*\*

Page 11509, lines 11–15

*These results are very interesting although hard to interpret. It would be difficult to believe that the particles suddenly converted from externally- to completely internally mixed. Even if the hydrophobic-mode grew through condensation of soluble chemical compounds such as sulphate and ammonium, there would still be a contribution from the hydrophobic core. This would show up as an increase in HGF from 1.1 up to 1.8 until the soluble components eventually dominate the hygroscopic growth. Do the authors have any insight?*

**Response:**

The water soluble materials condensed onto the pre-existing particles. As a result, the particles converted to from external to internal state. As indicated in the following figure, this process took around 4 hours after the new particle formation started, not an instant change.

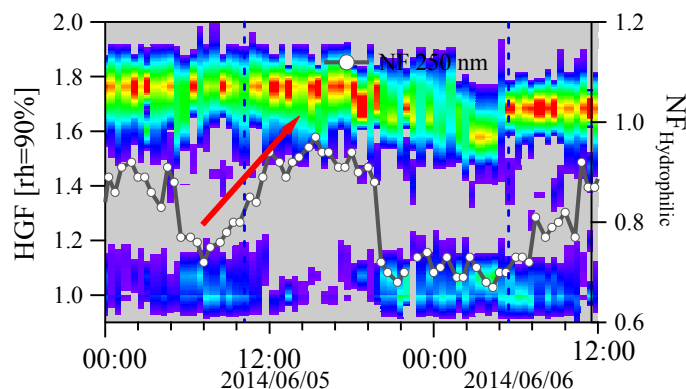


Figure: The variation in particle hygroscopicity during new particle formation event. HGF: hygroscopic growth factor,  $NF_{Hydrophilic}$ : number fraction of hydrophilic mode particle,  $VF_{soluble}$ : water soluble volume fraction.

\*\*\*\*\*

Page 11509, line 23

*Please include uncertainties associated with the listed \_ and the statistic used to represent these. This could be the 25th and 75th percentile or 1.5 times the interquartile distance or 1.95 times the standard deviation, etc.*

**Response:**

The mean values and standard deviation were given in the MS.

**Modification in the MS:**

“the mean hygroscopicity parameters ( $\kappa$ s) of 50, 100, 150, 200, and 250 nm particles

are respectively  $0.16\pm 0.07$ ,  $0.19\pm 0.06$ ,  $0.22\pm 0.06$ ,  $0.26\pm 0.07$ , and  $0.28\pm 0.10$ ”

\*\*\*\*\*

*Figure 2*

*Volume fraction would be a more appropriate right axis for the left figure.*

*Clarify the meaning of the whiskers on the right figure.*

**Response:**

This plot displays the size-dependency of particle hygroscopicity and its chemical composition. It is not used to make closure between  $\kappa$  and chemical compositions. Usage of mass fraction does not need to assume the densities of organic and inorganic fraction.

\*\*\*\*\*

*Figure 4*

*What is the RMSE of these fit?*

**Response:**

We calculated the RMSE of the linear fit in Fig.7. All the RMSEs are 0.04. The values were added into the caption of Fig. 7.

**Modification in the MS:**

“Figure 7:  $\kappa_{\text{HTDMA}}$  vs.  $\kappa_{\text{chem}}$  using size-resolved chemical composition data. All the root mean square errors (RMSE) of the linear fits are 0.04.”

\*\*\*\*\*

*Figure 5*

*All the data from the literature are from studies conducted at supersaturated conditions. HTDMA data, such as those included in Jimenez et al. (2009), would be more appropriate.*

**Response:**

This part was revised in the MS.

**Modification in the MS:**

Fig. 8 shows  $\kappa_{\text{org}}$  as a function of O:C ratio. From the degree of scatter point of view,  $\kappa_{\text{org}}$  is not correlated to the O:C ratio. Several previous studies reported the similar plots of  $\kappa_{\text{org}}$  values as a function of O:C ratios (Chang et al., 2010;Bhattu and Tripathi, 2015;Rickards et al., 2013). In order to derive an empirical relationship between  $\kappa_{\text{org}}$  and O:C ratios,  $\kappa_{\text{org}}$  values are usually binned by O:C in increments of 0.1. As displayed in Fig. 8, a linear fitting function ( $\kappa_{\text{org}}=(0.08\pm 0.02)*\text{O:C}+(0.02\pm 0.01)$ ) was obtained. Some empirical functions reported by other previous studies are also shown in Fig.8. In these previous studies (Wu et al., 2013;Jimenez et al., 2009;Rickards et al., 2013;Duplissy et al., 2011), the  $\kappa_{\text{org}}$  were derived from the measurements performed in the sub-saturation regime. In Massoli et al.’ study (2010) (not shown in the Fig. 8 due to the linear fitting based on HGF, not  $\kappa_{\text{org}}$ ), they reported a linear relationship ( $\text{HGF}_{90\%} = (0.58\pm 0.15)*\text{O:C} + (0.85 \pm 0.08)$ ) between  $\text{HGF}_{90\%}$  and O:C for the laboratory-generated SOA particles. Both results displayed in Fig. 8 and Massoli’s study showed a positive correlation between  $\kappa_{\text{org}}$  and O:C. Such positive correlation was also reported by those studies based on CCNc measurements, for examples, Chang et al. (2010) and Mei et al. (2013). We note that the slopes of the linear fitting varied with different studies, indicating there

is not a simple parametrization to describe the relationship between organic hygroscopic and its oxidation state through the various atmospheric environments. Recently, Richards et al. (2013) had undertaken an extensive review of  $\kappa_{\text{org}}$  values published in the literature and showed that  $\kappa_{\text{org}}$  vs. O:C plot has a large degree of scatter. This indicates that other factors, such as phase state (Pajunoja et al., 2015) and molecular structures (Suda et al., 2014) of organic aerosols (OA) other than oxidation state may also play a role in the determination of the OA hygroscopicity.

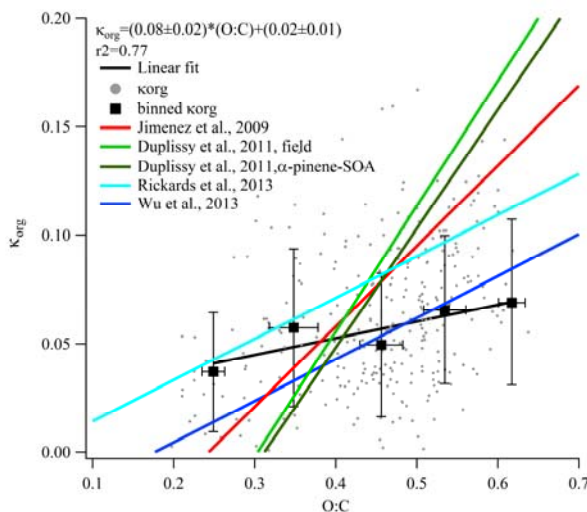


Figure 8: The relationship between organic hygroscopicity parameter ( $\kappa_{\text{org}}$ ) and oxygen to carbon ratio (O: C).

\*\*\*\*\*

**Technical corrections**

*As mentioned in the general comments, there are numerous grammatical errors in the manuscript which should be corrected before the article is resubmitted.*

**Response:**

We improved the English before resubmission.

*Page 11499, line 7*

*This should be “mass spectrometric”.*

**Response:**

It was corrected in the MS.

*Page 11500, lines 17, 18, 20*

*Ammonium sulphate in the subscript is incorrect.*

**Response:**

It was corrected in the MS.

*Page 11508, line 17*

*The time in the figure would suggest 9.50a.m.*

**Response:**

It was corrected in the MS.

*Page 11508, line 28*

*This should be “the hydrophobic mode appeared again”.*

**Response:** It was corrected in the MS.

## References

- Achtert, P., Birmili, W., Nowak, A., Wehner, B., Wiedensohler, A., Takegawa, N., Kondo, Y., Miyazaki, Y., Hu, M., and Zhu, T.: Hygroscopic growth of tropospheric particle number size distributions over the North China Plain, *Journal of Geophysical Research: Atmospheres*, 114, n/a-n/a, 10.1029/2008JD010921, 2009.
- Bhattu, D., and Tripathi, S. N.: CCN closure study: Effects of aerosol chemical composition and mixing state, *Journal of Geophysical Research: Atmospheres*, 120, 2014JD021978, 10.1002/2014JD021978, 2015.
- Chang, R. Y. W., Slowik, J. G., Shantz, N. C., Vlasenko, A., Liggio, J., Sjostedt, S. J., Leaitch, W. R., and Abbatt, J. P. D.: The hygroscopicity parameter ( $\kappa$ ) of ambient organic aerosol at a field site subject to biogenic and anthropogenic influences: relationship to degree of aerosol oxidation, *Atmos. Chem. Phys.*, 10, 5047-5064, 10.5194/acp-10-5047-2010, 2010.
- Cheng, Y. F., Wiedensohler, A., Eichler, H., Heintzenberg, J., Tesche, M., Ansmann, A., Wendisch, M., Su, H., Althausen, D., Herrmann, H., Gnauk, T., Brüggemann, E., Hu, M., and Zhang, Y. H.: Relative humidity dependence of aerosol optical properties and direct radiative forcing in the surface boundary layer at Xinken in Pearl River Delta of China: An observation based numerical study, *Atmospheric Environment*, 42, 6373-6397, <http://dx.doi.org/10.1016/j.atmosenv.2008.04.009>, 2008.
- Duplissy, J., DeCarlo, P. F., Dommen, J., Alfarra, M. R., Metzger, A., Barmpadimos, I., Prevot, A. S. H., Weingartner, E., Tritscher, T., Gysel, M., Aiken, A. C., Jimenez, J. L., Canagaratna, M. R., Worsnop, D. R., Collins, D. R., Tomlinson, J., and Baltensperger, U.: Relating hygroscopicity and composition of organic aerosol particulate matter, *Atmos. Chem. Phys.*, 11, 1155-1165, 10.5194/acp-11-1155-2011, 2011.
- Gunthe, S. S., King, S. M., Rose, D., Chen, Q., Roldin, P., Farmer, D. K., Jimenez, J. L., Artaxo, P., Andreae, M. O., Martin, S. T., and Pöschl, U.: Cloud condensation nuclei in pristine tropical rainforest air of Amazonia: size-resolved measurements and modeling of atmospheric aerosol composition and CCN activity, *Atmos. Chem. Phys.*, 9, 7551-7575, 10.5194/acp-9-7551-2009, 2009.
- Gysel, M., Crosier, J., Topping, D. O., Whitehead, J. D., Bower, K. N., Cubison, M. J., Williams, P. I., Flynn, M. J., McFiggans, G. B., and Coe, H.: Closure study between chemical composition and hygroscopic growth of aerosol particles during TORCH2, *Atmos. Chem. Phys.*, 7, 6131-6144, 10.5194/acp-7-6131-2007, 2007.
- Jimenez, J. L., Canagaratna, M. R., Donahue, N. M., Prevot, A. S. H., Zhang, Q., Kroll, J. H., DeCarlo, P. F., Allan, J. D., Coe, H., Ng, N. L., Aiken, A. C., Docherty, K. S., Ulbrich, I. M., Grieshop, A. P., Robinson, A. L., Duplissy, J., Smith, J. D., Wilson, K. R., Lanz, V. A., Hueglin, C., Sun, Y. L., Tian, J., Laaksonen, A., Raatikainen, T., Rautiainen, J., Vaattovaara, P., Ehn, M., Kulmala, M., Tomlinson, J. M., Collins, D. R., Cubison, M. J., E, Dunlea, J., Huffman, J. A., Onasch, T. B., Alfarra, M. R., Williams, P. I., Bower, K., Kondo, Y., Schneider, J., Drewnick, F., Borrmann, S., Weimer, S., Demerjian, K., Salcedo, D., Cottrell, L., Griffin, R., Takami, A., Miyoshi, T., Hatakeyama, S., Shimojo, A., Sun, J. Y., Zhang, Y. M., Dzepina, K., Kimmel, J. R., Sueper, D., Jayne, J. T., Herndon, S. C., Trimborn, A. M., Williams, L. R., Wood, E. C., Middlebrook, A. M., Kolb, C. E., Baltensperger, U., and Worsnop, D. R.: Evolution of organic aerosols in the atmosphere, *Science*, 326, 1525-1529, 10.1126/science.1180353, 2009.
- Jurányi, Z., Tritscher, T., Gysel, M., Laborde, M., Gomes, L., Roberts, G., Baltensperger, U., and Weingartner, E.: Hygroscopic mixing state of urban aerosol derived from size-resolved cloud

condensation nuclei measurements during the MEGAPOLI campaign in Paris, *Atmos. Chem. Phys.*, 13, 6431-6446, 10.5194/acp-13-6431-2013, 2013.

Kammermann, L., Gysel, M., Weingartner, E., and Baltensperger, U.: 13-month climatology of the aerosol hygroscopicity at the free tropospheric site Jungfraujoch (3580 m a.s.l.), *Atmos. Chem. Phys.*, 10, 10717-10732, 10.5194/acp-10-10717-2010, 2010.

Kreidenweis, S. M., and Asa-Awuku, A.: 5.13 - Aerosol Hygroscopicity: Particle Water Content and Its Role in Atmospheric Processes, in: *Treatise on Geochemistry (Second Edition)*, edited by: Turekian, H. D. H. K., Elsevier, Oxford, 331-361, 2014.

Lambe, A. T., Onasch, T. B., Massoli, P., Croasdale, D. R., Wright, J. P., Ahern, A. T., Williams, L. R., Worsnop, D. R., Brune, W. H., and Davidovits, P.: Laboratory studies of the chemical composition and cloud condensation nuclei (CCN) activity of secondary organic aerosol (SOA) and oxidized primary organic aerosol (OPOA), *Atmos. Chem. Phys.*, 11, 8913-8928, 10.5194/acp-11-8913-2011, 2011.

Lanz, V. A., Alfara, M. R., Baltensperger, U., Buchmann, B., Hueglin, C., and Prévôt, A. S. H.: Source apportionment of submicron organic aerosols at an urban site by factor analytical modelling of aerosol mass spectra, *Atmos. Chem. Phys.*, 7, 1503-1522, 10.5194/acp-7-1503-2007, 2007.

Levin, E. J. T., Prenni, A. J., Petters, M. D., Kreidenweis, S. M., Sullivan, R. C., Atwood, S. A., Ortega, J., DeMott, P. J., and Smith, J. N.: An annual cycle of size-resolved aerosol hygroscopicity at a forested site in Colorado, *J. Geophys. Res.*, 117, D06201, 10.1029/2011jd016854, 2012.

Levin, E. J. T., Prenni, A. J., Palm, B. B., Day, D. A., Campuzano-Jost, P., Winkler, P. M., Kreidenweis, S. M., DeMott, P. J., Jimenez, J. L., and Smith, J. N.: Size-resolved aerosol composition and its link to hygroscopicity at a forested site in Colorado, *Atmos. Chem. Phys.*, 14, 2657-2667, 10.5194/acp-14-2657-2014, 2014.

Liu, P. F., Zhao, C. S., Göbel, T., Hallbauer, E., Nowak, A., Ran, L., Xu, W. Y., Deng, Z. Z., Ma, N., Mildener, K., Henning, S., Stratmann, F., and Wiedensohler, A.: Hygroscopic properties of aerosol particles at high relative humidity and their diurnal variations in the North China Plain, *Atmos. Chem. Phys.*, 11, 3479-3494, 10.5194/acp-11-3479-2011, 2011.

Lopez-Yglesias, X. F., Yeung, M. C., Dey, S. E., Brechtel, F. J., and Chan, C. K.: Performance Evaluation of the Brechtel Mfg. Humidified Tandem Differential Mobility Analyzer (BMI HTDMA) for Studying Hygroscopic Properties of Aerosol Particles, *Aerosol Science and Technology*, 48, 969-980, 10.1080/02786826.2014.952366, 2014.

Massling, A., Stock, M., Wehner, B., Wu, Z. J., Hu, M., Brüggemann, E., Gnauk, T., Herrmann, H., and Wiedensohler, A.: Size segregated water uptake of the urban submicrometer aerosol in Beijing, *Atmospheric Environment*, 43, 1578-1589, <http://dx.doi.org/10.1016/j.atmosenv.2008.06.003>, 2009.

Massoli, P., Lambe, A. T., Ahern, A. T., Williams, L. R., Ehn, M., Mikkilä, J., Canagaratna, M. R., Brune, W. H., Onasch, T. B., Jayne, J. T., Petäjä, T., Kulmala, M., Laaksonen, A., Kolb, C. E., Davidovits, P., and Worsnop, D. R.: Relationship between aerosol oxidation level and hygroscopic properties of laboratory generated secondary organic aerosol (SOA) particles, *Geophysical Research Letters*, 37, n/a-n/a, 10.1029/2010GL045258, 2010.

Mei, F., Hayes, P. L., Ortega, A., Taylor, J. W., Allan, J. D., Gilman, J., Kuster, W., de Gouw, J., Jimenez, J. L., and Wang, J.: Droplet activation properties of organic aerosols observed at an urban site during CalNex-LA, *Journal of Geophysical Research: Atmospheres*, 118, 2903-2917, 10.1002/jgrd.50285, 2013.

Meier, J., Wehner, B., Massling, A., Birmili, W., Nowak, A., Gnauk, T., Brüggemann, E., Herrmann, H., Min, H., and Wiedensohler, A.: Hygroscopic growth of urban aerosol particles in Beijing (China)

during wintertime: a comparison of three experimental methods, *Atmos. Chem. Phys.*, 9, 6865-6880, 10.5194/acp-9-6865-2009, 2009.

Moore, R. H., Raatikainen, T., Langridge, J. M., Bahreini, R., Brock, C. A., Holloway, J. S., Lack, D. A., Middlebrook, A. M., Perring, A. E., Schwarz, J. P., Spackman, J. R., and Nenes, A.: CCN Spectra, Hygroscopicity, and Droplet Activation Kinetics of Secondary Organic Aerosol Resulting from the 2010 Deepwater Horizon Oil Spill, *Environmental Science & Technology*, 46, 3093-3100, 10.1021/es203362w, 2012.

Pajunoja, A., Lambe, A. T., Hakala, J., Rastak, N., Cummings, M. J., Brogan, J. F., Hao, L., Paramonov, M., Hong, J., Prisle, N. L., Malila, J., Romakkaniemi, S., Lehtinen, K. E. J., Laaksonen, A., Kulmala, M., Massoli, P., Onasch, T. B., Donahue, N. M., Riipinen, I., Davidovits, P., Worsnop, D. R., Petäjä, T., and Virtanen, A.: Adsorptive uptake of water by semisolid secondary organic aerosols, *Geophysical Research Letters*, 42, 3063-3068, 10.1002/2015GL063142, 2015.

Paramonov, M., Aalto, P. P., Asmi, A., Prisle, N., Kerminen, V. M., Kulmala, M., and Petäjä, T.: The analysis of size-segregated cloud condensation nuclei counter (CCNC) data and its implications for cloud droplet activation, *Atmos. Chem. Phys.*, 13, 10285-10301, 10.5194/acp-13-10285-2013, 2013.

Rickards, A. M. J., Miles, R. E. H., Davies, J. F., Marshall, F. H., and Reid, J. P.: Measurements of the Sensitivity of Aerosol Hygroscopicity and the  $\kappa$  Parameter to the O/C Ratio, *The Journal of Physical Chemistry A*, 117, 14120-14131, 10.1021/jp407991n, 2013.

Shantz, N. C., Pierce, J. R., Chang, R. Y. W., Vlasenko, A., Riipinen, I., Sjostedt, S., Slowik, J. G., Wiebe, A., Liggio, J., Abbatt, J. P. D., and Leaitch, W. R.: Cloud condensation nuclei droplet growth kinetics of ultrafine particles during anthropogenic nucleation events, *Atmospheric Environment*, 47, 389-398, <http://dx.doi.org/10.1016/j.atmosenv.2011.10.049>, 2012.

Sihto, S. L., Mikkilä, J., Vanhanen, J., Ehn, M., Liao, L., Lehtipalo, K., Aalto, P. P., Duplissy, J., Petäjä, T., Kerminen, V. M., Boy, M., and Kulmala, M.: Seasonal variation of CCN concentrations and aerosol activation properties in boreal forest, *Atmos. Chem. Phys.*, 11, 13269-13285, 10.5194/acp-11-13269-2011, 2011.

Suda, S. R., Petters, M. D., Yeh, G. K., Strollo, C., Matsunaga, A., Faulhaber, A., Ziemann, P. J., Prenni, A. J., Carrico, C. M., Sullivan, R. C., and Kreidenweis, S. M.: Influence of Functional Groups on Organic Aerosol Cloud Condensation Nucleus Activity, *Environmental Science & Technology*, 48, 10182-10190, 10.1021/es502147y, 2014.

Sun, T. L., He, L. Y., Zeng, L. W., and Huang, X. F.: Black carbon measurement during Beijing Paralympic Games, *China Environmental Science*, 32, 2123-2127, 2012a.

Sun, Y. L., Zhang, Q., Schwab, J. J., Yang, T., Ng, N. L., and Demerjian, K. L.: Factor analysis of combined organic and inorganic aerosol mass spectra from high resolution aerosol mass spectrometer measurements, *Atmos. Chem. Phys.*, 12, 8537-8551, 10.5194/acp-12-8537-2012, 2012b.

Swietlicki, E., Hansson, H. C., HäMeri, K., Svenningsson, B., Massling, A., McFiggans, G., McMurry, P. H., Petäjä, T., Tunved, P., Gysel, M., Topping, D., Weingartner, E., Baltensperger, U., Rissler, J., Wiedensohler, A., and Kulmala, M.: Hygroscopic properties of submicrometer atmospheric aerosol particles measured with H-TDMA instruments in various environments—a review, *Tellus B*, 60, 432-469, 10.1111/j.1600-0889.2008.00350.x, 2008.

Varutbangkul, V., Brechtel, F. J., Bahreini, R., Ng, N. L., Keywood, M. D., Kroll, J. H., Flagan, R. C., Seinfeld, J. H., Lee, A., and Goldstein, A. H.: Hygroscopicity of secondary organic aerosols formed by oxidation of cycloalkenes, monoterpenes, sesquiterpenes, and related compounds, *Atmos. Chem. Phys.*, 6, 2367-2388, 10.5194/acp-6-2367-2006, 2006.

Virkkula, A., Van Dingenen, R., Raes, F., and Hjorth, J.: Hygroscopic properties of aerosol formed by oxidation of limonene,  $\alpha$ -pinene, and  $\beta$ -pinene, *J. Geophys. Res.*, 104, 3569-3579, 10.1029/1998jd100017, 1999.

Wong, J. P. S., Lee, A. K. Y., Slowik, J. G., Cziczo, D. J., Leaitch, W. R., Macdonald, A., and Abbatt, J. P. D.: Oxidation of ambient biogenic secondary organic aerosol by hydroxyl radicals: Effects on cloud condensation nuclei activity, *Geophysical Research Letters*, 38, n/a-n/a, 10.1029/2011GL049351, 2011.

Wu, Z. J., Poulain, L., Henning, S., Dieckmann, K., Birmili, W., Merkel, M., van Pinxteren, D., Spindler, G., Mueller, K., Stratmann, F., Herrmann, H., and Wiedensohler, A.: Relating particle hygroscopicity and CCN activity to chemical composition during the HCCT-2010 field campaign, *Atmospheric Chemistry and Physics*, 13, 7983-7996, 10.5194/acp-13-7983-2013, 2013.

Ye, X., Tang, C., Yin, Z., Chen, J., Ma, Z., Kong, L., Yang, X., Gao, W., and Geng, F.: Hygroscopic growth of urban aerosol particles during the 2009 Mirage-Shanghai Campaign, *Atmospheric Environment*, 64, 263-269, <http://dx.doi.org/10.1016/j.atmosenv.2012.09.064>, 2013.

Yeung, M. C., Lee, B. P., Li, Y. J., and Chan, C. K.: Simultaneous HTDMA and HR-ToF-AMS measurements at the HKUST Supersite in Hong Kong in 2011, *Journal of Geophysical Research: Atmospheres*, 119, 9864-9883, 10.1002/2013JD021146, 2014.

Zhang, J., Wang, L., Chen, J., Feng, S., Shen, J., and Jiao, L.: Hygroscopicity of ambient submicron particles in urban Hangzhou, China, *Front. Environ. Sci. Eng. China*, 5, 342-347, 10.1007/s11783-011-0358-7, 2011.

Wu et al. conducted a set of ambient measurements from which they calculated size dependent hygroscopic growth factors (HGF) of aerosols in Beijing. Two primary results are reported. First, the hygroscopicity parameter calculated from HGF ( $\kappa$ HGF) increases with increasing particle diameter. Second,  $\kappa$ HGF of the organic aerosol fraction is correlated with the corresponding oxygen-to-carbon (O/C) ratio that is used as a surrogate for the aerosol oxidation level. The authors hypothesize that the increase in  $\kappa$ HGF with increasing particle diameter is associated with condensational aging processes that increase the hydrophilic fraction of the aerosol. New particle formation events are found to be responsible for aerosols with higher  $\kappa$ HGF. Overall, this manuscript addresses an important research topic regarding the influence of particle composition on hygroscopic properties. It extends previous laboratory and field studies with related measurements in an area that is subject to severe pollution problems. I would support publication in ACP after consideration of the following comments.

\*\*\*\*\*

We greatly thank to the referee to review this manuscript and provide many constructive suggestions. We modified the MS point by point.

\*\*\*\*\*

#### COMMENTS

1. P11497, L25: Several other studies have investigated the relationship between hygroscopicity and chemical composition of laboratory and ambient organic aerosols, including but not limited to: Massoli et al. (2010), Wong et al. (2011), Lambe et al. (2011), Moore et al. (2012a), Rickards et al. (2013), and Suda et al. (2014). None are referenced or discussed in this manuscript. In particular, Massoli et al. and Rickards et al. characterize water uptake under subsaturated conditions as is done in this work, and Suda et al. characterize functional-group-dependent trends in aerosol hygroscopicity at a specific O/C ratio. The introduction should be expanded to include discussion of prior work that is relevant to the current manuscript.

#### **Response:**

Thanks for this suggestion. We strengthened the comparisons and citation of the previous studies.

#### **Modifications in the MS:**

##### ***In introduction:***

Currently, some studies have been performed to investigate the relationship between particle hygroscopicity and chemical composition based on both field measurements and laboratory experiments (Massoli et al., 2010; Wong et al., 2011; Lambe et al., 2011; Rickards et al., 2013; Moore et al., 2012; Suda et al., 2014; Paramonov et al., 2013; Levin et al., 2012). These works specially focused on parametrizing the empirical correlations between the atomic Oxygen:Carbon (O:C) ratio and organic hygroscopicity parameter  $\kappa$  derived from either hygroscopic growth factor (Wu et al., 2013; Rickards et al., 2013) or Cloud Condensation Nuclei (CCN) activity (Mei et al., 2013; Wong et al., 2011; Lambe et al., 2011; Chang et al., 2010). Typically, a linear parametrization of the correlation between  $\kappa$  and O:C was presented. Rickards et al. (2013) recently summarized the literature data and pointed



out the systematic variability in parametrizations between organic  $\kappa$  and the O:C ratio determined from the different studies remains large. A recent work done by Suda et al. (2014) tested the influence of the number and location of molecular functional groups on the hygroscopicity of organic aerosols and may help us to find out the mechanisms of organics hygroscopicity from the chemistry point of view.

Over the past several decades, particle hygroscopicity measurements have been carried out world-wide, using the HTDMA technique. Atmospheric environments, in which those measurements were performed includes marine, Antarctic, boreal forest, rural, and urban areas. Swietlicki et al. (2008) and Kreidenweis and Asa-Awu (2014) compiled the existing observations on particle hygroscopic growth in the literature. Throughout these compilations, measurements of particle hygroscopicity have been rarely performed in China, which experiences frequently severe haze pollution episodes. These few particle hygroscopicity measurements using the HTDMA technique were deployed in Yangtze River Delta (Shanghai (Ye et al., 2013) and Hangzhou (Zhang et al., 2011)), Pearl River Delta (Xinken (Cheng et al., 2008) and Hong Kong (Lopez-Yglesias et al., 2014)) and North China Plain (Beijing (Massling et al., 2009; Meier et al., 2009), Yufa (Achtert et al., 2009), and Wuqing (Liu et al., 2011) ). Unfortunately, these measurements lack a linkage between particle hygroscopicity and chemical composition based on a high time resolution.

#### ***In section 4.2:***

Fig. 5 (left) shows the size-dependent particle hygroscopicity parameters and inorganic mass fraction of NR-PM<sub>1</sub> derived from averaging over the entire measuring period. The particle hygroscopicity increased with increasing particle size, displaying the same size-dependency with the mass fraction of inorganic composition in NR-PM<sub>1</sub>. This is because inorganics including ammonium sulfate and ammonium nitrate are major water-soluble chemical compounds in the atmospheric particles. Compared to inorganic components, the hygroscopicity parameter of organic aerosols were typically lower than 0.1 (Varutbangkul et al., 2006; Virkkula et al., 1999). The similar size-dependency of particle hygroscopicity was observed in various environments. For examples, Levin et al. (2012;2014) and Paramonov et al. (2013) reported that particle hygroscopicity increased with particle size at a forested site in Colorado and a boreal environment of southern Finland at the SMEAR station, respectively. Jurányi et al (2013) observed that particle hygroscopic growth increased with increasing dry diameter in the urban areas of Paris. Swietlicki et al. (2008) compiled worldwide H-TDMA data and found that the particle hgyroscopicity showed a pronounced size-dependency, with hygroscopicity increasing with particle diameter.

Over the entire study, the mean  $\kappa$ s of 50, 100, 150, 250, and 350 nm particles were  $0.16 \pm 0.07$ ,  $0.19 \pm 0.06$ ,  $0.22 \pm 0.06$ ,  $0.26 \pm 0.07$ , and  $0.28 \pm 0.10$ , respectively over the entire sampling period. These values were similar to the hygroscopicity parameter  $\kappa = 0.12$ - $0.27$  (measured at RH=90%) for 35–265 nm determined in the urban atmosphere of Paris (Jurányi et al., 2013). Yeung et al. (2014) observed that hygroscopicity  $\kappa$ s of particles with sizes of 75, 100, 150, and 200 nm were respectively 0.28, 0.29, 0.26,

and 0.27 when Hong Kong experienced a continental airstream. In their study, the particle hygroscopicity showed no obvious size-dependency and was higher than our observation in Beijing. In contrast,  $\kappa_s$  measured were relatively low at a forested site in Colorado ( $\kappa = 0.16 \pm 0.08$  detected by CCNc), a boreal forest in Finland ( $\kappa = 0.18$  at RH=90%) (Sihto et al., 2011), and a tropical forest site in the Amazon ( $\kappa = 0.16 \pm 0.06$  detected by CCNc) (Gunthe et al., 2009). At these forested locations, organic species were predominance in particles. Differently, in the atmosphere of Beijing, the inorganic fraction was relatively dominated, as shown in the Fig.3 (c).

### ***In section 4.3***

“Fig. 8 shows  $\kappa_{org}$  as a function of O:C ratio. From the degree of scatter point of view,  $\kappa_{org}$  is not correlated to the O:C ratio. Several previous studies reported the similar plots of  $\kappa_{org}$  values as a function of O:C ratios (Chang et al., 2010;Bhattu and Tripathi, 2015;Rickards et al., 2013). In order to derive an empirical relationship between  $\kappa_{org}$  and O:C ratios,  $\kappa_{org}$  values are usually binned by O:C in increments of 0.1. As displayed in Fig. 8, a linear fitting function ( $\kappa_{org} = (0.08 \pm 0.02) * O:C + (0.02 \pm 0.01)$ ) was obtained. Some empirical functions reported by other previous studies are also shown in Fig.8. In these previous studies (Wu et al., 2013;Jimenez et al., 2009;Rickards et al., 2013;Duplissy et al., 2011), the  $\kappa_{org}$  were derived from the measurements performed in the sub-saturation regime. In Massoli et al.’ study (2010) (not shown in the Fig. 8 due to the linear fitting based on HGF, not  $\kappa_{org}$ ), they reported a linear relationship ( $HGF_{90\%} = (0.58 \pm 0.15) * O:C + (0.85 \pm 0.08)$ ) between HGF90% and O:C for the laboratory-generated SOA particles. Both results displayed in Fig. 8 and Massoli’s study showed a positive correlation between  $\kappa_{org}$  and O:C. Such positive correlation was also reported by those studies based on CCNc measurements, for examples, Chang et al. (2010) and Mei et al. (2013). We note that the slopes of the linear fitting varied with different studies, indicating there is no a simple parametrization to describe the relationship between organic hygroscopic and its oxidation state though the various atmospheric environments. Recently, Richards et al. (2013) had undertaken an extensive review of  $\kappa$  values published in the literature and showed that  $\kappa_{org}$  vs. O:C plot has a large degree of scatter. This indicates that other factors, such as phase state (Pajunoja et al., 2015) and molecular structures (Suda et al., 2014) of organic aerosols (OA) other than oxidation state may also play a role in the determination of the OA hygroscopicity. ”

\*\*\*\*\*

2. In the abstract, the authors report median  $\kappa_{HGF}$  values ranging from 0.15 to 0.29; these values should be cited somewhere in Section 4.1 because as far as I can tell they are not mentioned anywhere except the abstract.

### **Response:**

The statistics of  $\kappa_s$  was given in the texts.

### **Modification in the MS:**

In the section 4.2: “Over the entire study, the mean  $\kappa_s$  of 50, 100, 150, 250, and 350 nm particles were  $0.16 \pm 0.07$ ,  $0.19 \pm 0.06$ ,  $0.22 \pm 0.06$ ,  $0.26 \pm 0.07$ , and  $0.28 \pm 0.10$ , respectively over the entire sampling period. These values were similar to the

hygroscopicity parameter  $\kappa = 0.12-0.27$  (measured at RH=90%) for 35–265 nm determined in the urban atmosphere of Paris (Jurányi et al., 2013). Yeung et al. (2014) observed that hygroscopicity  $\kappa$ s of particles with sizes of 75, 100, 150, and 200 nm were respectively 0.28, 0.29, 0.26, and 0.27 when Hong Kong experienced a continental airstream. In their study, the particle hygroscopicity showed no obvious size-dependency and was higher than our observation in Beijing. In contrast,  $\kappa$ s measured were relatively low at a forested site in Colorado ( $\kappa = 0.16 \pm 0.08$  detected by CCNc), a boreal forest in Finland ( $\kappa = 0.18$  at RH=90%) (Sihto et al., 2011), and a tropical forest site in the Amazon ( $\kappa = 0.16 \pm 0.06$  detected by CCNc) (Gunthe et al., 2009). At these forested locations, organic species were predominance in particles. Differently, in the atmosphere of Beijing, the inorganic fraction was relatively dominated, as shown in the Fig.3 (c).”

\*\*\*\*\*

3. I think it would be useful to compare results that are presented in Figure 2 with related measurements such as those presented in Moore et al. (2012b). This comparison could help to generalize the observations detailed in this work. Further, it would aid in the interpretation of other field measurements where chemical composition data may not be available.

**Response:**

Moore (2012)’s work was cited in the Introduction. Due to their study was performed at a supersaturation regime, not sub-saturated condition, the comparisons of size-dependency of particle hygroscopicity did not include Moore et al.’s study.

**Modification in the MS:**

Fig. 5 (left) shows the size-dependent particle hygroscopicity parameters and inorganic mass fraction of NR-PM<sub>1</sub> derived from averaging over the entire measuring period. The particle hygroscopicity increased with increasing particle size, displaying the same size-dependency with the mass fraction of inorganic composition in NR-PM<sub>1</sub>. This is because inorganics including ammonium sulfate and ammonium nitrate are major water-soluble chemical compounds in the atmospheric particles. Compared to inorganic components, the hygroscopicity parameter of organic aerosols are typically lower than 0.1 (Varutbangkul et al., 2006; Virkkula et al., 1999). The similar size-dependency of particle hygroscopicity was observed in various environments. For examples, Levin et al. (2012;2014) and Paramonov et al. (2013) reported that particle hygroscopicity increased with particle size at a forested site in Colorado and a boreal environment of southern Finland at the SMEAR station, respectively. Jurányi et al (2013) observed that particle hygroscopic growth increased with increasing dry diameter in the urban areas of Paris. Swietlicki et al. (2008) compiled worldwide H-TDMA data and found that the particle hgyroscopicity showed a pronounced size-dependency, with hygroscopicity increasing with particle diameter.

\*\*\*\*\*

4. P11505, L3-5: The growth factor probability distribution function is an important result. In my opinion the campaign average GF-PDF should be shown as a figure. It might also be interesting to contrast multiple GF-PDF’s during events that are dominated by specific sources or aging processes.

**Response:**

The GF-PDF during the entire sampling period was plotted and added into the MS. The analysis was also added into the MS.

**Modification in the MS:**

Fig. 3 (b) displays the time series of hygroscopicity parameters for 50 nm ( $\kappa_{50\text{nm}}$ ) and 250 nm ( $\kappa_{250\text{nm}}$ ) particles. Both  $\kappa_{50\text{nm}}$  and  $\kappa_{250\text{nm}}$  had an obvious temporal variability. Their variations were similar to that of inorganic mass fraction in NR-PM<sub>1</sub> displayed in Fig. 3 (c). An in-depth analysis of the relationship between particle hygroscopicity and chemical composition will be given in section 4.3. Fig. 4 gives an overview of growth factor probability density distributions (GF-PDF) for 50 and 250 nm particles during the entire field campaign. The GF-PDFs of both 50 and 250 nm showed two distinct modes, which are identified as hydrophobic mode (GF<1.2) and hydrophilic mode (GF>1.2). This implied that the particles were usually externally mixed. The hydrophilic mode of 250 nm particles is more prominent most of the time. Differently, the hydrophobic mode was dominated in 50 nm particles. As marked in the Fig. 4 (a) by the square with dashed line, the hydrophobic mode disappeared occasionally, indicating that the vast majority of particles in this size range can be fully hygroscopic. This phenomenon took place during the NPF events. A case study of particle hygroscopic behavior during new particle formation events will be given in section 4.4.

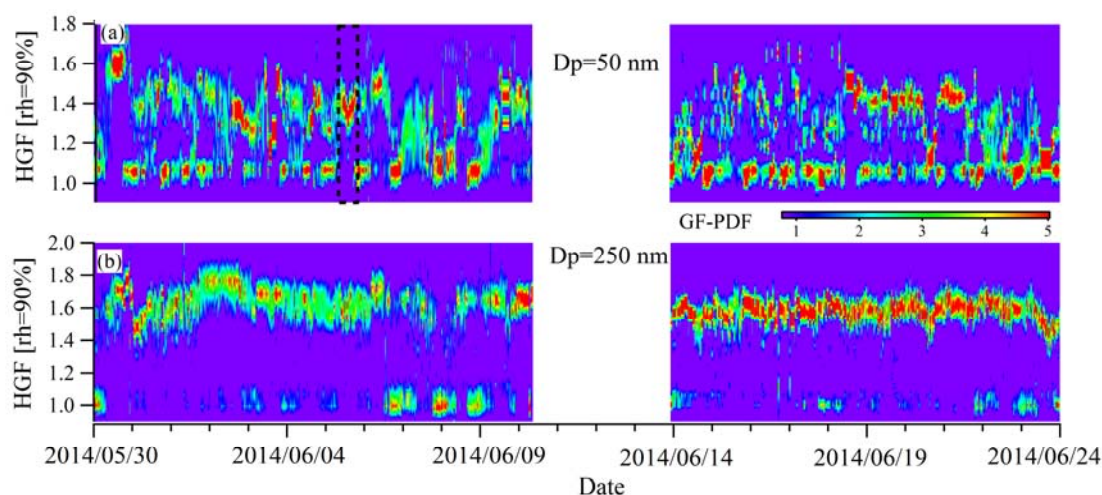


Figure 4: The time series of the GF-PDFs for 50 and 250 nm particles.

\*\*\*\*\*

5. P11507, L27 – P11508, L5: For the reasons that are mentioned in the text, it is not appropriate to compare  $\kappa\text{HGF}$  -versus-O/C trends observed here with  $\kappa\text{CCN}$  -versus-O/C parameterizations from other studies that are referenced in the Figure 5 caption (Bhattu and Tripathi, 2015; Chang et al., 2010 and Mei et al., 2013). I suggest modifying Figure 5 and related discussion by removing the  $\kappa\text{CCN}$  parameterizations and instead comparing with other  $\kappa\text{HGF}$  measurements. Some suggested studies for comparison include Jimenez et al. (2009), Massoli et al. (2010), Rickards et al. (2013), Pajunoja et al. (2015).

**Response:**

The MS was revised, see below:

**Modification in the MS:**

Fig. 8 shows  $\kappa_{\text{org}}$  as a function of O:C ratio. From the degree of scatter point of view,  $\kappa_{\text{org}}$  is not correlated to the O:C ratio. Several previous studies reported the similar plots of  $\kappa_{\text{org}}$  values as a function of O:C ratios (Chang et al., 2010;Bhattu and Tripathi, 2015;Rickards et al., 2013). In order to derive an empirical relationship between  $\kappa_{\text{org}}$  and O:C ratios,  $\kappa_{\text{org}}$  values are usually binned by O:C in increments of 0.1. As displayed in Fig. 8, a linear fitting function ( $\kappa_{\text{org}}=(0.08\pm 0.02)*\text{O:C}+(0.02\pm 0.01)$ ) was obtained. Some empirical functions reported by other previous studies are also shown in Fig.8. In these previous studies (Wu et al., 2013;Jimenez et al., 2009;Rickards et al., 2013;Duplissy et al., 2011), the  $\kappa_{\text{org}}$  were derived from the measurements performed in the sub-saturation regime. In Massoli et al.' study (2010) (not shown in the Fig. 8 due to the linear fitting based on HGF, not  $\kappa_{\text{org}}$ ), they reported a linear relationship ( $\text{HGF}_{90\%} = (0.58\pm 0.15)*\text{O:C} + (0.85 \pm 0.08)$ ) between HGF90% and O:C for the laboratory-generated SOA particles. Both results displayed in Fig. 8 and Massoli's study showed a positive correlation between  $\kappa_{\text{org}}$  and O:C. Such positive correlation was also reported by those studies based on CCNc measurements, for examples, Chang et al. (2010) and Mei et al. (2013). We note that the slopes of the linear fitting varied with different studies, indicating there is no a simple parametrization to describe the relationship between organic hygroscopic and its oxidation state though the various atmospheric environments. Recently, Richards et al. (2013) had undertaken an extensive review of  $\kappa$  values published in the literature and showed that  $\kappa_{\text{org}}$  vs. O:C plot has a large degree of scatter. This indicates that other factors, such as phase state (Pajunoja et al., 2015) and molecular structures (Suda et al., 2014) of organic aerosols (OA) other than oxidation state may also play a role in the determination of the OA hygroscopicity.

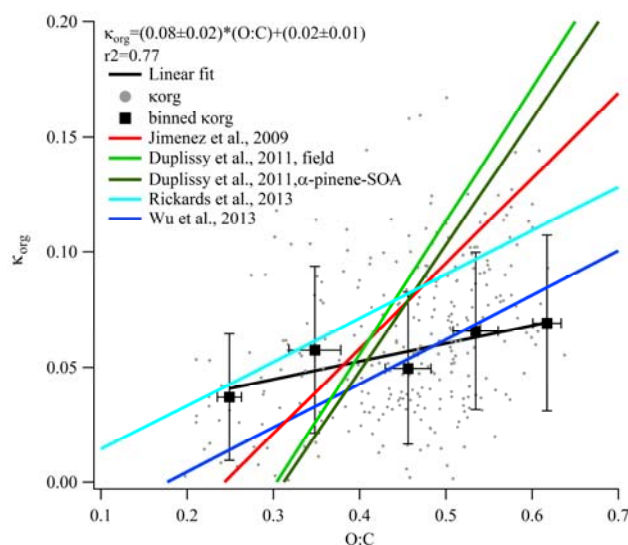


Figure 8: The relationship between organic hygroscopicity parameter ( $\kappa_{\text{org}}$ ) and oxygen to carbon ratio (O: C).

\*\*\*\*\*

6. P11508, L3: The authors state: “We should also note that the different aerosol formation ways in different environments could also be an explanation for the different relationship between  $\kappa_{\text{org}}$  and O:C.” Other studies also suggest that O:C does not encompass changes in detailed chemical composition that are responsible for changes in hygroscopicity (e.g. Mei et al., 2013; Rickards et al., 2013; Suda et al., 2014). However, AMS spectra obtained in this study are not discussed aside from the O/C ratio. This claim it should be supported by presentation of representative AMS spectra. Further, it would be useful to discuss what unique features of the Beijing aerosol chemical composition lead to different hygroscopic behavior relative to other studies.

**Response:**

As pointed out by the referee, several previous studies suggested that O:C does not encompass changes in detailed chemical composition that are responsible for changes in hygroscopicity (Rickards et al., 2013; Suda et al., 2014; Mei et al., 2013). Our results also showed that  $\kappa_{\text{org}}$  is not well correlated to the O:C ratio, as shown in the scattering plot ( $\kappa_{\text{org}}$  vs O:C) in the manuscript. There could be some other factors determining the organic hygroscopicity except for oxidation state. Our previous studies performed in the same sampling site with this study showed that no significant difference in the mass spectra observed between in Beijing and in other places (Huang et al., 2010). It would be difficult to find out the unique features of aerosol chemical composition in the atmosphere of Beijing. Suda et al. (2014) systematically studied the influence of the number and location of molecular functional groups on the hygroscopicity of organic aerosols. The great work done by Suda et al. (2014) may help us to find out the mechanisms of organics hygroscopicity from the chemistry point of view. In the future, we will make a deeper study using Suda et al.’s method, not in present study.

\*\*\*\*\*

**References**

Achtert, P., Birmili, W., Nowak, A., Wehner, B., Wiedensohler, A., Takegawa, N., Kondo, Y., Miyazaki, Y., Hu, M., and Zhu, T.: Hygroscopic growth of tropospheric particle number size distributions over the North China Plain, *Journal of Geophysical Research: Atmospheres*, 114, n/a-n/a, 10.1029/2008JD010921, 2009.

Bhattu, D., and Tripathi, S. N.: CCN closure study: Effects of aerosol chemical composition and mixing state, *Journal of Geophysical Research: Atmospheres*, 120, 2014JD021978, 10.1002/2014JD021978, 2015.

Chang, R. Y. W., Slowik, J. G., Shantz, N. C., Vlasenko, A., Liggio, J., Sjostedt, S. J., Leaitch, W. R., and Abbatt, J. P. D.: The hygroscopicity parameter ( $\kappa$ ) of ambient organic aerosol at a field site subject to biogenic and anthropogenic influences: relationship to degree of aerosol oxidation, *Atmos. Chem. Phys.*, 10, 5047-5064, 10.5194/acp-10-5047-2010, 2010.

Cheng, Y. F., Wiedensohler, A., Eichler, H., Heintzenberg, J., Tesche, M., Ansmann, A., Wendisch, M., Su, H., Althausen, D., Herrmann, H., Gnauk, T., Brüggemann, E., Hu, M., and Zhang, Y. H.: Relative humidity dependence of aerosol optical properties and direct radiative forcing in the surface boundary

layer at Xinken in Pearl River Delta of China: An observation based numerical study, *Atmospheric Environment*, 42, 6373-6397, <http://dx.doi.org/10.1016/j.atmosenv.2008.04.009>, 2008.

Duplissy, J., DeCarlo, P. F., Dommen, J., Alfarra, M. R., Metzger, A., Barmapadimos, I., Prevot, A. S. H., Weingartner, E., Tritscher, T., Gysel, M., Aiken, A. C., Jimenez, J. L., Canagaratna, M. R., Worsnop, D. R., Collins, D. R., Tomlinson, J., and Baltensperger, U.: Relating hygroscopicity and composition of organic aerosol particulate matter, *Atmos. Chem. Phys.*, 11, 1155-1165, 10.5194/acp-11-1155-2011, 2011.

Gunthe, S. S., King, S. M., Rose, D., Chen, Q., Roldin, P., Farmer, D. K., Jimenez, J. L., Artaxo, P., Andreae, M. O., Martin, S. T., and Pöschl, U.: Cloud condensation nuclei in pristine tropical rainforest air of Amazonia: size-resolved measurements and modeling of atmospheric aerosol composition and CCN activity, *Atmos. Chem. Phys.*, 9, 7551-7575, 10.5194/acp-9-7551-2009, 2009.

Huang, X. F., He, L. Y., Hu, M., Canagaratna, M. R., Sun, Y., Zhang, Q., Zhu, T., Xue, L., Zeng, L. W., Liu, X. G., Zhang, Y. H., Jayne, J. T., Ng, N. L., and Worsnop, D. R.: Highly time-resolved chemical characterization of atmospheric submicron particles during 2008 Beijing Olympic Games using an Aerodyne High-Resolution Aerosol Mass Spectrometer, *Atmos. Chem. Phys.*, 10, 8933-8945, 10.5194/acp-10-8933-2010, 2010.

Jimenez, J. L., Canagaratna, M. R., Donahue, N. M., Prevot, A. S. H., Zhang, Q., Kroll, J. H., DeCarlo, P. F., Allan, J. D., Coe, H., Ng, N. L., Aiken, A. C., Docherty, K. S., Ulbrich, I. M., Grieshop, A. P., Robinson, A. L., Duplissy, J., Smith, J. D., Wilson, K. R., Lanz, V. A., Hueglin, C., Sun, Y. L., Tian, J., Laaksonen, A., Raatikainen, T., Rautiainen, J., Vaattovaara, P., Ehn, M., Kulmala, M., Tomlinson, J. M., Collins, D. R., Cubison, M. J., E, Dunlea, J., Huffman, J. A., Onasch, T. B., Alfarra, M. R., Williams, P. I., Bower, K., Kondo, Y., Schneider, J., Drewnick, F., Borrmann, S., Weimer, S., Demerjian, K., Salcedo, D., Cottrell, L., Griffin, R., Takami, A., Miyoshi, T., Hatakeyama, S., Shimono, A., Sun, J. Y., Zhang, Y. M., Dzepina, K., Kimmel, J. R., Sueper, D., Jayne, J. T., Herndon, S. C., Trimborn, A. M., Williams, L. R., Wood, E. C., Middlebrook, A. M., Kolb, C. E., Baltensperger, U., and Worsnop, D. R.: Evolution of organic aerosols in the atmosphere, *Science*, 326, 1525-1529, 10.1126/science.1180353, 2009.

Jurányi, Z., Tritscher, T., Gysel, M., Laborde, M., Gomes, L., Roberts, G., Baltensperger, U., and Weingartner, E.: Hygroscopic mixing state of urban aerosol derived from size-resolved cloud condensation nuclei measurements during the MEGAPOLI campaign in Paris, *Atmos. Chem. Phys.*, 13, 6431-6446, 10.5194/acp-13-6431-2013, 2013.

Kreidenweis, S. M., and Asa-Awuku, A.: 5.13 - Aerosol Hygroscopicity: Particle Water Content and Its Role in Atmospheric Processes, in: *Treatise on Geochemistry (Second Edition)*, edited by: Turekian, H. D. H. K., Elsevier, Oxford, 331-361, 2014.

Lambe, A. T., Onasch, T. B., Massoli, P., Croasdale, D. R., Wright, J. P., Ahern, A. T., Williams, L. R., Worsnop, D. R., Brune, W. H., and Davidovits, P.: Laboratory studies of the chemical composition and cloud condensation nuclei (CCN) activity of secondary organic aerosol (SOA) and oxidized primary organic aerosol (OPOA), *Atmos. Chem. Phys.*, 11, 8913-8928, 10.5194/acp-11-8913-2011, 2011.

Levin, E. J. T., Prenni, A. J., Petters, M. D., Kreidenweis, S. M., Sullivan, R. C., Atwood, S. A., Ortega, J., DeMott, P. J., and Smith, J. N.: An annual cycle of size-resolved aerosol hygroscopicity at a forested site in Colorado, *J. Geophys. Res.*, 117, D06201, 10.1029/2011jd016854, 2012.

Levin, E. J. T., Prenni, A. J., Palm, B. B., Day, D. A., Campuzano-Jost, P., Winkler, P. M., Kreidenweis, S. M., DeMott, P. J., Jimenez, J. L., and Smith, J. N.: Size-resolved aerosol composition and its link to hygroscopicity at a forested site in Colorado, *Atmos. Chem. Phys.*, 14, 2657-2667,

10.5194/acp-14-2657-2014, 2014.

Liu, P. F., Zhao, C. S., Göbel, T., Hallbauer, E., Nowak, A., Ran, L., Xu, W. Y., Deng, Z. Z., Ma, N., Mildenerger, K., Henning, S., Stratmann, F., and Wiedensohler, A.: Hygroscopic properties of aerosol particles at high relative humidity and their diurnal variations in the North China Plain, *Atmos. Chem. Phys.*, 11, 3479-3494, 10.5194/acp-11-3479-2011, 2011.

Lopez-Yglesias, X. F., Yeung, M. C., Dey, S. E., Brechtel, F. J., and Chan, C. K.: Performance Evaluation of the Brechtel Mfg. Humidified Tandem Differential Mobility Analyzer (BMI HTDMA) for Studying Hygroscopic Properties of Aerosol Particles, *Aerosol Science and Technology*, 48, 969-980, 10.1080/02786826.2014.952366, 2014.

Massling, A., Stock, M., Wehner, B., Wu, Z. J., Hu, M., Brüggemann, E., Gnauk, T., Herrmann, H., and Wiedensohler, A.: Size segregated water uptake of the urban submicrometer aerosol in Beijing, *Atmospheric Environment*, 43, 1578-1589, <http://dx.doi.org/10.1016/j.atmosenv.2008.06.003>, 2009.

Massoli, P., Lambe, A. T., Ahern, A. T., Williams, L. R., Ehn, M., Mikkilä, J., Canagaratna, M. R., Brune, W. H., Onasch, T. B., Jayne, J. T., Petäjä, T., Kulmala, M., Laaksonen, A., Kolb, C. E., Davidovits, P., and Worsnop, D. R.: Relationship between aerosol oxidation level and hygroscopic properties of laboratory generated secondary organic aerosol (SOA) particles, *Geophysical Research Letters*, 37, n/a-n/a, 10.1029/2010GL045258, 2010.

Mei, F., Hayes, P. L., Ortega, A., Taylor, J. W., Allan, J. D., Gilman, J., Kuster, W., de Gouw, J., Jimenez, J. L., and Wang, J.: Droplet activation properties of organic aerosols observed at an urban site during CalNex-LA, *Journal of Geophysical Research: Atmospheres*, 118, 2903-2917, 10.1002/jgrd.50285, 2013.

Meier, J., Wehner, B., Massling, A., Birmili, W., Nowak, A., Gnauk, T., Brüggemann, E., Herrmann, H., Min, H., and Wiedensohler, A.: Hygroscopic growth of urban aerosol particles in Beijing (China) during wintertime: a comparison of three experimental methods, *Atmos. Chem. Phys.*, 9, 6865-6880, 10.5194/acp-9-6865-2009, 2009.

Moore, R. H., Raatikainen, T., Langridge, J. M., Bahreini, R., Brock, C. A., Holloway, J. S., Lack, D. A., Middlebrook, A. M., Perring, A. E., Schwarz, J. P., Spackman, J. R., and Nenes, A.: CCN Spectra, Hygroscopicity, and Droplet Activation Kinetics of Secondary Organic Aerosol Resulting from the 2010 Deepwater Horizon Oil Spill, *Environmental Science & Technology*, 46, 3093-3100, 10.1021/es203362w, 2012.

Pajunoja, A., Lambe, A. T., Hakala, J., Rastak, N., Cummings, M. J., Brogan, J. F., Hao, L., Paramonov, M., Hong, J., Prisle, N. L., Malila, J., Romakkaniemi, S., Lehtinen, K. E. J., Laaksonen, A., Kulmala, M., Massoli, P., Onasch, T. B., Donahue, N. M., Riipinen, I., Davidovits, P., Worsnop, D. R., Petäjä, T., and Virtanen, A.: Adsorptive uptake of water by semisolid secondary organic aerosols, *Geophysical Research Letters*, 42, 3063-3068, 10.1002/2015GL063142, 2015.

Paramonov, M., Aalto, P. P., Asmi, A., Prisle, N., Kerminen, V. M., Kulmala, M., and Petäjä, T.: The analysis of size-segregated cloud condensation nuclei counter (CCNC) data and its implications for cloud droplet activation, *Atmos. Chem. Phys.*, 13, 10285-10301, 10.5194/acp-13-10285-2013, 2013.

Rickards, A. M. J., Miles, R. E. H., Davies, J. F., Marshall, F. H., and Reid, J. P.: Measurements of the Sensitivity of Aerosol Hygroscopicity and the  $\kappa$  Parameter to the O/C Ratio, *The Journal of Physical Chemistry A*, 117, 14120-14131, 10.1021/jp407991n, 2013.

Sihto, S. L., Mikkilä, J., Vanhanen, J., Ehn, M., Liao, L., Lehtipalo, K., Aalto, P. P., Duplissy, J., Petäjä, T., Kerminen, V. M., Boy, M., and Kulmala, M.: Seasonal variation of CCN concentrations and aerosol activation properties in boreal forest, *Atmos. Chem. Phys.*, 11, 13269-13285,



10.5194/acp-11-13269-2011, 2011.

Suda, S. R., Petters, M. D., Yeh, G. K., Strollo, C., Matsunaga, A., Faulhaber, A., Ziemann, P. J., Prenni, A. J., Carrico, C. M., Sullivan, R. C., and Kreidenweis, S. M.: Influence of Functional Groups on Organic Aerosol Cloud Condensation Nucleus Activity, *Environmental Science & Technology*, 48, 10182-10190, 10.1021/es502147y, 2014.

Swietlicki, E., Hansson, H. C., HÄMeri, K., Svenningsson, B., Massling, A., McFiggans, G., McMurry, P. H., PetÄJÄ, T., Tunved, P., Gysel, M., Topping, D., Weingartner, E., Baltensperger, U., Rissler, J., Wiedensohler, A., and Kulmala, M.: Hygroscopic properties of submicrometer atmospheric aerosol particles measured with H-TDMA instruments in various environments—a review, *Tellus B*, 60, 432-469, 10.1111/j.1600-0889.2008.00350.x, 2008.

Varutbangkul, V., Brechtel, F. J., Bahreini, R., Ng, N. L., Keywood, M. D., Kroll, J. H., Flagan, R. C., Seinfeld, J. H., Lee, A., and Goldstein, A. H.: Hygroscopicity of secondary organic aerosols formed by oxidation of cycloalkenes, monoterpenes, sesquiterpenes, and related compounds, *Atmos. Chem. Phys.*, 6, 2367-2388, 10.5194/acp-6-2367-2006, 2006.

Virkkula, A., Van Dingenen, R., Raes, F., and Hjorth, J.: Hygroscopic properties of aerosol formed by oxidation of limonene,  $\alpha$ -pinene, and  $\beta$ -pinene, *J. Geophys. Res.*, 104, 3569-3579, 10.1029/1998jd100017, 1999.

Wong, J. P. S., Lee, A. K. Y., Slowik, J. G., Cziczo, D. J., Leaitch, W. R., Macdonald, A., and Abbatt, J. P. D.: Oxidation of ambient biogenic secondary organic aerosol by hydroxyl radicals: Effects on cloud condensation nuclei activity, *Geophysical Research Letters*, 38, n/a-n/a, 10.1029/2011GL049351, 2011.

Wu, Z. J., Poulain, L., Henning, S., Dieckmann, K., Birmili, W., Merkel, M., van Pinxteren, D., Spindler, G., Mueller, K., Stratmann, F., Herrmann, H., and Wiedensohler, A.: Relating particle hygroscopicity and CCN activity to chemical composition during the HCCT-2010 field campaign, *Atmospheric Chemistry and Physics*, 13, 7983-7996, 10.5194/acp-13-7983-2013, 2013.

Ye, X., Tang, C., Yin, Z., Chen, J., Ma, Z., Kong, L., Yang, X., Gao, W., and Geng, F.: Hygroscopic growth of urban aerosol particles during the 2009 Mirage-Shanghai Campaign, *Atmospheric Environment*, 64, 263-269, <http://dx.doi.org/10.1016/j.atmosenv.2012.09.064>, 2013.

Yeung, M. C., Lee, B. P., Li, Y. J., and Chan, C. K.: Simultaneous HTDMA and HR-ToF-AMS measurements at the HKUST Supersite in Hong Kong in 2011, *Journal of Geophysical Research: Atmospheres*, 119, 9864-9883, 10.1002/2013JD021146, 2014.

Zhang, J., Wang, L., Chen, J., Feng, S., Shen, J., and Jiao, L.: Hygroscopicity of ambient submicron particles in urban Hangzhou, China, *Front. Environ. Sci. Eng. China*, 5, 342-347, 10.1007/s11783-011-0358-7, 2011.

1 **Particle hygroscopicity and its link to chemical composition in the urban**  
2 **atmosphere of Beijing, China during summertime**

3 Z. J. Wu<sup>1</sup>, J. Zheng<sup>1</sup>, D. J. Shang<sup>1</sup>, Z. F. Du<sup>1</sup>, Y. S. Wu<sup>1</sup>, L. M. Zeng<sup>1</sup>, A.

4 Wiedensohler<sup>2</sup>, M. Hu<sup>1</sup>

5 [1] State Key Joint Laboratory of Environmental Simulation and Pollution Control, College of  
6 Environmental Sciences and Engineering, Peking University, Beijing 100871, China

7 [2] Leibniz Institute for Tropospheric Research, 04318, Leipzig, Germany

8 Corresponding to: Min Hu ([minhu@pku.edu.cn](mailto:minhu@pku.edu.cn)) or Zhijun Wu ([zhijunwu@pku.edu.cn](mailto:zhijunwu@pku.edu.cn))

9  
10 **Abstract:**

11 Simultaneous measurements of particle number size distribution, particle  
12 hygroscopic properties, and size-resolved chemical composition were made during the  
13 summer of 2014 in Beijing, China. During the measurement period, the mean  
14 hygroscopicity parameters ( $\kappa$ s) of 50, 100, 150, 200, and 250 nm particles were  
15 respectively  $0.16 \pm 0.07$ ,  $0.19 \pm 0.06$ ,  $0.22 \pm 0.06$ ,  $0.26 \pm 0.07$ , and  $0.28 \pm 0.10$ , showing an  
16 increasing trend with increasing particle size. Such size-dependency of particle  
17 hygroscopicity was similar to that of the inorganic mass fraction in  $PM_{10}$ . The  
18 hydrophilic mode ( $HGF > 1.2$ ) was more prominent in growth factor probability  
19 density distributions and its dominance of hydrophilic mode became more  
20 pronounced with increasing particle size. When  $PM_{2.5}$  mass concentration is greater  
21 than  $50 \mu\text{g}/\text{m}^3$ , the fractions of the hydrophilic mode for 150, 250, and 350 nm  
22 particles increased towards 1 as  $PM_{2.5}$  mass concentration increased. This indicates  
23 that aged particles dominated during severe pollution periods in the atmosphere of  
24 Beijing. Particle hygroscopic growth can be well predicted using high time-resolution  
25 size-resolved chemical composition derived from AMS measurement using the ZSR  
26 mixing rule. The organic hygroscopicity parameter ( $\kappa_{\text{org}}$ ) showed a positive  
27 correlation with oxygen to carbon ratio. During the new particle formation event  
28 associating with strongly active photochemistry, the hygroscopic growth factor or  $\kappa$  of  
29 newly formed particles is greater than for particle with the same sizes during non-NPF  
30 periods. A quick transformation from external mixture to internal mixture for  
31 pre-existing particles (for example 250 nm particle) was observed. Such

1 transformations may modify the state of mixture of pre-existing particles and thus  
2 modify properties such as the light absorption coefficient and cloud condensation  
3 nuclei activation.

## 4 **1 Introduction**

5 Hygroscopic growth of atmospheric particles is one of the important parameters  
6 controlling their direct and indirect climate effects (McFiggans et al., 2006; Haywood  
7 and Boucher, 2000). Due to water uptake, hydrophilic particles grow significantly in  
8 size at high relative humidity (RH), which influences the particle light scattering and  
9 extinction coefficients, thereby impairing visibility (Sloane and Wolff, 1985). In  
10 addition, the water content of atmospheric aerosol particles can serve as a site for  
11 heterogeneous nucleation and reactions that perturb local photochemistry  
12 (Kreidenweis and Asa-Awuku, 2014). Therefore, a better understanding of  
13 hygroscopic behavior of atmospheric aerosol particle is required to further elucidate  
14 the physicochemical processes in the atmosphere.

15 The association of the particle chemical composition with their size-dependent  
16 hygroscopic behavior is rather complex. In order to overcome such complexities,  
17 Petters and Kreidenweis (2007) proposed a single hygroscopicity parameter  
18 ( $\kappa$ ), namely  $\kappa$ -Köhler theory. On the basis of the  $\kappa$ -Köhler theory and  
19 Zdanovskii-Stokes-Robinson (ZSR) mixing rule (Stokes and Robinson,  
20 1966; Zdanovskii, 1948), particle hygroscopic growth of a homogeneous chemical  
21 mixture can be predicted, knowing hygroscopic growth factors of pure chemical  
22 species. Aerosol mass spectrometers (AMS), which have been increasingly deployed  
23 in atmospheric aerosol studies, can provide a high time resolution of the size-resolved  
24 chemical composition of non-refractory particle material (DeCarlo et al., 2006).  
25 Therefore, coupled measurements of an AMS and a Hygroscopicity Tandem  
26 Differential Mobility Analyzer (H-TDMA) are able to capture highly variable changes  
27 in chemical particle composition and hygroscopicity in real time. Some studies  
28 highlighted the advantage of using size-selected AMS information over size-averaged

1 information from off-line chemical characterization (Medina et al., 2007;Gunthe et al.,  
2 2009;Cerully et al., 2011;Wu et al., 2013).

3 Another key product of AMS measurements is the oxidation level and chemical  
4 information of organic aerosols. Compared to inorganic species, which exhibit a  
5 well-characterized hygroscopic behavior, knowledge on the influence of the water  
6 uptake of the organic aerosols remains limited (Kanakidou et al., 2005;Hallquist et al.,  
7 2009). The hygroscopicity of organic material varies with its oxidation state (Jimenez  
8 et al., 2009), which may be highly variable in the real atmosphere, depending on the  
9 history of an air mass. Such variation may present a significant challenge when  
10 predicting hygroscopicity assuming a constant hygroscopic growth factor of the  
11 organic aerosol fraction at a given relative humidity, as has usually been done in  
12 closure studies.

13 Currently, some studies have been performed to investigate the relationship  
14 between particle hygroscopicity and chemical composition in both field  
15 measurements and laboratory experiments (Massoli et al., 2010;Wong et al.,  
16 2011;Lambe et al., 2011;Rickards et al., 2013;Moore et al., 2012b;Suda et al.,  
17 2014;Paramonov et al., 2013;Levin et al., 2012;Moore et al., 2012a). These works  
18 specially focused on parametrizing the empirical correlations between the atomic  
19 Oxygen : Carbon (O:C) ratio and organic hygroscopicity parameter ( $\kappa$ ) derived from  
20 either hygroscopic growth factor (e.g. Wu et al., 2013;Rickards et al., 2013) or Cloud  
21 Condensation Nuclei (CCN) activity (e.g. Mei et al., 2013;Wong et al., 2011;Lambe et  
22 al., 2011;Chang et al., 2010). Typically, a linear parametrization of the correlation  
23 between  $\kappa$  and O:C was presented. Rickards et al. (2013) recently summarized the  
24 literature data and pointed out the systematic variability in parametrizations between  
25 organic  $\kappa$  and the O:C ratio determined from the different studies remains large. A  
26 recent work done by Suda et al. (2014) tested the influence of the number and location  
27 of molecular functional groups on the hygroscopicity of organic aerosols and may  
28 improve our understanding the mechanisms of organics hygroscopicity.

29 Over the past several decades, particle hygroscopicity measurements have been  
30 carried out world-wide, using the H-TDMA technique. Atmospheric environments, in

1 which those measurements were performed included marine, Antarctic, boreal forest,  
2 rural, and urban areas. Swietlicki et al. (2008) and Kreidenweis and Asa-Awu (2014)  
3 compiled the existing observations on particle hygroscopic growth in the literature.  
4 Throughout these compilations, measurements of particle hygroscopicity have been  
5 rarely performed in China, which is experiencing frequently severe haze pollution  
6 episodes. These few particle hygroscopicity measurements using the H-TDMA  
7 technique were deployed in Yangtze River Delta (Shanghai (Ye et al., 2013) and  
8 Hangzhou (Zhang et al., 2011)), Pearl River Delta (Xinken (Cheng et al., 2008) and  
9 Hong Kong (Lopez-Yglesias et al., 2014;Yeung et al., 2014)) and North China Plain  
10 (Beijing (Massling et al., 2009;Meier et al., 2009), Yufa (Achtert et al., 2009), and  
11 Wuqing (Liu et al., 2011) ). Unfortunately, most of measurements lack a linkage  
12 between particle hygroscopicity and chemical composition with a high time  
13 resolution.

14 This study investigated the size-resolved particle hygroscopicity and chemical  
15 composition in Beijing, China, during summertime. Our work provided a general  
16 overview of particle hygroscopic behavior as well as a comparison of the observed  
17 hygroscopic particle growth and simulated one using AMS-based chemical particle  
18 composition, emphasizing on the organic mass fraction. Additionally, the evolution of  
19 particle hygroscopicity during the new particle formation event was investigated to  
20 understand the effects of strong photochemistry-driven atmospheric oxidation  
21 processes on particle hygroscopicity and the mixing state.

## 22 **2 Measurements**

### 23 **2.1 The Sampling site**

24 The sampling site is on the campus of Peking University, located in northwest  
25 Beijing. The laboratory was equipped with a suit of aerosol instruments sites on the  
26 roof of a building (30 m above the ground). The relative humidity (RH) of the  
27 sampled air was kept to below 30% using a silica gel dryer and a Nafion dryer in

1 series. The particle number size distribution, particle hygroscopicity, and aerosol mass  
2 spectrometric measurements were concurrently made. Particle number size  
3 distributions from 3 to 800 nm were measured by TSI-SMPS  
4 (Long-DMA3081+CPC3775 and Nano-DMA3085+UCPC3776). The multiple charge  
5 correction and particle loss correction were carried out. Other core instruments will be  
6 briefly described below.

## 7 **2.2 Particle hygroscopicity measurements**

8 The H-TDMA used in this study has been described in detail in previous  
9 publications (Wu et al., 2011; Massling et al., 2003), and complied to the instrumental  
10 standards and quality assurance prescribed in Massling et al. (2011). The H-TDMA  
11 consists of three main parts: (1) A Differential Mobility Analyzer (DMA1) that selects  
12 quasi-monodisperse particles, and a Condensation Particle Counter (CPC1) that  
13 measures the particle number concentration leaving the DMA1 at the selected particle  
14 size; (2) An aerosol humidifier conditioning the particles selected by DMA1 to a  
15 defined relative humidity (RH); (3) The second DMA (DMA2) coupled with another  
16 condensation particle counter (CPC2) to measure the number size distributions of the  
17 humidified particles. The second DMA and the aerosol humidification were placed in  
18 a temperature-controlled box. Hygroscopicity scans with 100 nm ammonium sulfate  
19 particles were performed every 3 hours to analyze the stability of the relative  
20 humidity of 90% in the second DMA. Hygroscopicity scan with a deviation of more  
21 than 3% in relative humidity to the set-point of 90% was not considered for further  
22 analysis.

23 The hygroscopic growth factor (*HGF*) is defined as the ratio of the particle  
24 mobility diameter,  $Dp(RH)$ , at a given RH to the dry diameter,  $Dp_{dry}$ :

$$25 \text{ HGF}(RH) = \frac{Dp(RH)}{Dp_{dry}} \quad [1]$$

26 The TDMA<sub>inv</sub> method developed by Gysel et al. (2009) was used to invert the  
27 H-TDMA data. Dry scans (under RH<10%) were used to calibrate a possible offset  
28 between DMA1 and DMA2 and define the width of the H-TDMA's transfer function

1 (Gysel et al., 2009).

2 Based on the ZSR method , the *HGF* of a mixture can be estimated from the  
3 *HGF<sub>i</sub>* of the pure components and their respective volume fractions,  $\varepsilon_i$  (Malm and  
4 Kreidenweis, 1997):

$$5 \quad HGF_{mixed} = (\sum_i \varepsilon_i HGF_i^3)^{1/3} \quad [2]$$

6 Here, we assumed that two components including soluble and insoluble fractions  
7 consist of aerosols (also refer to Ehn et al., 2007; Swietlicki et al., 1999). The soluble  
8 fraction was assumed to be ammonium sulfate. Then, the water-soluble volume  
9 fraction ( $\varepsilon_{soluble}$ ) can be calculated by:

$$10 \quad \varepsilon_{soluble} = \frac{HGF_{measured}^3 - 1}{HGF_{(NH_4)_2SO_4}^3 - 1} \quad [3]$$

11 where  $HGF_{measured}$  is the HGF of the particles measured by H-TDMA, and  
12  $HGF_{(NH_4)_2SO_4}$  is the HGF of pure  $(NH_4)_2SO_4$  particles with the same size. When  
13 calculating  $HGF_{(NH_4)_2SO_4}$  in different diameters, the parameterizations for  $(NH_4)_2SO_4$   
14 water activity developed by Potukuchi and Wexler (1995) and the density reported by  
15 Tang and Munkelwitz (1994) were used. The Kelvin term was considered in the  
16 calculation. In this study, the hygroscopic growth factors of 50, 100, 150, 250, and  
17 350 nm particles were measured at RH=90%.

## 18 **2.3 Particle chemical composition**

19 The Aerodyne HR-ToF-AMS (here simply referred to as AMS) (DeCarlo et al.,  
20 2006) was operated with a time resolution of 5 minutes. Due to the 600°C surface  
21 temperature of the vaporizer, the AMS can only analyze the non-refractory chemical  
22 composition of the particles. Elemental carbon, crustal material, and sea-salt cannot  
23 be detected. Therefore, based on the transmission efficiency of the aerodynamic  
24 lenses and the detected compounds, the AMS can provide the size-resolved chemical  
25 composition of the submicrometer non-refractory aerosol particle fraction (NR-PM<sub>1</sub>)  
26 (Canagaratna et al., 2007). Applying the method developed by Canagaratna et al.  
27 (2015) the high resolution organic particle mass spectra were used to determine the  
28 elemental composition and the Oxygen to Carbon atomic ratio (O:C). The vacuum

1 aerodynamic diameter for AMS measurements was converted to the particle mobility  
2 diameter by division of AMS vacuum aerodynamic diameter by the estimated particle  
3 density ( $1500 \text{ kg/m}^3$ ). Here, the particle density is estimated by dividing the  
4 AMS-measured  $\text{PM}_{10}$  and black carbon mass concentrations by the SMPS-derived  
5 particle volume concentration. Hereafter, the mobility diameter (assuming spherical  
6 particles) was used for AMS data below.

7 AMS-positive matrix factor (PMF) analysis was performed to identify different  
8 organic aerosols (OA) factors on the basis of the high resolution mass spectra of  
9 organics (Ulbrich et al., 2009). Four OA components were resolved by PMF,  
10 including low-volatility oxygenated organic aerosol (LV-OOA), semi-volatile  
11 oxygenated OA (SV-OOA), hydrocarbon-like OA (HOA) and cooking OA (COA).  
12 LV-OOA and SV-OOA typically represented aged SOA and freshly formed SOA,  
13 respectively (Ulbrich et al., 2009). HOA and COA were both anthropogenic primary  
14 organic aerosol (POA) components (Lanz et al., 2007).

15 Black carbon (BC) mass concentration in  $\mu\text{g/m}^3$  is derived from Photoacoustic  
16 Extinctionmeter (PAX) measurements (DMT Company) (Arnott et al., 1999) equipped  
17 with  $\text{PM}_{10}$  cut-off inlet. In this study, PAX measurements were performed at  
18 wavelength 532 nm.

## 19 **2.4 Meteorological parameters**

20 Additionally, a weather station (Met One Instruments Inc.) provided the  
21 meteorological parameters. The wind speed, wind direction, ambient temperature, and  
22 relative humidity (RH) were detected.

23 Air mass backward trajectories arriving at the sampling site were calculated  
24 using the NOAA “HYSPLIT-4” (Hybrid Single-Particle Lagrangian Integrated  
25 Trajectory) model (Draxler and Hess, 1998). The 48 h trajectories terminated on a  
26 height of 200 m above the ground at 00:00, 06:00, 12:00 and 18:00 local time  
27 (UTC+08). In total, 100 air mass backward trajectories were grouped by assigning to  
28 five clusters using a k-means clustering algorithm. The number of clusters was



1 identified according to the changes of total spatial variance (TSV) (cf. HYSPLIT4  
2 user's guide). Five was chosen as the final number of clusters considering optimum  
3 separation of trajectories (larger number of clusters) and simplicity of display (lower  
4 number of cluster).

## 5 **3 Theory**

### 6 **3.1 Hygroscopicity parameter**

7 The hygroscopicity parameter,  $\kappa$ , can be calculated from the hygroscopic growth  
8 factor ( $HGF$ ) measured by H-TDMA (Petters and Kreidenweis, 2007):

$$9 \quad \kappa_{HTDMA} = (HGF^3 - 1) \left( \frac{\exp\left(\frac{A}{D_{Pdry} \cdot HGF}\right) - 1}{RH} \right) \quad [4]$$

$$10 \quad A = \frac{4\sigma_{s/a}M_w}{RT\rho_w} \quad [5]$$

11 Where  $D_{Pdry}$  and  $HGF$  are the initial dry particle diameter and the hygroscopic growth  
12 factor at 90% RH measured by H-TDMA, respectively.  $\sigma_{s/a}$  is the droplet surface  
13 tension (assumed to be that of pure water,  $\sigma_{s/a} = 0.0728 \text{ N m}^{-2}$ ),  $M_w$  the molecular  
14 weight of water,  $\rho_w$  the density of liquid water,  $R$  the universal gas constant, and  $T$  the  
15 absolute temperature.

16 For a given internal mixture,  $\kappa$  can also be predicted by a simple mixing rule on  
17 the basis of chemical volume fractions  $\varepsilon_i$  (Petters and Kreidenweis, 2007):

$$18 \quad \kappa_{chem} = \sum_i \varepsilon_i \kappa_i \quad [6]$$

19 Here,  $\kappa_i$  and  $\varepsilon_i$  are the hygroscopicity parameters and volume fraction for the  
20 individual (dry) component in the mixture with  $i$  the number of components in the  
21 mixture. We derived  $\varepsilon_i$  from the particle chemical composition measured by AMS and  
22 PAX. The detailed description of how to calculate volume fraction is given in section  
23 3.2. In the following discussions,  $\kappa_{HTDMA}$  and  $\kappa_{chem}$  denote respectively the values  
24 derived from H-TDMA and predicted using the ZSR mixing rule.

## 1 3.2 Hygroscopicity-chemical composition closure

2 The AMS provided the particle mass size distribution of sulfate ( $\text{SO}_4^{2-}$ ), nitrate  
3 ( $\text{NO}_3^-$ ), and ammonium ( $\text{NH}_4^+$ ) ions as well that of organic compounds. We used a  
4 simplified ion pairing scheme as presented in Gysel et al. (2007) to convert the ion  
5 mass concentrations to the mass concentrations of their corresponding inorganic salts  
6 as listed in Table 1. Unlike inorganic salts, the hygroscopicity of organic aerosols is  
7 not well-recognized. In the literature, there were different approaches in representing  
8  $\kappa_{\text{org}}$  in the closure studies. Typically,  $\kappa_{\text{org}}$  is assumed as a constant value. Chang et al.,  
9 (2010) represented  $\kappa_{\text{org}}$  by using the factors from the PMF analysis to group organics  
10 measured by AMS into two components: a non-hygroscopic, unoxygenated  
11 component consisting of the hydrocarbon-like organic aerosol (HOA) factor and a  
12 hygroscopic component, consisting of the oxygenated factors LV-OOA, SV-OOA, and  
13 biomass burning organic aerosol (BBOA). In our study, organic materials derived  
14 from AMS measurements were grouped into two components including secondary  
15 organic aerosols (SOA) and primary organic aerosols (POA) based on AMS-PMF  
16 analysis. SOA, including LV-OOA and SV-OOA factors, is a more oxygenated  
17 organic aerosol, thereby more hygroscopic and has a  $\kappa_{\text{SOA}}$  of 0.1, which was  
18 calculated from the hygroscopic growth factor of organics at RH=90% as given in  
19 Gysel et al. (2007) using Eq. (4) in section 3.1. By taking  $\kappa_{\text{SOA}}=0.1$ , the best fit  
20 between  $\kappa_{\text{HTDMA}}$  and  $\kappa_{\text{chem}}$  was obtained in this study. One should note that kappa of  
21 SOA may varied with its oxidation state (Jimenez et al., 2009). The usage of a  
22 constant kappa value may introduce uncertainty in the closure of particle  
23 hygroscopicity and chemical composition. POA is the unoxygenated component  
24 consisting of the HOA and COA factors and is treated as hydrophobic material with  
25  $\kappa_{\text{POA}}=0$ . Then,  $\kappa_{\text{org}}$  can be calculated as:

$$26 \quad \kappa_{\text{org}} = f_{\text{POA}} * \kappa_{\text{POA}} + f_{\text{SOA}} * \kappa_{\text{SOA}} \quad [7]$$

27 Here,  $\kappa_{\text{org}}$  is overall  $\kappa$  for organic aerosols.  $f_{\text{POA}}$  and  $f_{\text{SOA}}$  are volume fraction of  
28 POA and SOA in total organic aerosols measured by AMS. One should note that Sun  
29 et al. (2012b) found that the contributions of POA and SOA to OA showed a

1 size-dependency. The relative contribution of POA to OA significantly increased with  
2 decreasing particle sizes. In this study, the closure studies were performed for  
3 particles with the mobility diameters of 150, 250, and 350 nm (larger than 200 nm in  
4 vacuum aerodynamic diameter). Using the relative contribution of POA to OA in PM<sub>1</sub>  
5 tended to overestimate percentage of POA for the size range focused in this study,  
6 thus underestimate the  $\kappa$ . In our case, the POA/OA and SOA/OA were respectively  
7 0.39 and 0.61. According to equation [7], the  $\kappa_{\text{org}}$  can be calculated as 0.06 assuming  
8  $\kappa_{\text{SOA}}=0.1$ . On the basis of Sun et al.'s study, the POA/OAs for 150, 250, and 350 nm  
9 particles were 0.30, 0.23, and 0.19, respectively. Using these ratios and equation [7],  
10 the calculated  $\kappa_{\text{orgs}}$  were 0.07, 0.08, and 0.08, respectively, which were slightly higher  
11 than the one ( $\kappa_{\text{org}}=0.06$ ) in our case. This minor difference can be negligible.

12 The volume fraction of each species was calculated from the particle mass  
13 concentration divided by its density as given in Table 1. The densities for inorganic  
14 salts were well defined. By summarizing the articles published (Park et al.,  
15 2004;McMurry et al., 2002;Kondo et al., 2011;Kiselev et al., 2010), 1700 kg/m<sup>3</sup> was  
16 selected as BC density. The hygroscopicity parameter  $\kappa$  of the hydrophobic black  
17 carbon was considered to be zero. The density of organic particle mass fraction  
18 including both SOA and POA was taken to be 1400 kg/m<sup>3</sup> (Gysel et al., 2007;Alfarra  
19 et al., 2006;Dinar et al., 2006). The  $\kappa_{\text{HTDMA}}$  values for the individual compounds listed  
20 in the Table 1 were calculated from the hygroscopic growth factor at 90% RH as  
21 given in Gysel et al. (2007) using equation [4] in the section 3.1.

## 22 4 Results and discussion

### 23 4.1 Meteorological condition during the sampling period

24 Fig. 1 showed the mean air mass backward trajectories for five clusters arriving at  
25 the sampling site from May 31 to June 24, 2014. The mean backward trajectories in  
26 five cluster showed the significant differences in direction and length. The air masses  
27 from the east (45%) and the south (26%) were the dominate trajectories. The

1 short-length air mass backward trajectories in cluster 1 and 2 indicated that air parcels  
2 moved slowly and spent much more time over the industrialized regions south and  
3 east of Beijing. As a result, the southerly and easterly air masses may be heavily  
4 polluted once they arrived at Beijing (Wehner et al., 2008). Cluster 3 spent much more  
5 time over the sea and may be associated with humid air masses. Northerly (8%) and  
6 north-westerly (10%) air masses, as represented by clusters 4–5, typically lead to the  
7 advection of dry and continental air into the Beijing area.

8 Fig. 2 displays the time series of wind speed, wind direction, ambient temperature,  
9 and RH during the sampling period. There was a clear diurnal cycle for all  
10 meteorological parameters. During nighttime, the wind speed was usually very low  
11 (around 1 m/s) and started to increase around noon on each day. The nighttime static  
12 wind may lead to very poor dilution with clean air and dispersion of pollutants and  
13 result in the local emissions were trapped in the urban atmosphere. The ambient  
14 temperature usually was above 30 °C during daytime and around 20 °C during  
15 nighttime. The average temperature and RH were respectively  $24\pm 7$  °C and  $45\pm 20\%$ .  
16 It rained several times during the measuring period, as indicated in the Fig. 2 (a). The  
17 heaviest wet deposition occurred on 17, June. The wet deposition obviously removed  
18 the atmospheric particles, as can be seen from the particle number size distribution  
19 shown in Fig. 3 (a).

20 In summer, the new particle formation and traffic emissions are the major sources  
21 of ultrafine particles in the atmosphere of Beijing (Wu et al., 2008; Wu et al., 2007). In  
22 addition, air masses across the industrialized regions in the south and east typically  
23 bring the high concentrations of accumulation mode particles to urban areas of  
24 Beijing (Wehner et al., 2008).

## 25 4.2 Overview of particle hygroscopic growth and the mixing state

26 Fig. 3 provides an overview of the particle number size distribution (a),  
27 hygroscopicity parameters ( $\kappa$ ) (b), and chemical composition of  $PM_{10}$  (c) during the  
28 entire field campaign. The trajectory clusters were marked as black circles in the Fig.

1 3 (a). As shown in the Fig. 3 (a), new particle formation (NPF) events were observed  
2 frequently. During the sampling period, the inorganic species and SOA were  
3 dominated in NR-PM<sub>1</sub> when air masses came from south and east of Beijing  
4 (trajectory cluster 1 and 2 as indicated by black circles in Fig.3 (a)). SOA was usually  
5 dominated in the organic compounds during the sampling period. Differently, the  
6 POA was a major fraction on June 7, 8, and 9, on which the BC mass fraction  
7 increased too. During this time period, the northerly air masses (trajectory cluster 5  
8 marked in Fig. 3 (a)) arriving at the measurement site may be influenced by the wheat  
9 straw burning, which usually takes place from late May to early June over North  
10 China Plain. Several previous studies showed that wheat straw burning significantly  
11 contributes to degradation of air quality in Beijing during the harvest season in the  
12 summer (Li et al., 2008;Zheng et al., 2005).

13 Fig. 3 (b) displays the time series of hygroscopicity parameters for 50 nm ( $\kappa_{50\text{nm}}$ )  
14 and 250 nm ( $\kappa_{250\text{nm}}$ ) particles. Both  $\kappa_{50\text{nm}}$  and  $\kappa_{250\text{nm}}$  had an obvious temporal  
15 variability. Their variations were similar to that of inorganic mass fraction in PM<sub>1</sub>  
16 displayed in Fig. 3 (c). An in-depth analysis of the relationship between particle  
17 hygroscopicity and chemical composition will be given in section 4.3. Fig. 4 gives an  
18 overview of growth factor probability density distributions (GF-PDF) for 50 and 250  
19 nm particles during the entire field campaign. The GF-PDFs of both 50 and 250 nm  
20 showed two distinct modes, which are identified as hydrophobic mode (GF<1.2) and  
21 hydrophilic mode (GF>1.2). This implied that the particles were usually externally  
22 mixed. The hydrophilic mode of 250 nm particles is more prominent most of the time.  
23 Differently, the hydrophobic mode was dominated in 50 nm particles. As marked in  
24 the Fig. 4 (a) by the square with dashed line, the hydrophobic mode disappeared  
25 occasionally, indicating that the vast majority of particles in this size range can be  
26 fully hygroscopic. This phenomenon took place during the NPF events. A case study  
27 of particle hygroscopic behavior during the NPF event will be given in section 4.4.

28 Fig. 5 (left) shows the size-dependent particle hygroscopicity parameters and  
29 inorganic mass fraction of NR-PM<sub>1</sub> derived from averaging over the entire measuring  
30 period. The particle hygroscopicity increased with increasing particle size, displaying

1 the same size-dependency with the mass fraction of inorganic composition in  
2 NR-PM<sub>1</sub>. This is because inorganics including ammonium sulfate and ammonium  
3 nitrate are major water-soluble chemical compounds in the atmospheric particles.  
4 Compared to inorganic components, the hygroscopicity parameter of organic aerosols  
5 are typically lower than 0.1 (Varutbangkul et al., 2006; Virkkula et al., 1999). The  
6 similar size-dependency of particle hygroscopicity was observed in various  
7 environments. For examples, Levin et al. (2012;2014) and Paramonov et al. (2013)  
8 reported that particle hygroscopicity increased with particle size at a forested site in  
9 Colorado and a boreal environment of southern Finland at the SMEAR station,  
10 respectively. Jurányi et al (2013) observed that particle hygroscopic growth increased  
11 with increasing dry diameter in the urban areas of Paris. Swietlicki et al. (2008)  
12 compiled worldwide H-TDMA data and found that the particle hygroscopicity showed  
13 a pronounced size-dependency, with hygroscopicity increasing with particle diameter.

14 Fig. 5 (right) shows the size-dependency of the fraction of the hydrophilic mode.  
15 It can be seen that the hydrophilic mode was more prominent, no matter what particle  
16 size was considered. With increasing particle size, the dominance of hydrophilic mode  
17 became more pronounced. Above 150 nm, the number fraction of hydrophilic mode  
18 was around 0.8, and its size-dependency was insignificant. Below 150 nm, the number  
19 fraction of hydrophilic mode increases significantly with increasing particle size. The  
20 median number fraction of hydrophilic mode for 50 nm particles was 0.6, which was  
21 smaller than those of larger particles. Fors et al. (2011) also reported that smaller  
22 particles had a higher fraction of less hygroscopic particles in southern Sweden.  
23 Larger particles (here, above 150 nm) constituting a larger fraction of the hydrophilic  
24 mode can be explained as such: In the urban area, traffic emissions are major sources  
25 for particles below 100 nm. Typically, freshly emitted particles, such as soot, are  
26 initially hydrophobic and externally mixed. In contrast, larger particles have  
27 undergone atmospheric aging processes during transport (such as coagulation,  
28 condensation, chemical reaction) (Pöschl, 2005) for a longer time. These aging  
29 processes enhance the particle's water solubility (Pöschl, 2005; Jimenez et al., 2009)  
30 and result in more internally mixed particles.

1 Over the entire study, the mean  $\kappa$ s of 50, 100, 150, 250, and 350 nm particles were  
2  $0.16\pm 0.07$ ,  $0.19\pm 0.06$ ,  $0.22\pm 0.06$ ,  $0.26\pm 0.07$ , and  $0.28\pm 0.10$ , respectively. These  
3 values were similar to the hygroscopicity parameter  $\kappa = 0.12\text{--}0.27$  (measured at  
4  $\text{RH}=90\%$ ) for 35–265 nm determined in the urban atmosphere of Paris (Jurányi et al.,  
5 2013). Yeung et al. (2014) observed that hygroscopicity  $\kappa$ s of particles with sizes of  
6 75, 100, 150, and 200 nm were respectively 0.28, 0.29, 0.26, and 0.27 when Hong  
7 Kong experienced a continental airstream. In their study, the particle hygroscopicity  
8 showed no obvious size-dependency and was higher than our observation in Beijing.  
9 In contrast,  $\kappa$ s measured were relatively low at a forested site in Colorado ( $\kappa =$   
10  $0.16\pm 0.08$  detected by CCNc), a boreal forest in Finland ( $\kappa = 0.18$  at  $\text{RH}=90\%$ ) (Sihto  
11 et al., 2011), and a tropical forest site in the Amazon ( $\kappa = 0.16\pm 0.06$  detected by  
12 CCNc) (Gunthe et al., 2009). At these forested locations, organic species were  
13 predominance in particles. Differently, in the atmosphere of Beijing, the inorganic  
14 fraction was relatively dominated, as shown in the Fig.3 (c).

15 The haze issue caused by high aerosol loadings over the northern plain of China is  
16 a major concern, for both air quality and climate effects. Here, the  $\text{PM}_{2.5}$  mass  
17 concentration which measured by TEOM<sup>®</sup> Monitor (Series 1400ab), a key factor  
18 characterizing air pollution, vs. the fraction of the hydrophilic mode is plotted (Fig. 6)  
19 to analyze the relationship between the particle mixing state and air pollution. There  
20 was no obvious dependency between the  $\text{PM}_{2.5}$  mass concentration and the number  
21 fraction of hydrophilic mode for 50 nm particles, which can be expected due to the  
22 low mass fraction of ultrafine particles. This was however also true for 150, 250, and  
23 350 nm particles, if  $\text{PM}_{2.5}$  mass concentration is lower than  $50 \mu\text{g}/\text{m}^3$ . The reason for  
24 this is that the particle mass concentration is dominated by local sources and less by  
25 secondary aerosol particles formed during long-range transport. Conversely, when  
26  $\text{PM}_{2.5}$  mass concentration was larger than  $50 \mu\text{g}/\text{m}^3$ , the fraction of the hydrophilic  
27 mode was larger than 0.7. With the increasing  $\text{PM}_{2.5}$  mass concentration, the fraction  
28 rose towards to 1, indicating that the aged aerosols were dominant. This means that  
29 secondary aerosol particles were dominant during severe particulate pollution  
30 episodes, occurring frequently in Beijing. Our results were consistent to recent

1 scientific findings (Guo et al., 2014;Huang et al., 2014), which pointed out that the  
2 haze pollution events were mainly attributable to secondary aerosol formation.

### 3 **4.3 Closure between particle hygroscopicity and chemical components**

4 The AMS-derived particle mass concentrations for different chemical compounds  
5 were used to perform a closure study. The particle mass concentrations for individual  
6 species were integrated over the size interval of  $D_{\text{Pdry}} \pm 50$  nm. Here,  $D_{\text{Pdry}}$  is the dry  
7 particle diameter selected by H-TDMA. Considering the limited signal statistics in  
8 this narrow size range, AMS data were used to carry out the closure only if the sum of  
9 sulfate, nitrate, ammonium, and organics mass concentrations derived from  
10 integrating size range of  $D_{\text{Pdry}} \pm 50$  nm was greater than  $1 \mu\text{g}/\text{m}^3$ .

11 The BC particle mass concentration within the size range of  $D_{\text{Pdry}} \pm 50$  nm was  
12 estimated as follows: First, the ratio ( $R_{\text{BC}/\text{PM1}}$ ) of BC particle mass concentration  
13 (derived from PAX) to bulk particle mass concentration (derived from AMS  
14 measurement) was calculated, assuming this ratio was independent on the particle size.  
15 Afterwards, the BC particle mass concentration in a certain size range, e.g.,  $150 \pm 50$   
16 nm was estimated by multiplying the mass concentration derived from integrating  
17 particle size range of  $150 \pm 50$  nm (AMS data) and  $R_{\text{BC}/\text{PM1}}$ . One should note that this  
18 assumption may give an uncertainty in the closure, because the BC mass  
19 concentration has a dependency with particle size (Huang et al., 2006). Sun et al.  
20 (2012a) reported that the average mass size distribution of BC had one mode peaking  
21 at a volume-equivalent diameter of 207 nm. The sizes of 150, 250, 350 nm covered  
22 the peak of BC mass size distribution. As a result, the BC mass concentration for  
23 particles in diameter of 150, 250, and 350 nm should be higher than that estimated  
24 with the assumption of uniformly distributed BC across the whole particle size range.

25 The SOA and POA mass fractions within the size range of  $D_{\text{Pdry}} \pm 50$  nm were  
26 estimated using a similar method as the calculation of BC mass concentration given  
27 above. The POA ( $MF_{\text{POA}}$ ) and SOA ( $MF_{\text{SOA}}$ ) mass fractions in total organic aerosols  
28 in NR-PM1 are calculated on a basis of the AMS-PMF analysis results. Assuming



1  $MF_{\text{POA}}$  and  $MF_{\text{SOA}}$  were independent of the particle diameter, the POA or SOA mass  
2 concentration in the size range  $D_{\text{p,dry}} \pm 50$  nm can be calculated by multiplying the  
3 organic mass concentration derived from integrating particle size range of  $150 \pm 50$  nm  
4 (AMS data) and  $MF_{\text{POA}}$  or  $MF_{\text{SOA}}$ . Fig. 7 shows the scattering plots of  $\kappa_{\text{chem}}$  calculated  
5 from the size-resolved chemical composition against  $\kappa_{\text{HTDMA}}$ . The fitted slopes for  
6 150, 250, and 350 nm particles were 1.02, 0.99, and 0.97, respectively, which is close  
7 to unit. The root mean square errors (RMSE) of these linear fits were 0.04. This  
8 indicates that the measured  $\kappa$  can be well predicted on a basis of AMS data and the  
9 ZSR mixing rule. While, one should note that the assumption of BC mass size  
10 distribution and  $\kappa_{\text{org}}$  value in the closure as well as the measurement uncertainties for  
11 both H-TDMA and AMS could introduce the biases in the closure. This may lead to a  
12 scatter of data point around the fitting line.

13 Assuming the inorganic fraction was fully explained by the ZSR mixing rule,  $\kappa_{\text{org}}$   
14 can be calculated by subtracting  $\kappa$  of inorganic fraction and BC from  $\kappa_{\text{HTDMA}}$ .  
15 Here,  $\kappa_{\text{org}}$  for 150 nm particles was calculated because it provided a better closure  
16 result and higher organic fraction in contrast to other particle sizes. Duplissy et al.  
17 (2011) pointed out that the uncertainty in the estimation of  $\kappa_{\text{org}}$  decreases with  
18 increasing organic fraction, thereby, only data featuring organic fractions larger than  
19 50% were used in this calculation. In addition, the evaporation of  $\text{NH}_4\text{NO}_3$  could  
20 occur in the DMAs and the humidification section. This leads to a positive prediction  
21 bias because the volatile  $\text{NH}_4\text{NO}_3$ , which is fully detected by AMS, can evaporate in  
22 the H-TDMA system (Gysel et al., 2007). Here, only data with  $\text{NH}_4\text{NO}_3$  volume  
23 fraction below 20% were considered in order to reduce the evaporation artifact of  
24  $\text{NH}_4\text{NO}_3$ . Restricting data to times when ammonium nitrate is below 20% and  
25 organics were greater than 50% may lead to a bias in data points between daytime and  
26 nighttime. The statistics showed that nighttime data points (204 data points) were  
27 more than those during daytime (160 data points). This is because that the organic  
28 mass fraction during nighttime was higher than that during daytime. This bias could  
29 make the fit between  $\kappa_{\text{org}}$  and O:C ratio more representative for nighttime situation  
30 than daytime.

1 Fig. 8 shows  $\kappa_{\text{org}}$  as a function of O:C ratio. From the degree of scatter point of  
2 view,  $\kappa_{\text{org}}$  was not correlated to the O:C ratio. Several previous studies reported the  
3 similar plots of  $\kappa_{\text{org}}$  values as a function of O:C ratios (Chang et al., 2010;Bhattu and  
4 Tripathi, 2015;Rickards et al., 2013). In order to derive an empirical relationship  
5 between  $\kappa_{\text{org}}$  and O:C ratios,  $\kappa_{\text{org}}$  values were usually binned by O:C in increments of  
6 0.1. As displayed in Fig. 8, a linear fitting function  
7 ( $\kappa_{\text{org}}=(0.08\pm 0.02)*\text{O:C}+(0.02\pm 0.01)$ ) was obtained. Some empirical functions  
8 reported by other previous studies were also shown in Fig.8. In these previous studies  
9 (Wu et al., 2013;Jimenez et al., 2009;Rickards et al., 2013;Duplissy et al., 2011), the  
10  $\kappa_{\text{org}}$  were derived from the measurements performed in the sub-saturation regime. In  
11 Massoli et al.' study (2010) (not shown in the Fig. 8 due to the linear fitting using  
12 HGF, not  $\kappa_{\text{org}}$ ), they reported a linear relationship ( $\text{HGF}_{90\%} = (0.58\pm 0.15)*\text{O:C} + (0.85$   
13  $\pm 0.08)$ ) between  $\text{HGF}_{90\%}$  and O:C for the laboratory-generated SOA particles. Both  
14 results displayed in Fig. 8 and Massoli's study showed a positive correlation between  
15  $\kappa_{\text{org}}$  and O:C. Such positive correlation was also reported by those studies based on  
16 CCNc measurements, for examples, Chang et al. (2010) and Mei et al. (2013). We  
17 note that the slopes of the linear fitting varied with different studies, indicating there  
18 was no a simple parametrization to describe the relationship between organic  
19 hygroscopicity and its oxidation state though the various atmospheric environments.  
20 Recently, Richards et al. (2013) had undertaken an extensive review of  $\kappa$  values  
21 published in the literature and showed that  $\kappa_{\text{org}}$  vs. O:C plot has a large degree of  
22 scatter. This indicates that other factors, such as phase state (Pajunoja et al., 2015) and  
23 molecular structures (Suda et al., 2014) of organic aerosols (OA) other than oxidation  
24 state may also play a role in the determination of the OA hygroscopicity.

#### 25 4.4 Case study: particle hygroscopicity during a NPF event

26 As shown in Fig. 3 (a), the NPF events frequently took place during the sampling  
27 period. In order to understand the effects of NPF on particle hygroscopic behavior,  
28 this section will exemplify the evolution of particle hygroscopicity during a NPF

1 event. As an example, Fig. 9 displays the time series of particle number size  
2 distribution, GF-PDFs and water soluble fraction of 50 and 250 nm particles, and  
3 chemical composition of PM<sub>1</sub> during a NPF event occurred on 5<sup>th</sup> June, 2014. Here,  
4 the particles with 50 nm in diameter represented the newly formed particles, and  
5 particles with 250 nm in diameter represented the pre-existing particles.

6 The NPF event started at around 10:30 am and ended at 5:30 am the next day.  
7 After the starting of new particle formation, the number fraction of the hydrophilic  
8 mode for 50 nm particles increased from 0.5 to around 1, showing the conversion of  
9 externally to more internally mixed particles, as marked by the black dashed lines in  
10 Fig. 9 (b). Around 8:30 pm, the fraction of the hydrophilic mode particles dropped to  
11 0.6, and the hydrophobic mode appeared again. This is attributed to the intensive  
12 traffic emissions at the time of rush hour, which can clearly be seen from the particle  
13 number size distribution. During nighttime, the growth factor of hydrophilic mode  
14 particles decreased. This can be explained by sulfuric acid condensation playing a  
15 minor role in particle growth during nighttime. Simultaneously, ambient temperature  
16 decreased from 27 to 20 °C. Lower temperature facilitated the condensation of  
17 semi-volatile organic vapors onto the newly formed particles. The chemical  
18 composition of PM<sub>1</sub> also (Fig. 9 (d)) showed that the inorganic species and SOA were  
19 dominated before 8:30 pm, while mass fraction of organic compounds, especially  
20 POA increased significantly afterwards.

21 Clearly, an obvious enhancement in the water soluble fraction of 50 nm particles  
22 took place after the NPF event started. Similar phenomenon was also observed by  
23 Shantz et al. (2012), which showed that the 36 nm particles became increasingly CCN  
24 active within 1-4 h after the nucleation during the NPF events. They hypothesized that  
25 the condensation of sulphate on these small particles enhanced their CCN activity.  
26 The water soluble fraction accounted for 42% in 50 nm newly formed particles. The  
27 water soluble fraction was most likely ammonium sulfate formed from neutralization  
28 reaction between ammonia and sulfuric acid. In contrast, the newly formed particles  
29 consisted a minor fraction of water soluble fraction (16%) in Hyytiälä, Finland (Ehn  
30 et al., 2007). Other observations in the clean atmospheric environments (relative to

1 Beijing), such as a forested site in Colorado (Levin et al., 2012), Mace Head, Ireland  
2 (Väkevä et al., 2002), Melpitz, Germany (Wu et al., 2015) also showed that low water  
3 soluble compounds, most likely secondary organic species mainly contributed to new  
4 particle growth. Differently, in urban Atlanta (Sakurai et al., 2005), the water soluble  
5 fraction was dominated in the newly formed particles, which was similar to our  
6 observation in this study.

7 As shown in Figure 9 (c), the fraction of the hydrophilic mode of 250 nm particles  
8 increased significantly and approached 1 after the NPF event started. This can be  
9 explained as such: during the particle formation, a large amount of condensable  
10 vapors, such as sulfuric acid and secondary organic species produced because of the  
11 strongly active photochemistry. These condensable vapors can condense onto the  
12 pre-existing particle and result in the transformation of external mixture to internal  
13 mixture. Such transformation may alter the atmospheric behaviors of pre-existing  
14 particles, such as optical property and cloud condensation nuclei activation during the  
15 new particle formation events.

## 16 **5 Conclusions**

17 Particle number size distribution, particle hygroscopicity, and size-resolved  
18 chemical composition were measured concurrently during summertime 2014 in  
19 Beijing, China. The particle hygroscopicity showed a pronounced size-dependency. It  
20 increased with increasing particle size. During the measurement period, the mean  $\kappa$ s  
21 of 50, 100, 150, 200, and 250 nm particles are  $0.16 \pm 0.07$ ,  $0.19 \pm 0.06$ ,  $0.22 \pm 0.06$ ,  
22  $0.26 \pm 0.07$ , and  $0.28 \pm 0.10$ , respectively. The size-dependency behavior of particle  
23 hygroscopicity was similar to that of inorganic compounds in  $PM_{10}$ . The hydrophilic  
24 mode ( $HGF > 1.2$ ) was more prominent, no matter what particle size was considered.  
25 With increasing particle size, the dominance of hydrophilic mode became more  
26 pronounced. When  $PM_{2.5}$  mass concentration was below  $50 \mu\text{g}/\text{m}^3$ , no dependency  
27 between  $PM_{2.5}$  mass concentration and the number fraction of hydrophilic mode was  
28 found. Above  $50 \mu\text{g}/\text{m}^3$ , the number fraction of hydrophilic mode for 150, 250, 350

1 nm particles increased and rose towards to 1 with the increasing PM<sub>2.5</sub> mass  
2 concentration. This means that aged particles was dominated the particle mass  
3 concentration, especially during severe particulate pollution events in Beijing. Based  
4 on the size-resolved AMS data, the particle hygroscopic growth can be well predicted  
5 using the ZSR method. The organic hygroscopicity parameter showed a positive  
6 correlation with O:C ratio.

7 Frequent new particle formation events took place during the measuring period.  
8 The hygroscopic growth factor or  $\kappa$  of newly formed particles was greater than the  
9 hygroscopic growth factor of particles with the same sizes during non-NPF periods.  
10 During the new particle formation, fast transformations of external mixture to internal  
11 mixture for existing particles (for example 250 nm particle) have been observed. This  
12 was a strong indication that secondary aerosol material such as organics and sulfates  
13 were produced due to the strongly active photochemistry during NPF events, and  
14 subsequently condensed onto the particles. Such transformation may modify the  
15 atmospheric behaviors of pre-existing particles, such as optical property and cloud  
16 condensation nuclei activation.

17

### 18 **Acknowledgement**

19 This work is supported by the following projects: National Natural Science  
20 Foundation of China (41475127), National Basic Research Program of China  
21 (2013CB228503), and Special Fund of State Key Joint Laboratory of Environment  
22 Simulation and Pollution Control (14L02ESPC). The authors would like to thank  
23 Douglas R. Worsnop for useful discussion about the AMS size distribution data  
24 processing.

### 25 **Reference**

26 Achtert, P., Birmili, W., Nowak, A., Wehner, B., Wiedensohler, A., Takegawa, N., Kondo, Y.,  
27 Miyazaki, Y., Hu, M., and Zhu, T.: Hygroscopic growth of tropospheric particle number size  
28 distributions over the North China Plain, *Journal of Geophysical Research: Atmospheres*, 114,  
29 n/a-n/a, 10.1029/2008JD010921, 2009.

1 Alfarra, M. R., Paulsen, D., Gysel, M., Garforth, A. A., Dommen, J., Prévôt, A. S. H.,  
2 Worsnop, D. R., Baltensperger, U., and Coe, H.: A mass spectrometric study of secondary  
3 organic aerosols formed from the photooxidation of anthropogenic and biogenic precursors in  
4 a reaction chamber, *Atmos. Chem. Phys.*, 6, 5279-5293, 10.5194/acp-6-5279-2006, 2006.

5 Arnott, P., Moosmüller, H., Fred Rogers, C., Jin, T., and Bruch, R.: Photoacoustic  
6 spectrometer for measuring light absorption by aerosol: instrument description, *Atmospheric  
7 Environment*, 33, 2845-2852, [http://dx.doi.org/10.1016/S1352-2310\(98\)00361-6](http://dx.doi.org/10.1016/S1352-2310(98)00361-6), 1999.

8 Bhattu, D., and Tripathi, S. N.: CCN closure study: Effects of aerosol chemical composition  
9 and mixing state, *Journal of Geophysical Research: Atmospheres*, 120, 2014JD021978,  
10 10.1002/2014JD021978, 2015.

11 Canagaratna, M. R., Jayne, J. T., Jimenez, J. L., Allan, J. D., Alfarra, M. R., Zhang, Q.,  
12 Onasch, T. B., Drewnick, F., Coe, H., Middlebrook, A., Delia, A., Williams, L. R., Trimborn,  
13 A. M., Northway, M. J., DeCarlo, P. F., Kolb, C. E., Davidovits, P., and Worsnop, D. R.:  
14 Chemical and microphysical characterization of ambient aerosols with the aerodyne aerosol  
15 mass spectrometer, *Mass Spectrometry Reviews*, 26, 185-222, 10.1002/mas.20115, 2007.

16 Canagaratna, M. R., Jimenez, J. L., Kroll, J. H., Chen, Q., Kessler, S. H., Massoli, P.,  
17 Hildebrandt Ruiz, L., Fortner, E., Williams, L. R., Wilson, K. R., Surratt, J. D., Donahue, N.  
18 M., Jayne, J. T., and Worsnop, D. R.: Elemental ratio measurements of organic compounds  
19 using aerosol mass spectrometry: characterization, improved calibration, and implications,  
20 *Atmos. Chem. Phys.*, 15, 253-272, 10.5194/acp-15-253-2015, 2015.

21 Cerully, K. M., Raatikainen, T., Lance, S., Tkacik, D., Tiitta, P., Petäjä, T., Ehn, M., Kulmala,  
22 M., Worsnop, D. R., Laaksonen, A., Smith, J. N., and Nenes, A.: Aerosol hygroscopicity and  
23 CCN activation kinetics in a boreal forest environment during the 2007 EUCAARI campaign,  
24 *Atmos. Chem. Phys.*, 11, 12369-12386, 10.5194/acp-11-12369-2011, 2011.

25 Chang, R. Y. W., Slowik, J. G., Shantz, N. C., Vlasenko, A., Liggio, J., Sjostedt, S. J., Leitch,  
26 W. R., and Abbatt, J. P. D.: The hygroscopicity parameter ( $\kappa$ ) of ambient organic aerosol at a  
27 field site subject to biogenic and anthropogenic influences: relationship to degree of aerosol  
28 oxidation, *Atmos. Chem. Phys.*, 10, 5047-5064, 10.5194/acp-10-5047-2010, 2010.

29 Cheng, Y. F., Wiedensohler, A., Eichler, H., Heintzenberg, J., Tesche, M., Ansmann, A.,  
30 Wendisch, M., Su, H., Althausen, D., Herrmann, H., Gnauk, T., Brüggemann, E., Hu, M., and  
31 Zhang, Y. H.: Relative humidity dependence of aerosol optical properties and direct radiative  
32 forcing in the surface boundary layer at Xinken in Pearl River Delta of China: An observation  
33 based numerical study, *Atmospheric Environment*, 42, 6373-6397,  
34 <http://dx.doi.org/10.1016/j.atmosenv.2008.04.009>, 2008.

35 DeCarlo, P. F., Kimmel, J. R., Trimborn, A., Northway, M. J., Jayne, J. T., Aiken, A. C., Gonin,  
36 M., Fuhrer, K., Horvath, T., Docherty, K. S., Worsnop, D. R., and Jimenez, J. L.:  
37 Field-Deployable, High-Resolution, Time-of-Flight Aerosol Mass Spectrometer, *Analytical  
38 Chemistry*, 78, 8281-8289, 10.1021/ac061249n, 2006.

- 1 Dinar, E., Mentel, T. F., and Rudich, Y.: The density of humic acids and humic like substances  
2 (HULIS) from fresh and aged wood burning and pollution aerosol particles, *Atmos. Chem.  
3 Phys.*, 6, 5213-5224, 10.5194/acp-6-5213-2006, 2006.
- 4 Draxler, R. R., and Hess, G. D.: An overview of the HYSPLIT\_4 modelling system for  
5 trajectories dispersion and deposition, *Australian Meteorological Magazine*, 47, 295-308,  
6 1998.
- 7 Duplissy, J., DeCarlo, P. F., Dommen, J., Alfarra, M. R., Metzger, A., Barmpadimos, I., Prevot,  
8 A. S. H., Weingartner, E., Tritscher, T., Gysel, M., Aiken, A. C., Jimenez, J. L., Canagaratna,  
9 M. R., Worsnop, D. R., Collins, D. R., Tomlinson, J., and Baltensperger, U.: Relating  
10 hygroscopicity and composition of organic aerosol particulate matter, *Atmos. Chem. Phys.*, 11,  
11 1155-1165, 10.5194/acp-11-1155-2011, 2011.
- 12 Ehn, M., Petäjä, T., Aufmhoff, H., Aalto, P., Hämeri, K., Arnold, F., Laaksonen, A., and  
13 Kulmala, M.: Hygroscopic properties of ultrafine aerosol particles in the boreal forest: diurnal  
14 variation, solubility and the influence of sulfuric acid, *Atmos. Chem. Phys.*, 7, 211-222,  
15 10.5194/acp-7-211-2007, 2007.
- 16 Fors, E. O., Swietlicki, E., Svenningsson, B., Kristensson, A., Frank, G. P., and Sporre, M.:  
17 Hygroscopic properties of the ambient aerosol in southern Sweden – a two year study, *Atmos.  
18 Chem. Phys.*, 11, 8343-8361, 10.5194/acp-11-8343-2011, 2011.
- 19 Gunthe, S. S., King, S. M., Rose, D., Chen, Q., Roldin, P., Farmer, D. K., Jimenez, J. L.,  
20 Artaxo, P., Andreae, M. O., Martin, S. T., and Pöschl, U.: Cloud condensation nuclei in  
21 pristine tropical rainforest air of Amazonia: size-resolved measurements and modeling of  
22 atmospheric aerosol composition and CCN activity, *Atmos. Chem. Phys.*, 9, 7551-7575,  
23 10.5194/acp-9-7551-2009, 2009.
- 24 Guo, S., Hu, M., Zamora, M. L., Peng, J., Shang, D., Zheng, J., Du, Z., Wu, Z., Shao, M.,  
25 Zeng, L., Molina, M. J., and Zhang, R.: Elucidating severe urban haze formation in China,  
26 *Proceedings of the National Academy of Sciences*, 111, 17373-17378,  
27 10.1073/pnas.1419604111, 2014.
- 28 Gysel, M., Crosier, J., Topping, D. O., Whitehead, J. D., Bower, K. N., Cubison, M. J.,  
29 Williams, P. I., Flynn, M. J., McFiggans, G. B., and Coe, H.: Closure study between chemical  
30 composition and hygroscopic growth of aerosol particles during TORCH2, *Atmos. Chem.  
31 Phys.*, 7, 6131-6144, 10.5194/acp-7-6131-2007, 2007.
- 32 Gysel, M., McFiggans, G. B., and Coe, H.: Inversion of tandem differential mobility analyser  
33 (TDMA) measurements, *Journal of Aerosol Science*, 40, 134-151,  
34 10.1016/j.jaerosci.2008.07.013, 2009.
- 35 Hallquist, M., Wenger, J. C., Baltensperger, U., Rudich, Y., Simpson, D., Claeys, M.,  
36 Dommen, J., Donahue, N. M., George, C., Goldstein, A. H., Hamilton, J. F., Herrmann, H.,  
37 Hoffmann, T., Iinuma, Y., Jang, M., Jenkin, M. E., Jimenez, J. L., Kiendler-Scharr, A.,

- 1 Maenhaut, W., McFiggans, G., Mentel, T. F., Monod, A., Prevot, A. S. H., Seinfeld, J. H.,  
2 Surratt, J. D., Szmigielski, R., and Wildt, J.: The formation, properties and impact of  
3 secondary organic aerosol: current and emerging issues, *Atmospheric Chemistry and Physics*,  
4 9, 5155-5236, 2009.
- 5 Haywood, J., and Boucher, O.: Estimates of the direct and indirect radiative forcing due to  
6 tropospheric aerosols: A review, *Reviews of Geophysics*, 38, 513-543,  
7 10.1029/1999RG000078, 2000.
- 8 Huang, R.-J., Zhang, Y., Bozzetti, C., Ho, K.-F., Cao, J.-J., Han, Y., Daellenbach, K. R.,  
9 Slowik, J. G., Platt, S. M., Canonaco, F., Zotter, P., Wolf, R., Pieber, S. M., Bruns, E. A.,  
10 Crippa, M., Ciarelli, G., Piazzalunga, A., Schwikowski, M., Abbaszade, G., Schnelle-Kreis, J.,  
11 Zimmermann, R., An, Z., Szidat, S., Baltensperger, U., Haddad, I. E., and Prevot, A. S. H.:  
12 High secondary aerosol contribution to particulate pollution during haze events in China,  
13 *Nature*, 514, 218-222, 10.1038/nature13774  
14 [http://www.nature.com/nature/journal/v514/n7521/abs/nature13774.html#supplementary-info](http://www.nature.com/nature/journal/v514/n7521/abs/nature13774.html#supplementary-information)  
15 [rmation](http://www.nature.com/nature/journal/v514/n7521/abs/nature13774.html#supplementary-information), 2014.
- 16 Huang, X. F., Yu, J. Z., He, L. Y., and Hu, M.: Size distribution characteristics of elemental  
17 carbon emitted from Chinese vehicles: Results of a tunnel study and atmospheric implications,  
18 *Environmental Science & Technology*, 40, 5355-5360, 10.1021/es0607281, 2006.
- 19 Jimenez, J. L., Canagaratna, M. R., Donahue, N. M., Prevot, A. S. H., Zhang, Q., Kroll, J. H.,  
20 DeCarlo, P. F., Allan, J. D., Coe, H., Ng, N. L., Aiken, A. C., Docherty, K. S., Ulbrich, I. M.,  
21 Grieshop, A. P., Robinson, A. L., Duplissy, J., Smith, J. D., Wilson, K. R., Lanz, V. A.,  
22 Hueglin, C., Sun, Y. L., Tian, J., Laaksonen, A., Raatikainen, T., Rautiainen, J., Vaattovaara, P.,  
23 Ehn, M., Kulmala, M., Tomlinson, J. M., Collins, D. R., Cubison, M. J., E, Dunlea, J.,  
24 Huffman, J. A., Onasch, T. B., Alfarra, M. R., Williams, P. I., Bower, K., Kondo, Y., Schneider,  
25 J., Drewnick, F., Borrmann, S., Weimer, S., Demerjian, K., Salcedo, D., Cottrell, L., Griffin,  
26 R., Takami, A., Miyoshi, T., Hatakeyama, S., Shimono, A., Sun, J. Y., Zhang, Y. M., Dzepina,  
27 K., Kimmel, J. R., Sueper, D., Jayne, J. T., Herndon, S. C., Trimborn, A. M., Williams, L. R.,  
28 Wood, E. C., Middlebrook, A. M., Kolb, C. E., Baltensperger, U., and Worsnop, D. R.:  
29 Evolution of organic aerosols in the atmosphere, *Science*, 326, 1525-1529,  
30 10.1126/science.1180353, 2009.
- 31 Jurányi, Z., Tritscher, T., Gysel, M., Laborde, M., Gomes, L., Roberts, G., Baltensperger, U.,  
32 and Weingartner, E.: Hygroscopic mixing state of urban aerosol derived from size-resolved  
33 cloud condensation nuclei measurements during the MEGAPOLI campaign in Paris, *Atmos.*  
34 *Chem. Phys.*, 13, 6431-6446, 10.5194/acp-13-6431-2013, 2013.
- 35 Kanakidou, M., Seinfeld, J. H., Pandis, S. N., Barnes, I., Dentener, F. J., Facchini, M. C., Van  
36 Dingenen, R., Ervens, B., Nenes, A., Nielsen, C. J., Swietlicki, E., Putaud, J. P., Balkanski, Y.,  
37 Fuzzi, S., Horth, J., Moortgat, G. K., Winterhalter, R., Myhre, C. E. L., Tsigaridis, K., Vignati,  
38 E., Stephanou, E. G., and Wilson, J.: Organic aerosol and global climate modelling: a review,  
39 *Atmospheric Chemistry and Physics*, 5, 1053-1123, 2005.



- 1 Kiselev, A., Wennrich, C., Stratmann, F., Wex, H., Henning, S., Mentel, T. F., Kiendler-Scharr,  
2 A., Schneider, J., Walter, S., and Lieberwirth, I.: Morphological characterization of soot  
3 aerosol particles during LACIS Experiment in November (LEXNo), *Journal of Geophysical*  
4 *Research-Atmospheres*, 115, Artn D11204  
5 Doi 10.1029/2009jd012635, 2010.
- 6 Kondo, Y., Sahu, L., Moteki, N., Khan, F., Takegawa, N., Liu, X., Koike, M., and Miyakawa,  
7 T.: Consistency and Traceability of Black Carbon Measurements Made by Laser-Induced  
8 Incandescence, Thermal-Optical Transmittance, and Filter-Based Photo-Absorption  
9 Techniques, *Aerosol Science and Technology*, 45, 295-312, 10.1080/02786826.2010.533215,  
10 2011.
- 11 Kreidenweis, S. M., and Asa-Awuku, A.: 5.13 - Aerosol Hygroscopicity: Particle Water  
12 Content and Its Role in Atmospheric Processes, in: *Treatise on Geochemistry (Second*  
13 *Edition)*, edited by: Turekian, H. D. H. K., Elsevier, Oxford, 331-361, 2014.
- 14 Lambe, A. T., Onasch, T. B., Massoli, P., Croasdale, D. R., Wright, J. P., Ahern, A. T.,  
15 Williams, L. R., Worsnop, D. R., Brune, W. H., and Davidovits, P.: Laboratory studies of the  
16 chemical composition and cloud condensation nuclei (CCN) activity of secondary organic  
17 aerosol (SOA) and oxidized primary organic aerosol (OPOA), *Atmos. Chem. Phys.*, 11,  
18 8913-8928, 10.5194/acp-11-8913-2011, 2011.
- 19 Lanz, V. A., Alfarra, M. R., Baltensperger, U., Buchmann, B., Hueglin, C., and Prévôt, A. S.  
20 H.: Source apportionment of submicron organic aerosols at an urban site by factor analytical  
21 modelling of aerosol mass spectra, *Atmos. Chem. Phys.*, 7, 1503-1522,  
22 10.5194/acp-7-1503-2007, 2007.
- 23 Levin, E. J. T., Prenni, A. J., Petters, M. D., Kreidenweis, S. M., Sullivan, R. C., Atwood, S.  
24 A., Ortega, J., DeMott, P. J., and Smith, J. N.: An annual cycle of size-resolved aerosol  
25 hygroscopicity at a forested site in Colorado, *J. Geophys. Res.*, 117, D06201,  
26 10.1029/2011jd016854, 2012.
- 27 Levin, E. J. T., Prenni, A. J., Palm, B. B., Day, D. A., Campuzano-Jost, P., Winkler, P. M.,  
28 Kreidenweis, S. M., DeMott, P. J., Jimenez, J. L., and Smith, J. N.: Size-resolved aerosol  
29 composition and its link to hygroscopicity at a forested site in Colorado, *Atmos. Chem. Phys.*,  
30 14, 2657-2667, 10.5194/acp-14-2657-2014, 2014.
- 31 Li, L., Wang, Y., Zhang, Q., Li, J., Yang, X., and Jin, J.:  
32 Wheat straw burning and its associated impacts on Beijing air quality, *Science in China Series*  
33 *D: Earth Sciences*, 51, 403-414, 2008.
- 34 Liu, P. F., Zhao, C. S., Göbel, T., Hallbauer, E., Nowak, A., Ran, L., Xu, W. Y., Deng, Z. Z.,  
35 Ma, N., Mildenberger, K., Henning, S., Stratmann, F., and Wiedensohler, A.: Hygroscopic  
36 properties of aerosol particles at high relative humidity and their diurnal variations in the  
37 North China Plain, *Atmos. Chem. Phys.*, 11, 3479-3494, 10.5194/acp-11-3479-2011, 2011.

1 Lopez-Yglesias, X. F., Yeung, M. C., Dey, S. E., Brechtel, F. J., and Chan, C. K.: Performance  
2 Evaluation of the Brechtel Mfg. Humidified Tandem Differential Mobility Analyzer (BMI  
3 HTDMA) for Studying Hygroscopic Properties of Aerosol Particles, *Aerosol Science and  
4 Technology*, 48, 969-980, 10.1080/02786826.2014.952366, 2014.

5 Malm, W. C., and Kreidenweis, S. M.: The effects of models of aerosol hygroscopicity on the  
6 apportionment of extinction, *Atmospheric Environment*, 31, 1965-1976,  
7 10.1016/s1352-2310(96)00355-x, 1997.

8 Massling, A., Wiedensohler, A., Busch, B., Neusüß, C., Quinn, P., Bates, T., and Covert, D.:  
9 Hygroscopic properties of different aerosol types over the Atlantic and Indian Oceans, *Atmos.  
10 Chem. Phys.*, 3, 1377-1397, 10.5194/acp-3-1377-2003, 2003.

11 Massling, A., Stock, M., Wehner, B., Wu, Z. J., Hu, M., Brüggemann, E., Gnauk, T.,  
12 Herrmann, H., and Wiedensohler, A.: Size segregated water uptake of the urban  
13 submicrometer aerosol in Beijing, *Atmospheric Environment*, 43, 1578-1589,  
14 <http://dx.doi.org/10.1016/j.atmosenv.2008.06.003>, 2009.

15 Massling, A., Niedermeier, N., Hennig, T., Fors, E. O., Swietlicki, E., Ehn, M., Hämeri, K.,  
16 Villani, P., Laj, P., Good, N., McFiggans, G., and Wiedensohler, A.: Results and  
17 recommendations from an intercomparison of six Hygroscopicity-TDMA systems, *Atmos.  
18 Meas. Tech.*, 4, 485-497, 10.5194/amt-4-485-2011, 2011.

19 Massoli, P., Lambe, A. T., Ahern, A. T., Williams, L. R., Ehn, M., Mikkilä, J., Canagaratna, M.  
20 R., Brune, W. H., Onasch, T. B., Jayne, J. T., Petäjä, T., Kulmala, M., Laaksonen, A., Kolb, C.  
21 E., Davidovits, P., and Worsnop, D. R.: Relationship between aerosol oxidation level and  
22 hygroscopic properties of laboratory generated secondary organic aerosol (SOA) particles,  
23 *Geophysical Research Letters*, 37, n/a-n/a, 10.1029/2010GL045258, 2010.

24 McFiggans, G., Artaxo, P., Baltensperger, U., Coe, H., Facchini, M. C., Feingold, G., Fuzzi, S.,  
25 Gysel, M., Laaksonen, A., Lohmann, U., Mentel, T. F., Murphy, D. M., O'Dowd, C. D., Snider,  
26 J. R., and Weingartner, E.: The effect of physical and chemical aerosol properties on warm  
27 cloud droplet activation, *Atmospheric Chemistry and Physics*, 6, 2593-2649, 2006.

28 McMurry, P. H., Wang, X., Park, K., and Ehara, K.: The Relationship between Mass and  
29 Mobility for Atmospheric Particles: A New Technique for Measuring Particle Density,  
30 *Aerosol Science and Technology*, 36, 227-238, 10.1080/027868202753504083, 2002.

31 Medina, J., Nenes, A., Sotiropoulou, R.-E. P., Cottrell, L. D., Ziemba, L. D., Beckman, P. J.,  
32 and Griffin, R. J.: Cloud condensation nuclei closure during the International Consortium for  
33 Atmospheric Research on Transport and Transformation 2004 campaign: Effects of  
34 size-resolved composition, *J. Geophys. Res.*, 112, D10S31, 10.1029/2006jd007588, 2007.

35 Mei, F., Hayes, P. L., Ortega, A., Taylor, J. W., Allan, J. D., Gilman, J., Kuster, W., de Gouw,  
36 J., Jimenez, J. L., and Wang, J.: Droplet activation properties of organic aerosols observed at  
37 an urban site during CalNex-LA, *Journal of Geophysical Research: Atmospheres*, 118,

1 2903-2917, 10.1002/jgrd.50285, 2013.

2 Meier, J., Wehner, B., Massling, A., Birmili, W., Nowak, A., Gnauk, T., Brüggemann, E.,  
3 Herrmann, H., Min, H., and Wiedensohler, A.: Hygroscopic growth of urban aerosol particles  
4 in Beijing (China) during wintertime: a comparison of three experimental methods, *Atmos.*  
5 *Chem. Phys.*, 9, 6865-6880, 10.5194/acp-9-6865-2009, 2009.

6 Moore, R. H., Cerully, K., Bahreini, R., Brock, C. A., Middlebrook, A. M., and Nenes, A.:  
7 Hygroscopicity and composition of California CCN during summer 2010, *Journal of*  
8 *Geophysical Research: Atmospheres*, 117, n/a-n/a, 10.1029/2011JD017352, 2012a.

9 Moore, R. H., Raatikainen, T., Langridge, J. M., Bahreini, R., Brock, C. A., Holloway, J. S.,  
10 Lack, D. A., Middlebrook, A. M., Perring, A. E., Schwarz, J. P., Spackman, J. R., and Nenes,  
11 A.: CCN Spectra, Hygroscopicity, and Droplet Activation Kinetics of Secondary Organic  
12 Aerosol Resulting from the 2010 Deepwater Horizon Oil Spill, *Environmental Science &*  
13 *Technology*, 46, 3093-3100, 10.1021/es203362w, 2012b.

14 Pöschl, U.: Atmospheric aerosols: Composition, transformation, climate and health effects,  
15 *Angewandte Chemie-International Edition*, 44, 7520-7541, citeulike-article-id:6549360,  
16 2005.

17 Pajunoja, A., Lambe, A. T., Hakala, J., Rastak, N., Cummings, M. J., Brogan, J. F., Hao, L.,  
18 Paramonov, M., Hong, J., Prisle, N. L., Malila, J., Romakkaniemi, S., Lehtinen, K. E. J.,  
19 Laaksonen, A., Kulmala, M., Massoli, P., Onasch, T. B., Donahue, N. M., Riipinen, I.,  
20 Davidovits, P., Worsnop, D. R., Petäjä, T., and Virtanen, A.: Adsorptive uptake of water by  
21 semisolid secondary organic aerosols, *Geophysical Research Letters*, 42, 3063-3068,  
22 10.1002/2015GL063142, 2015.

23 Paramonov, M., Aalto, P. P., Asmi, A., Prisle, N., Kerminen, V. M., Kulmala, M., and Petäjä,  
24 T.: The analysis of size-segregated cloud condensation nuclei counter (CCNC) data and its  
25 implications for cloud droplet activation, *Atmos. Chem. Phys.*, 13, 10285-10301,  
26 10.5194/acp-13-10285-2013, 2013.

27 Park, K., Kittelson, D. B., Zachariah, M. R., and McMurry, P. H.: Measurement of inherent  
28 material density of nanoparticle agglomerates, *Journal of Nanoparticle Research*, 6, 267-272,  
29 2004.

30 Petters, M. D., and Kreidenweis, S. M.: A single parameter representation of hygroscopic  
31 growth and cloud condensation nucleus activity, *Atmos. Chem. Phys.*, 7, 1961-1971,  
32 10.5194/acp-7-1961-2007, 2007.

33 Potukuchi, S., and Wexler, A. S.: Identifying solid-aqueous phase transitions in atmospheric  
34 aerosols—I. Neutral-acidity solutions, *Atmospheric Environment*, 29, 1663-1676,  
35 [http://dx.doi.org/10.1016/1352-2310\(95\)00074-9](http://dx.doi.org/10.1016/1352-2310(95)00074-9), 1995.

36 Rickards, A. M. J., Miles, R. E. H., Davies, J. F., Marshall, F. H., and Reid, J. P.:  
37 Measurements of the Sensitivity of Aerosol Hygroscopicity and the  $\kappa$  Parameter to the O/C

1 Ratio, *The Journal of Physical Chemistry A*, 117, 14120-14131, 10.1021/jp407991n, 2013.

2 Sakurai, H., Fink, M. A., McMurry, P. H., Mauldin, L., Moore, K. F., Smith, J. N., and Eisele,  
3 F. L.: Hygroscopicity and volatility of 4–10 nm particles during summertime atmospheric  
4 nucleation events in urban Atlanta, *Journal of Geophysical Research: Atmospheres*, 110,  
5 n/a-n/a, 10.1029/2005JD005918, 2005.

6 Shantz, N. C., Pierce, J. R., Chang, R. Y. W., Vlasenko, A., Riipinen, I., Sjostedt, S., Slowik, J.  
7 G., Wiebe, A., Liggio, J., Abbatt, J. P. D., and Leaitch, W. R.: Cloud condensation nuclei  
8 droplet growth kinetics of ultrafine particles during anthropogenic nucleation events,  
9 *Atmospheric Environment*, 47, 389-398, <http://dx.doi.org/10.1016/j.atmosenv.2011.10.049>,  
10 2012.

11 Sihto, S. L., Mikkilä, J., Vanhanen, J., Ehn, M., Liao, L., Lehtipalo, K., Aalto, P. P., Duplissy,  
12 J., Petäjä, T., Kerminen, V. M., Boy, M., and Kulmala, M.: Seasonal variation of CCN  
13 concentrations and aerosol activation properties in boreal forest, *Atmos. Chem. Phys.*, 11,  
14 13269-13285, 10.5194/acp-11-13269-2011, 2011.

15 Sloane, C. S., and Wolff, G. T.: Prediction of ambient light scattering using a physical model  
16 responsive to relative humidity: Validation with measurements from detroit, *Atmospheric*  
17 *Environment* (1967), 19, 669-680, [http://dx.doi.org/10.1016/0004-6981\(85\)90046-0](http://dx.doi.org/10.1016/0004-6981(85)90046-0), 1985.

18 Stokes, R. H., and Robinson, R. A.: Interactions in Aqueous Nonelectrolyte Solutions. I.  
19 Solute-Solvent Equilibria, *Journal of Physical Chemistry*, 70, 2126-2130, 1966.

20 Suda, S. R., Petters, M. D., Yeh, G. K., Strollo, C., Matsunaga, A., Faulhaber, A., Ziemann, P.  
21 J., Prenni, A. J., Carrico, C. M., Sullivan, R. C., and Kreidenweis, S. M.: Influence of  
22 Functional Groups on Organic Aerosol Cloud Condensation Nucleus Activity, *Environmental*  
23 *Science & Technology*, 48, 10182-10190, 10.1021/es502147y, 2014.

24 Sun, T. L., He, L. Y., Zeng, L. W., and Huang, X. F.: Black carbon measurement during  
25 Beijing Paralympic Games, *China Environmental Science*, 32, 2123-2127, 2012a.

26 Sun, Y. L., Zhang, Q., Schwab, J. J., Yang, T., Ng, N. L., and Demerjian, K. L.: Factor  
27 analysis of combined organic and inorganic aerosol mass spectra from high resolution aerosol  
28 mass spectrometer measurements, *Atmos. Chem. Phys.*, 12, 8537-8551,  
29 10.5194/acp-12-8537-2012, 2012b.

30 Swietlicki, E., Zhou, J., Berg, O. H., Martinsson, B. G., Frank, G., Cederfelt, S.-I., Dusek, U.,  
31 Berner, A., Birmili, W., Wiedensohler, A., Yuskiewicz, B., and Bower, K. N.: A closure study  
32 of sub-micrometer aerosol particle hygroscopic behaviour, *Atmospheric Research*, 50,  
33 205-240, 10.1016/s0169-8095(98)00105-7, 1999.

34 Swietlicki, E., Hansson, H. C., HÄMeri, K., Svenningsson, B., Massling, A., McFiggans, G.,  
35 McMurry, P. H., PetÄJÄ, T., Tunved, P., Gysel, M., Topping, D., Weingartner, E.,  
36 Baltensperger, U., Rissler, J., Wiedensohler, A., and Kulmala, M.: Hygroscopic properties of  
37 submicrometer atmospheric aerosol particles measured with H-TDMA instruments in various

1 environments—a review, *Tellus B*, 60, 432-469, 10.1111/j.1600-0889.2008.00350.x, 2008.

2 Tang, I. N., and Munkelwitz, H. R.: Water activities, densities, and refractive indices of  
3 aqueous sulfates and sodium nitrate droplets of atmospheric importance, *J. Geophys. Res.*, 99,  
4 18801-18808, 10.1029/94jd01345, 1994.

5 Ulbrich, I. M., Canagaratna, M. R., Zhang, Q., Worsnop, D. R., and Jimenez, J. L.:  
6 Interpretation of organic components from Positive Matrix Factorization of aerosol mass  
7 spectrometric data, *Atmos. Chem. Phys.*, 9, 2891-2918, 10.5194/acp-9-2891-2009, 2009.

8 Väkevää, M., Hämeri, K., and Aalto, P. P.: Hygroscopic properties of nucleation mode and  
9 Aitken mode particles during nucleation bursts and in background air on the west coast of  
10 Ireland, *Journal of Geophysical Research: Atmospheres*, 107, PAR 9-1-PAR 9-11,  
11 10.1029/2000JD000176, 2002.

12 Varutbangkul, V., Brechtel, F. J., Bahreini, R., Ng, N. L., Keywood, M. D., Kroll, J. H.,  
13 Flagan, R. C., Seinfeld, J. H., Lee, A., and Goldstein, A. H.: Hygroscopicity of secondary  
14 organic aerosols formed by oxidation of cycloalkenes, monoterpenes, sesquiterpenes, and  
15 related compounds, *Atmos. Chem. Phys.*, 6, 2367-2388, 10.5194/acp-6-2367-2006, 2006.

16 Virkkula, A., Van Dingenen, R., Raes, F., and Hjorth, J.: Hygroscopic properties of aerosol  
17 formed by oxidation of limonene,  $\alpha$ -pinene, and  $\beta$ -pinene, *J. Geophys. Res.*, 104, 3569-3579,  
18 10.1029/1998jd100017, 1999.

19 Wehner, B., Birmili, W., Ditas, F., Wu, Z., Hu, M., Liu, X., Mao, J., Sugimoto, N., and  
20 Wiedensohler, A.: Relationships between submicrometer particulate air pollution and air mass  
21 history in Beijing, China, 2004–2006, *Atmos. Chem. Phys.*, 8, 6155-6168,  
22 10.5194/acp-8-6155-2008, 2008.

23 Wong, J. P. S., Lee, A. K. Y., Slowik, J. G., Cziczo, D. J., Leaitch, W. R., Macdonald, A., and  
24 Abbatt, J. P. D.: Oxidation of ambient biogenic secondary organic aerosol by hydroxyl  
25 radicals: Effects on cloud condensation nuclei activity, *Geophysical Research Letters*, 38,  
26 n/a-n/a, 10.1029/2011GL049351, 2011.

27 Wu, Z., Hu, M., Liu, S., Wehner, B., Bauer, S., Maßling, A., Wiedensohler, A., Petäjä, T., Dal  
28 Maso, M., and Kulmala, M.: New particle formation in Beijing, China: Statistical analysis of  
29 a 1-year data set, *Journal of Geophysical Research: Atmospheres*, 112, n/a-n/a,  
30 10.1029/2006JD007406, 2007.

31 Wu, Z., Hu, M., Lin, P., Liu, S., Wehner, B., and Wiedensohler, A.: Particle number size  
32 distribution in the urban atmosphere of Beijing, China, *Atmospheric Environment*, 42,  
33 7967-7980, <http://dx.doi.org/10.1016/j.atmosenv.2008.06.022>, 2008.

34 Wu, Z. J., Nowak, A., Poulain, L., Herrmann, H., and Wiedensohler, A.: Hygroscopic  
35 behavior of atmospherically relevant water-soluble carboxylic salts and their influence on the  
36 water uptake of ammonium sulfate, *Atmos. Chem. Phys.*, 11, 12617-12626,  
37 10.5194/acp-11-12617-2011, 2011.

1 Wu, Z. J., Poulain, L., Henning, S., Dieckmann, K., Birmili, W., Merkel, M., van Pinxteren,  
2 D., Spindler, G., Mueller, K., Stratmann, F., Herrmann, H., and Wiedensohler, A.: Relating  
3 particle hygroscopicity and CCN activity to chemical composition during the HCCT-2010  
4 field campaign, *Atmospheric Chemistry and Physics*, 13, 7983-7996,  
5 10.5194/acp-13-7983-2013, 2013.

6 Wu, Z. J., Poulain, L., Birmili, W., Größ, J., Niedermeier, N., Wang, Z. B., Herrmann, H., and  
7 Wiedensohler, A.: Some insights into the condensing vapors driving new particle growth to  
8 CCN sizes on the basis of hygroscopicity measurements, *Atmos. Chem. Phys. Discuss.*, 15,  
9 8403-8427, 10.5194/acpd-15-8403-2015, 2015.

10 Ye, X., Tang, C., Yin, Z., Chen, J., Ma, Z., Kong, L., Yang, X., Gao, W., and Geng, F.:  
11 Hygroscopic growth of urban aerosol particles during the 2009 Mirage-Shanghai Campaign,  
12 *Atmospheric Environment*, 64, 263-269, <http://dx.doi.org/10.1016/j.atmosenv.2012.09.064>,  
13 2013.

14 Yeung, M. C., Lee, B. P., Li, Y. J., and Chan, C. K.: Simultaneous HTDMA and  
15 HR-ToF-AMS measurements at the HKUST Supersite in Hong Kong in 2011, *Journal of*  
16 *Geophysical Research: Atmospheres*, 119, 9864-9883, 10.1002/2013JD021146, 2014.

17 Zdanovskii, B.: Novyi Metod Rascheta Rastvorimostei Elektrolitov v Mnogokomponentnykh  
18 Sistema, , *Zh. Fiz. Khim+*, 22, 1478-1485, 1486-1495, 1948.

19 Zhang, J., Wang, L., Chen, J., Feng, S., Shen, J., and Jiao, L.: Hygroscopicity of ambient  
20 submicron particles in urban Hangzhou, China, *Front. Environ. Sci. Eng. China*, 5, 342-347,  
21 10.1007/s11783-011-0358-7, 2011.

22 Zheng, X., Liu, X., Zhao, F., Duan, F., Yu, T., and Cachier, H.: Seasonal characteristics of  
23 biomass burning contribution to Beijing aerosol, *Science in China Ser. B Chemistry*, 48,  
24 481-488, 2005.

25  
26  
27  
28  
29  
30  
31  
32  
33  
34  
35  
36  
37  
38  
39  
40

1  
2  
3  
4

5 **Table and figures**

6

7 Table 1: Gravimetric densities ( $\rho$ ) and hygroscopicity parameters ( $\kappa$ ) used in this  
8 study.

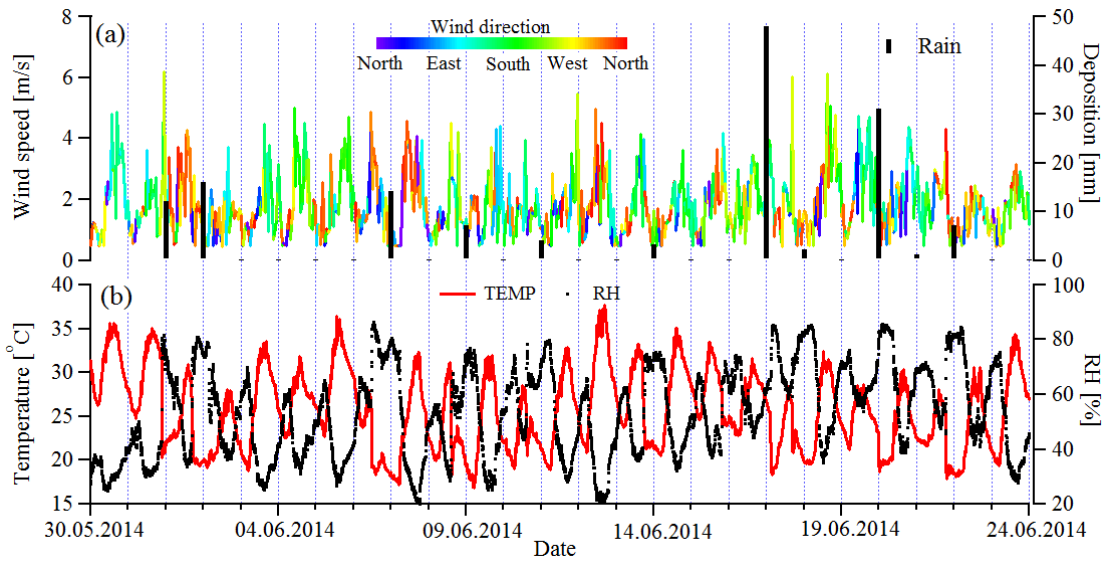
Species	$\text{NH}_4\text{NO}_3$	$\text{NH}_4\text{HSO}_4$	$(\text{NH}_4)_2\text{SO}_4$	SOA	POA	BC
[ $\text{kg}/\text{m}^3$ ]	1720	1780	1769	1400	1400	1700
$\kappa$	0.58	0.56	0.48	0.1	0	0

9  
10  
11  
12



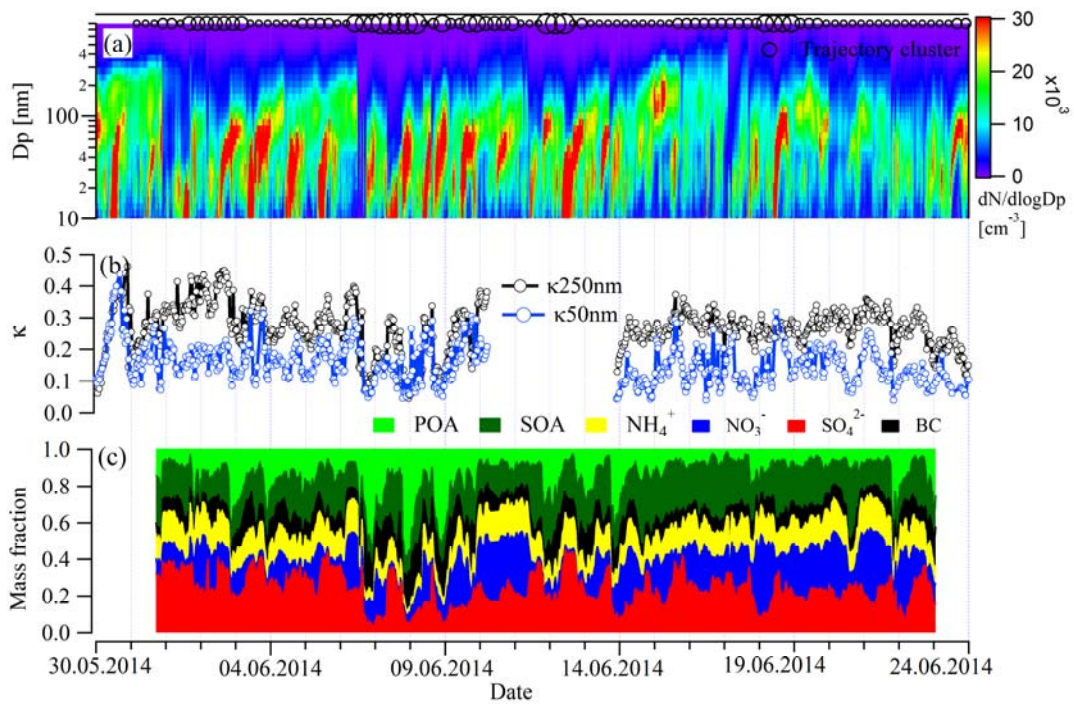
13  
14  
15  
16  
17

Figure 1: Mean air mass backward trajectories for five clusters arriving at the sampling site.



1  
2  
3  
4  
5

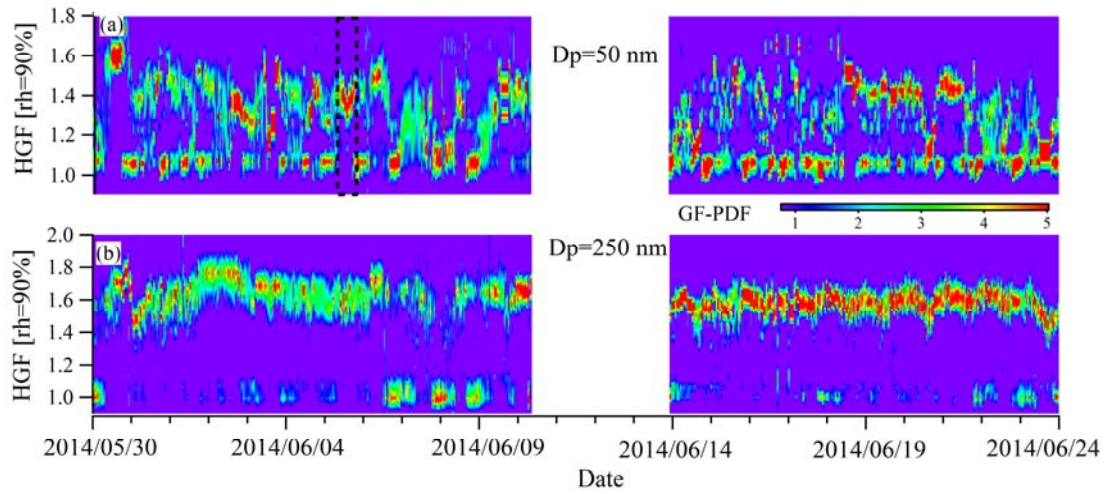
Figure 2: The time series of wind speed, wind direction, wet deposition (a) and temperature and RH (b) during the sampling period.



6  
7  
8  
9  
10  
11

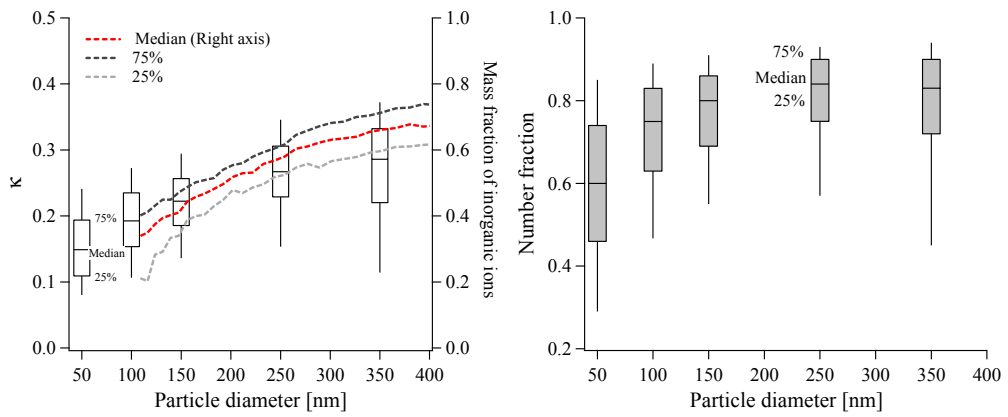
Figure 3: Time series of particle number size distribution (a), hygroscopicity parameters ( $\kappa$ ) (b), and chemical composition of PM1 (c) during the measuring period. The black circles in the upper panel (a) indicate the trajectory clusters. The smallest circle means cluster 1, and the biggest one is cluster 5.





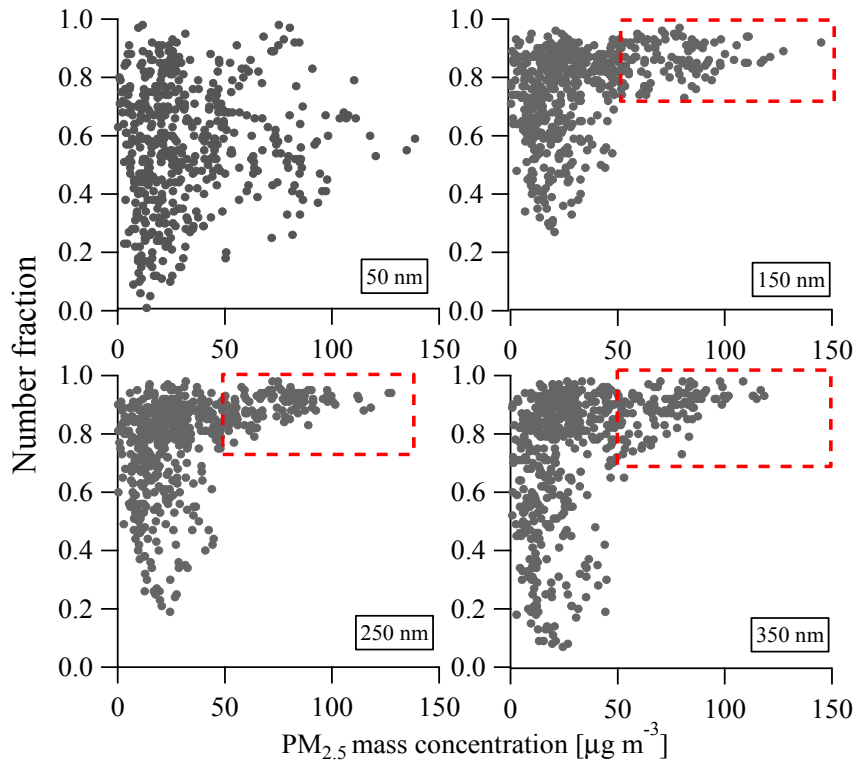
1  
2  
3  
4  
5  
6

Figure 4: The time series of the GF-PDFs for 50 and 250 nm particles.



7  
8  
9  
10  
11

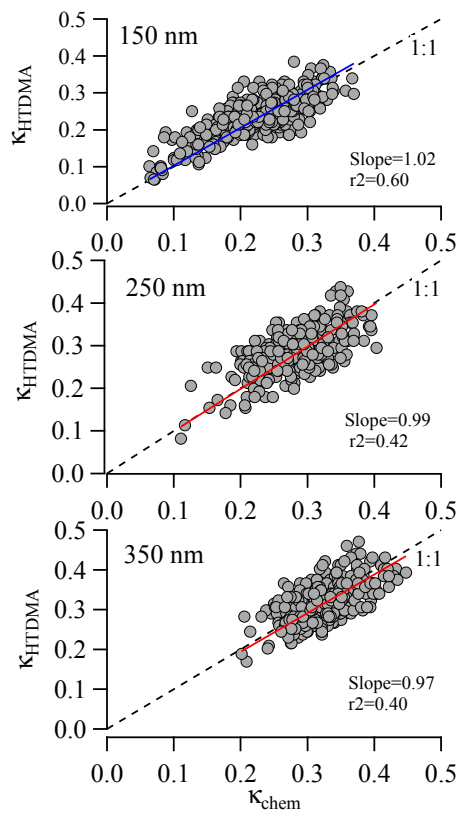
Figure 5: Size-resolved particle hygroscopicity and inorganic mass fraction (left) in NR-PM1 and Size-dependent number fraction of hydrophilic mode (right).



1

2

Figure 6: Number fraction of hydrophilic mode vs  $PM_{2.5}$  mass concentration

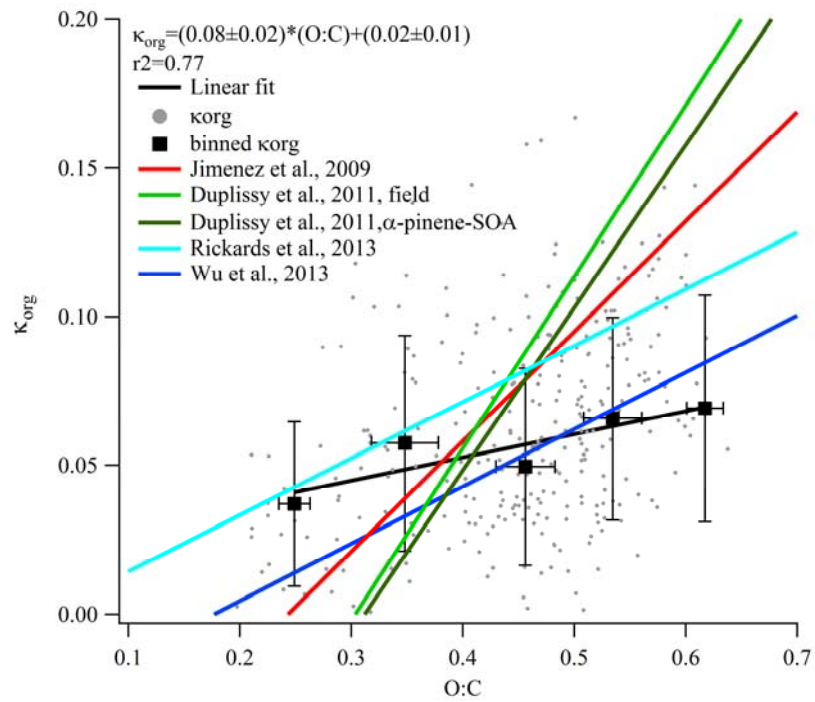


3

4

5

Figure 7:  $\kappa_{HTDMA}$  vs.  $\kappa_{chem}$  using size-resolved chemical composition data. All the root mean square errors (RMSE) of the linear fits were 0.04.



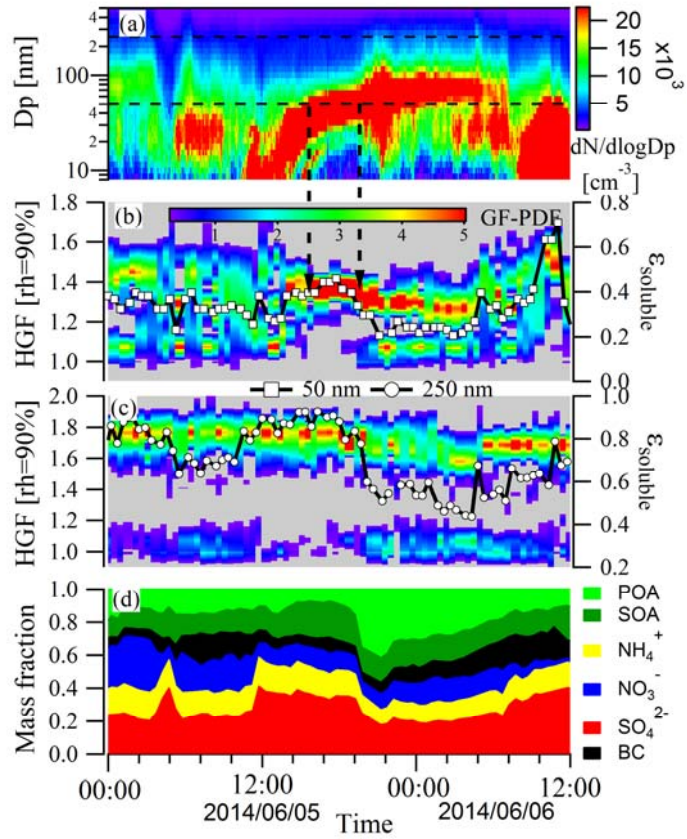
1

2 Figure 8: The relationship between organic hygroscopicity parameter ( $\kappa_{\text{org}}$ ) and  
 3 oxygen to carbon ratio (O: C).

4

5

6



1  
2  
3  
4  
5  
6  
7

Figure 9: The variation in particle number size distribution (a), GF-PDF (b, c), water soluble volume fraction (b, c), and chemical composition of PM<sub>1</sub> (d) during a NPF event.